POTENTIOMETRIC AND SPECTROPHOTOMETRIC STUDIES OF α-CYCLODEXTRIN COMPLEXES OF WEAK ACIDS AND BASES

Shu-Fen Lin

(Under the supervision of Professor Kenneth A. Connors)

The theory of the potentiometric method for studying complexes of ionizable substrates is developed, and graphical techniques are described for obtaining stability constant estimates from the data. The method is described for a system in which the conjugate acid and base forms of the substrate (S) are capable of forming 1:1 (SL) and 1:2 (SL_2) complexes with the ligand L. It is applied to complexes of α-cyclodextrin with 4-substituted benzoic acids, phenols, anilines and some heterocyclic amines. The stability of the complex formation is described in terms of the corresponding equilibrium constants: K_{11a}, K_{12a}, K_{11b} and K_{12b}. It was found that a maximum of three complex equilibria is sufficient to describe any of the systems studied.

The theory of the methyl orange competitive spectrophotometric method for studying 1:1 complexing is extended and a graphical technique is developed for obtaining the stability constant. The method is applicable and is useful when the complexation is accompanied by no significant substrate spectral change.

The stoichiometric model introduced earlier by this

laboratory is applied to describe the extent of binding to specific sites. Let gG represent the 1,4-disubstituted benzene derivatives having two binding sites, and hH a ligand having two sites, in the case of cyclodextrins the two ends of the cavity. If no 2:1 complexes are present, it is inferred that only one end of L can be entered. It follows that there are only two 1:1 complexes (say gH and GH) and one 1:2 complex (HgGH) in the system. Then it is shown that $K_{11} = K_{gH} + K_{GH}$ and $K_{12} = aK_{gH}K_{GH}/K_{11}$, where K_{gH} and K_{GH} are 1:1 binding constants for sites g and G, and a is a parameter measuring interaction between the sites in a 1:2 complex.

K_{11} and K_{12} are reported for many 1,4-disubstituted benzene derivatives with α-cyclodextrin at 25.0°C and these are interpreted in terms of the 2-site binding model. The dependence of the experimental stability constants on substituent sigma constants is used to establish the primary site of binding. It is concluded that binding site electron density is the primary factor contributing to binding at the site, however, the binding stability is aided by high site polarizability and opposed by high site polarity. For the benzoic acid series, it is determined that the carboxylic acid end is the primary binding site, but the 4-substituted end is for benzoates; for phenols, phenolates, anilines and anilinium series, the primary

binding site is the 4-substituted end.

Binding site constants are established by making use of some chemically reasonable assumptions about the systems. These site binding constants suggest that one simple 1:1 complex system tends to be generated when the two binding sites are very much different in size and electronic properties, but substantial fractions of two isomeric 1:1 complexes may co-exist when the two sites have similar properties.

APPROVED: Kenneth A. Connors

DATE: Aug. 14, 1981

POTENTIOMETRIC AND SPECTROPHOTOMETRIC STUDIES OF α-CYCLODEXTRIN COMPLEXES OF WEAK ACIDS AND BASES

BY

SHU-FEN LIN

A thesis submitted in partial fulfillment of the requirements for the degree of

DOCTOR OF PHILOSOPHY
(Pharmacy)

at the

UNIVERSITY OF WISCONSIN-MADISON

1981

ACKNOWLEDGEMENTS

I wish to express my sincere appreciation to Professor Kenneth A. Connors for his guidance and suggestions throughout the course of this investigation. His inspiration and encouragement provided me with rich and rewarding experiences during my graduate studies.

I gratefully acknowledge the scholarship from the Ministry of Education of the Republic of China.

To my parents

Their constant love made the journey worth the effort.

TABLE OF CONTENTS

Page

I. INTRODUCTION

The cyclodextrins, sometimes called Schardinger dextrins or cycloamyloses, are a series of water-soluble, non-reducing cyclic oligosaccharides produced by the enzymatic degradation and cyclization of starch by Bacillus macerans. They were first discovered in 1891 by Villiers (1), and their definite structural elucidation was accomplished in 1940 by Schardinger (2,3).

Cyclodextrins are composed of a number of D(+)-glucopyranose units with α-(1,4) linkages. Greek letters are used to denote the number of glucose units on the ring: α- for 6, β- for 7, γ- for 8, and so on. Cyclodextrins containing 6-12 glucose units have been isolated by Pulley and French (4) and they found α-, β- and γ-cyclodextrins were the main fractions. Five and lower-membered rings were not observed, probably because of the ring strain (5).

The considerable number of publications and patents dealing with the investigation of cyclodextrin chemistry reveal the widespread interest in the physical and chemical properties of these compounds. Cyclodextrins form inclusion complexes with a variety of molecules and ions (6). The "host-guest" stoichiometric complexes pave the way for the fundamental research to study molecular interactions and lead to their use as catalysts in several chemical

reactions (7,8).

A. Physical and Chemical Properties of Cyclodextrins

The cyclodextrins have conical-doughnut shapes. All the glucose units in solution are substantially in the undistorted C1 chair conformation (9) with α-(1,4) acetal oxygen bridges (Fig. 1). Bender et al. (10,11) describe the cavities as slightly "V" shaped. The wider rim, as shown in Fig. 2, is lined with the secondary hydroxyl groups on the C-2 and C-3 atoms of the glucose units. The C-3 hydroxyl group of one glucose unit interacts with the C-2 hydroxyl group of an adjacent glucose unit by hydrogen bonding. The secondary hydroxyl groups are, therefore, relatively rigid. The comparatively low pK_a of 12.3 (13) of the secondary hydroxyl group is due to stabilization of the alkoxide ion by means of these intramolecular hydrogen bonds, which also have a great effect on the reactivity of these groups. The narrower rim of the molecule is lined with the primary hydroxyl groups on C-6 atoms, which have freedom to rotate so as to partially block the cavity.

From a Corey-Pauling-Koltun molecular model, the interior of the cavity appears to consist only of a ring of C-H groups, a ring of glucosidic oxygens and another ring of C-H groups, thus the cavity interior is considered to be relatively apolar compared to water. The bridging oxygens

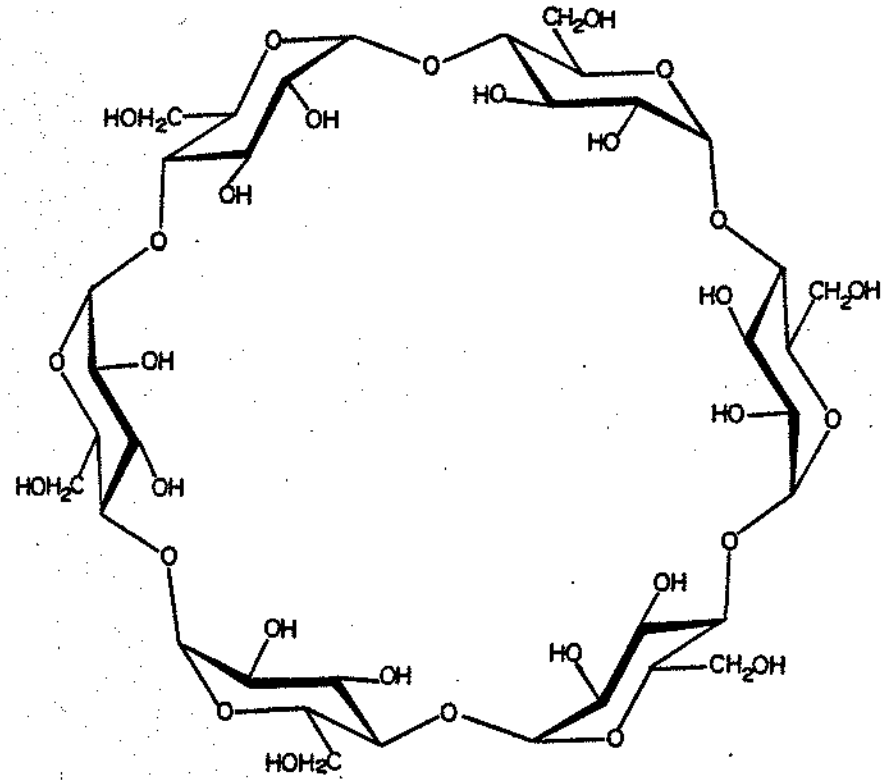

Figure 1. Structure of α-cyclodextrin.

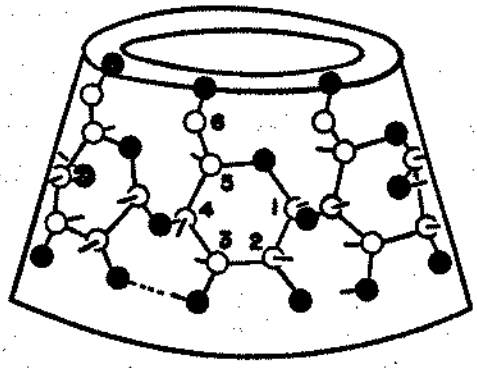

Figure 2. Diagram of cyclodextrins. o: carbon atom; ●: oxygen atom; —: C-H bond; ····: hydrogen bonding. [Ref. (12).].

are symmetrically distributed with their lone pair orbitals orthogonal to the cylindrical axis of the molecule (14), suggesting that the cavity is a region of high electron density and may behave like a Lewis base (6,15,16).

Some physical properties of α-, β- and γ-cyclodextrins are well-characterized and are collected in Table I.

Cyclodextrins are very stable in alkaline media, but are hydrolytically cleaved by strong acids (20-23). The acid hydrolysis by ring opening follows first order kinetics. The half-lives for α- and β-cyclodextrins in 7.7 N HCl solution at 30°C are 7.2 hrs and 4.5 hrs, respectively (20). Other thermodynamic parameters of the reaction were determined by Szejtli and Budai (23).

An important property of the cyclodextrins is their ability to form inclusion complexes, in aqueous solution and the crystalline state, with smaller molecules which fit into their cavity (6,24). Many kinds of reactions, as listed in Table II, have been found to be catalyzed by cyclodextrins after the inclusion complexes are formed. The catalyses are divided into covalent and noncovalent catalysis depending upon whether or not a covalently bonded intermediate is formed (7). A general scheme for covalent catalysis is

Table I. Some Physical Properties of the Cyclodextrins.

Cyclodextrin	# of Glucose Units	Mol. Wt.	Water Solubility (g/100 ml)	$[\alpha]_D^{25}$[b]	Melting Point[d]	Diameter[a] (Å)	
						Cavity	External
α	6	972	14.5[b] 12.1[c]	150.5 ± 0.5	278 (dec.)	4.7-5.2	14.6 ± 0.4
β	7	1135	1.85[b]	162.5 ± 0.5	300 (dec.)	6.0-6.4	15.4 ± 0.4
γ	8	1297	23.2[b]	177.4 ± 0.5	---	7.5-8.3	17.5 ± 0.4

Height of the cyclodextrin ring: 7.9-8 Å.[a]

[a]Ref. (17).

[b]At 25°C, Ref. (18).

[c]Ref. (19).

[d]Ref. (12).

Table II. Reactions Catalyzed by Cyclodextrins [According to (11)].

Reactions	Substrates	Acceleration Factor[a]	Nature of Catalysis[b]
Ester hydrolysis	Alkyl benzoates[c]	4.8	C
	Phenyl esters	300	C
	Mandelic esters	1.4	U
Amide hydrolysis	Penicillins	89	C
	N-Acylimidazoles	50	C
	Acetanilides	16	C
Cleavage of phosphoric	Pyrophosphates	>200	C
and phosphonic ester	Diaryl methyl phosphonates	66	C
Cleavage of carbonates	Aryl carbonates	7.5	C
Cleavage of sulfonates	Aryl sulfonates	19	N
Intramolecular acyl migration	2-Hydroxymethyl-4-nitrophenyl pivalate	6	N
Decarboxylation	Cyanoacetate ion	44	N
	Glyoxylate ion	4.0	N
Oxidation	α-Hydroxy ketones	3	N

[a] Ratio of rate catalyzed by cyclodextrin to the uncatalyzed reaction rate.

[b] C, N, and U respectively denote that catalysis proceed via a covalent bound intermediate, noncovalent catalysis, and unknown.

[c] Ref. (25).

$$S + L \underset{k_{-1}}{\overset{k_1}{\rightleftharpoons}} SL \xrightarrow{k_2} P^1\text{-}L + P^2 \xrightarrow{k_3} P^1 + L + P^2$$

$$\downarrow k_{un}$$

$$P^1 + P^2$$

where S and L denote the reaction substrate and cyclodextrin, respectively; k_{un} is the rate constant for the uncatalyzed reaction without cyclodextrin, k_1 is the rate of complex formation, k_2 describes the formation of covalent intermediate P^1-L which is hydrolyzed according to k_3 to give end products and regenerate cyclodextrin. For noncovalent catalysis, there is no intermediate P^1-L formation but all the other reaction steps proceed. Cramer and Bender et al. described this noncovalent catalysis as a result of a "microsolvent" effect of the "microheterogeneous" cavity and the steric properties within the cyclodextrin (26,11).

Since the substrate reacts in the form of an inclusion complex (SL), it has been observed, as expected, that the pseudo-first-order rate constants reach a limiting value with increasing cyclodextrin concentration (27-34). Furthermore, inhibitions occur when an inert molecule is added to compete with the substrate for the binding site of cyclodextrin (7,28,35). These rate effects are qualitatively identical with that in many enzymatic reactions.

Enantiomeric specificity and stereospecificity are also observed in the cyclodextrin catalyzed hydrolysis of mandelic acid esters (16) and phenylacetates (23). These properties of cyclodextrins have led to intensive study of these compounds as enzyme models.

However, there are shortcomings preventing cyclodextrins from acting as good enzyme models. First, maximum catalytic effects are observed at pH 13 (11), whereas enzymatic reactions exhibit maximal rates near neutral pH. Second, the hydrolysis rates of acyl-cyclodextrins, intermediates in covalent catalysis of ester hydrolysis, are very slow. Attempts have been made to facilitate cleavage of the intermediate by substituting the O (2) and O (3) of the cyclodextrin with various amine groups as more reactive nucleophiles. Imidazoyl (36), histamine (37), benzimidazole (38), and various acetohydroxamic acid derivatives (39) have been synthesized and results have shown a $\sim 10^3$ fold acceleration, relative to α-cyclodextrin, of some phenyl acetate hydrolysis reactions (40).

The cyclodextrins are also modified by "capping" several N-formyl groups to the primary alcohol, so that the molecules become more hydrophobic to favor the complexation with the substrate (41-43). Substitutions of cyclodextrins with 1,4-diaminoethane (44), polyamines (45), or pyridinecarbaldehyde oxime (46) furnish derivatives that can

complex metal ions and which can be considered as models for metalloenzymes. β-Cyclodextrins capped with divalent metal ions Cu^{++}, Zn^{++} and Mg^{++} are reported to be able to bind anions with hydrophobic moieties more strongly than the parent cyclodextrin (49).

In preparative chemistry, α-cyclodextrin catalyzes chlorination of anisole exclusively at the para position (47). For synthesizing vitamin K_1 and K_2 derivatives, the presence of cyclodextrin increases the yield from 22% to 60% in one step (48). The conversion of prostaglandin A_1 to its B_1 isomer is accelerated by α- and β-cyclodextrins (49,50).

B. Inclusion Complexation with Cyclodextrin

The cyclodextrins have been the subject of two books (11,26), eleven review articles (6,8,12,17,24,51-56) and hundreds of papers. This is because they form inclusion complexes with a wide variety of compounds ranging from polar reagents such as acids, amines, small ions such as ClO_4^-, SCN^- and halogen anions (57) to highly apolar aliphatic and aromatic hydrocarbons and even rare gases (58). The studies of inclusion compounds are of interest as they furnish information about intermolecular forces and hydrophobic interactions which are important in chemical and biological systems. In the industrial applications,

the "microencapsulation" of guest molecules within the inclusion complexes protects the substance from exposure to light and oxygen (59) and improves the storage and handling of volatile or toxic substances (17). Lach and Cohen (60) reported the solubility changes of 19 pharmaceuticals in water upon complexation with cyclodextrins.

Direct evidence for the apparent formation of inclusion compounds has resulted from proton NMR studies of β-cyclodextrin complexes with substituted benzoic acids, phenols, aspirin and tetracycline (61). DeMarco and Thakkar (61) demonstrated that protons H-3 and H-5, located in the interior of β-cyclodextrin cavity, were shielded by guest protons upon the formation of an inclusion compound. The chemical shifts of H-3 and H-5 are directly proportional to the increase in substrate concentration up to saturation. This study and the subsequent study (62) demonstrated that large molecules can form inclusion complexes if an aromatic moiety or other group of a suitable size and shape can fit into the cyclodextrin cavity.

The rate of inclusion complex formation is high. The temperature jump method (63) has been used for kinetic studies. The rate of recombination of the bimolecular reaction of p-nitrophenol, its anion, azo dyes and a number of other organic compounds (64-66) with α-cyclodextrin in aqueous solution was found to be about $10^8 \sim 10^9$ $M^{-1}sec^{-1}$,

which is almost diffusion controlled. Cramer et al. (64) proposed that the rate of complex formation depends upon:

1) approach of the guest molecule to the cyclodextrin molecule;
2) loss of water structure within the cyclodextrin cavity with removal of some water molecules;
3) breakdown of the water structure around the portion of the substrate that will be included and transport of some water molecules into the bulk solution;
4) interactions of substituent groups of the substrate with groups on the rim and inside the cyclodextrin ring;
5) possible formation of hydrogen bonds between the substrate and the cyclodextrin;
6) reconstitution of water structure around the exposed parts of the substrate after the inclusion process.

Which of these steps is rate determining depends on the nature of the enclosed guest molecule. That the diffusion-controlled limit (67) is not quite reached may be due to the special steric conditions of the inclusion reaction in step 1. Other factors, however, cannot be excluded.

The complex stabilities are quantitatively described by equilibrium constants. A number of classical methods as

well as some novel techniques based on the specific properties of the guest molecules have been developed. A 1:1 stoichiometry is often assumed. Spectrophotometric measurements (64,68-72) employing the Benesi-Hildebrand method (73,74) rely on the differing absorptivities of free and complexes substrates; a competitive spectrophotometric method (75,76) measures the spectral change of an indicator, methyl orange, when competing with a substrate for the binding site on the cyclodextrin molecule; a novel acid-base spectrophotometric analysis was also developed (77); the pH potentiometric method (72,78,79) exploits different complexation strengths of the acid-base conjugates; conductance determinations (57,80) rely on differing mobilities of free and complexed ionic substrates; the kinetic method (81) depends on the catalytic or inhibitory properties in certain ester hydrolysis reactions; the solubility method (60,82,83) measures the solubility changes of the substrate in water. Other methods such as proton and carbon-13 nuclear magnetic resonance spectroscopy (70,72,79,84-86), fluorometry (43,87,88), polarography (89,90) and circular dichroism spectroscopy (70-72,91) have been used. Microcalorimetry (87,92,93) measures the thermodynamic properties of complex formation directly.

The driving force for complex formation remains controversial. It has been suggested that several forces act

simultaneously (11,64,94). The dependence of complex stability constant on substrate polarizability (7,95) indicates that van der Waals forces play a role. The van der Waals forces include both dipole-induced dipole interactions and London dispersion forces (95,96). Dipole-dipole interactions are not as important, since guests without permanent dipoles can form stable complexes with cyclodextrins. On the contrary, the dipoles of guest molecules decrease the stability of the complex (97,98). This is consistent with the view that the interior of the cyclodextrin cavity is less polar than the surrounding medium, hence the more polar the substrate, the less is its tendency to complex with the host (other factors being equal).

Hydrogen bonding also functions in inclusion complex formation. The formation of hydrogen bonds between the guest and the O (6) H group of the cyclodextrin has been demonstrated crystallographically (99) in the structures of α-cyclodextrin/p-nitrophenol and α-cyclodextrin/p-hydroxybenzoic acid systems.

Hydrophobic interactions are also involved (64,100, 101). As described by Cramer et al. (64), the water molecules surrounding the guest molecules must be liberated and taken up by the bulk before the inclusion complexation. Thus, they gain degrees of freedom and contribute to the stability of the complex owing to the resulting increase in

entropy as well as the gain in potential energy. Bender et al. (7,8) proposed that the water molecules in the cyclodextrin cavity are enthalpy-rich, since they cannot form their full complement of hydrogen bonds to adjacent water molecules. This water is in an unfavorable, hydrophobic environment and is thus "activated". Expulsion of this enthalpy-rich water on complexation would be the driving force for the process (101,102).

Saenger et al. (103,105) suggested that cyclodextrin can release the strain energy of its macrocyclic ring on inclusion complex formation, according to the result of their X-ray crystallography and potential energy calculations, thus contributing to the stability of the complex. However, this gain in energy can only occur with α-cyclodextrin; β- and γ-cyclodextrins before inclusion complex formation are not strained (102,106).

Bergeron et al. (95,107) evaluated the contribution of strain energy relief and the release of high energy water in inclusion complex formation. They concluded that the effects are not the main driving force. Though more recent experiments (101,108) and theoretical considerations (109) have shown that van der Waals forces and the hydrophobic interactions probably are the main driving forces, the other forces inherent in the cyclodextrin-water complex may also be involved. In addition, the ring structure of

cyclodextrins is decisive as inclusion complexes are only formed if there is a good spatial fit between the guest and host components.

C. Stoichiometry in Cyclodextrin Complexation

A 1:1 stoichiometry between the substrate and the cyclodextrin molecule is typical and is often assumed in evaluating complex stabilities. However, evidence is accumulating (80,110,111) that in α-cyclodextrin systems both 1:1 and 1:2 (one substrate and two cyclodextrins) complexes must be taken into account.

Cramer et al. (64) observed the loss of isosbestic point in the spectra of methyl orange at varying cyclodextrin concentrations in alkaline solutions, and inferred the presence of complexes of higher than 1:1 stoichiometry. Pauli and Lach (112) used the solubility method and calculated the stoichiometric ratios of 1:1 and 1:2 for complexes of cinnamic acid and a series of phenyl-substituted carboxylic acids with β-cyclodextrin from the phase diagram. n-Heptane and cyclohexane (113) were also reported to form 1:2 complexes with α-cyclodextrin. Complexes involving three cyclodextrins were suggested for palmitoyl Co-A (114). However, none of these systems was described quantitatively.

Gelb et al. (80,110) identified 1:2 complexes of

4-biphenylcarboxylate and 4-methylcinnamate ions with α-cyclodextrin, using a combination of conductometric and carbon-13 NMR techniques. They were unable to resolve the complex stability constants K_{11} and K_{12} for 1:1 and 1:2 complexes. Connors et al. (97,111) have developed systematic methods for studying 1:1 and 1:2 complexes of α-cyclodextrin with trans-cinnamic acid and some related compounds, using solubility, spectral, kinetic and potentiometric techniques. Their results showed that at the relatively low total cyclodextrin concentration of 0.01 M, about 37% of the complexed cinnamic acid is present as the 1:2 complex form. Therefore, one cannot overlook the involvement of multiple complexes in these systems. They further described a stoichiometric model based on the assumption that the 1:2 complex is formed by adding another host molecule to a preformed 1:1 complex without perturbing the structure of the 1:1 complex (97). The binding constants for the sites on the substrate that are responsible for the complexation interaction were thus estimated.

D. Plan of Research

The potentiometric method as developed by Connors et al. (78,111,115) for 1:1 + 1:2 stoichiometric systems appeared to offer a convenient experimental approach to obtain all the complexation stability constants

simultaneously for ionizable substrates. However, the calculation procedures required a form of iterative non-linear regression analysis and the curve-fitting approach (115) resulted, for many systems, in an infinite number of acceptable solutions, obviously an unsatisfactory situation.

The objectives of this research were (1) to improve the systematic treatment of the theory of the potentiometric method, and to develop simple and reliable techniques to extract the stability constants for routine applications; and (2) to apply this technique to many substrates, seeking trends and explanations of complex stability.

para-Substituted benzoic acids, phenols, anilines and some heterocyclic amines were studied as substrates. One reason for using these compounds is that some of them have been studied by other techniques (76-78,116). Therefore the validity of the newly developed method can be tested by comparison of the results. Second, the apolar nature of the cavity has been demonstrated by the stronger complexation of benzoic acids over the negatively charged benzoate anion (78). For phenols, the phenolate anion complexes more strongly than the corresponding phenol (64,78,95). This anomalous phenomenon is of interest. Third, only few amines have been studied (116). The complexation of aniline with α-cyclodextrin was too weak to be determined

by the calorimetric method. Therefore, some amines were studied as a class.

For simple 1:1 complex systems, spectrophotometric measurement as developed by Benesi and Hildebrand (73) is one of the most convenient methods to determine the stability constant. However, an alternative approach was explored for studying compounds in a 1:1 system unaccompanied by significant spectral change upon complexation. The methyl orange competitive spectrophotometric method, which was first introduced by Broser et al. (75) and then was applied to study benzoic acid complex systems (76), is the method of interest. The theory of the competitive spectrophotometry is examined in depth so as to develop an applicable method.

The acquisition of stability constants for systems of established stoichiometry leads to an interpretation in terms of models to describe the extent of binding to specific binding sites.

II. THEORY OF METHODS FOR COMPLEXATION STUDIES

A. Potentiometric Method

1. The Basic Model Equations

If the conjugate acid and base forms of a weak acid/base substrate form cyclodextrin complexes of different strengths, then addition of cyclodextrin to a solution of the substrate will result in a pH change. The basic equations to describe the potentiometric studies of a 1:1 and 1:2 complexation have been developed by Connors' group (111,115).

Let L, HA and A^- represent cyclodextrin, a neutral weak acid substrate and the conjugate base, respectively. For 1:1 + 1:2 stoichiometry, the four complexation equilibria are presented as

$$HA + L \rightleftharpoons HAL \qquad (1\text{-}1)$$

$$A^- + L \rightleftharpoons AL^- \qquad (1\text{-}2)$$

$$HAL + L \rightleftharpoons HAL_2 \qquad (1\text{-}3)$$

$$AL^- + L \rightleftharpoons AL_2^- \qquad (1\text{-}4)$$

with their corresponding stability constants

$$K_{11a} = \frac{[HAL]}{[HA][L]} \qquad (2)$$

$$K_{11b} = \frac{[AL^-]}{[A^-][L]} \quad (3)$$

$$K_{12a} = \frac{[HAL_2]}{[HAL][L]} \quad (4)$$

$$K_{12b} = \frac{[AL_2^-]}{[AL^-][L]} \quad (5)$$

where brackets signify molar concentrations, and activity coefficients are assumed to be constant (79); thus the stability constants may be interpreted as thermodynamic quantities having the experimental solvent as the reference state.

There are three acid-base equilibria

$$HA \rightleftharpoons H^+ + A^- \quad (6\text{-}1)$$

$$HAL \rightleftharpoons H^+ + AL^- \quad (6\text{-}2)$$

$$HAL_2 \rightleftharpoons H^+ + AL_2^- \quad (6\text{-}3)$$

with their corresponding acid-base dissociation constants

$$K_a = \frac{[H^+][A^-]}{[HA]} \quad (7)$$

$$K_{a11} = \frac{[H^+][AL^-]}{[HAL]} \quad (8)$$

$$K_{a12} = \frac{[H^+][AL_2^-]}{[HAL_2]} \quad (9)$$

However, not all of the constants defined are independent; the following relationships are found:

$$K_{11a}K_{a11} = K_aK_{11b} \tag{10}$$

$$K_{12a}K_{a12} = K_{a11}K_{12b} \tag{11}$$

Letting S_t and L_t be the total molar concentrations of substrate and ligand, respectively, the mass-balance equations are:

$$S_t = [HA] + [A^-] + [HAL] + [AL^-] + [HAL_2] + [AL_2^-] \tag{12}$$

$$L_t = [L] + [HAL] + [AL^-] + 2[HAL_2] + 2[AL_2^-] \tag{13}$$

Substitution with the equilibrium expressions in Eqs. (2)-(5) and (7) yields functions of S_t and L_t in terms of the variables [L], [HA], $[H^+]$ and the stability constants.

$$S_t = [HA]\left[\frac{A[H^+] + BK_a}{[H^+]}\right] \tag{14}$$

$$L_t = [L] + [HA]\left[\frac{M[H^+] + NK_a}{[H^+]}\right] \tag{15}$$

where $A = 1 + K_{11a}[L] + K_{11a}K_{12a}[L]^2$ (16)

$$B = 1 + K_{11b}[L] + K_{11b}K_{12b}[L]^2 \tag{17}$$

$$M = K_{11a}[L] + 2K_{11a}K_{12a}[L]^2 \tag{18}$$

$$N = K_{11b}[L] + 2K_{11b}K_{12b}[L]^2 \tag{19}$$

Eliminating [HA] from Eqs. (14) and (15) gives a general

relationship between [L] and L_t:

$$L_t = [L] + S_t\left[\frac{M[H^+] + NK_a}{A[H^+] + BK_a}\right] \qquad (20)$$

The electroneutrality equation for this system is:

$$[Na^+] + [H^+] = [OH^-] + [A^-] + [AL^-] + [AL_2^-] \qquad (21)$$

where it is supposed that sodium is the counter-ion to the conjugate base form of the substrate. Combining Eq. (21) with Eqs. (3), (5), (7) and (14) gives

$$[Na^+] + [H^+] - [OH^-] = \frac{S_t BK_a}{A[H^+] + BK_a} \qquad (22)$$

The quantity $[Na^+]/S_t$ is the analytical fraction of substrate in the conjugate base form.

Eq. (22) is the general equation relating $[H^+]$ to free ligand concentration [L]. By means of Eqs. (20) and (22), $[H^+]$ is related to total ligand concentration L_t. In these equations $[Na^+]$, S_t and L_t are independent variables; $[H^+]$ and [L] are dependent variables.

Eq. (22) can be cast in a more useful form. In case $[Na^+] >> ([H^+] - [OH^-])$, Eq. (22) becomes

$$[Na^+] = \frac{S_t BK_a}{A[H^+] + BK_a} \qquad (23)$$

For a solution in which $L_t = 0$, it follows that $[L] = 0$, $A = 1$, $B = 1$ and Eq. (23) becomes

$$[Na^+]_0 = \frac{S_t K_a}{[H^+]_0 + K_a} \tag{24}$$

A series of measurements of $[H^+]$ as a function of L_t is made at constant S_t and $[Na^+]$, hence $[Na^+] = [Na^+]_0$, and these equations give

$$\frac{[H^+]_0}{[H^+]} = \frac{A}{B} = C \tag{25}$$

where C is the ratio of A/B. Defining a quantity $\Delta pH = pH - pH_0$:

$$\Delta pH = \log C \tag{26}$$

Eq. (26) describes the change in pH of the solution as a function of free ligand concentration, for fixed $[Na^+]/S_t$. If the substrate is half-neutralized, i.e., $[Na^+] = S_t/2$, then pH can be interpreted as pK_a' (apparent dissociation constant), and Eq. (26) becomes $\Delta pK_a' = \log C$ or

$$\Delta pK_a' = \log\left[\frac{1 + K_{11a}[L] + K_{11a}K_{12a}[L]^2}{1 + K_{11b}[L] + K_{11b}K_{12b}[L]^2}\right] \tag{27}$$

which is the equation used earlier (111) to interpret the cinnamic acid:α-cyclodextrin system. The present derivation is instructive in showing the level of approximation involved in interpreting ΔpH as $\Delta pK_a'$.

More generally, the exact Eq. (22) must be used. Defining the operational dissociation constant K_a' by Eq. (28):

$$K_a' = \frac{[H^+]([Na^+] + [H^+] - [OH^-])}{S_t - ([Na^+] + [H^+] - [OH^-])} \qquad (2\text{&}$$

Substitution into Eq. (28) from Eq. (22) leads to $K_a/K_a' = A/B = C$ or $\Delta pK_a' = \log C$. That is, Eq. (27) is general, provided the dissociation constants are evaluated by Eq. (28), which takes into account the dissociation of the solvent.

An important feature of this equation is that C is a ratio of polynomials. If $\Delta pK_a' = 0$ at all L_t, then $K_{11a} = K_{11b}$ and $K_{12a} = K_{12b}$.

On chemical grounds, and also by means of Eq. (20), it can be seen that the limits of [L] are $[L] = L_t$ and $[L] = L_t - 2S_t$. In the potentiometric method S_t must be appreciable in order to provide buffer capacity, hence it is seldom permissible to set $[L] = L_t$, as may often be done in other experimental techniques (such as spectroscopy).

For 1:1 + 1:2 complexation of a neutral weak base substrate (B) with α-cyclodextrin, the four complexation equilibria are similarly presented as:

$$B + L \rightleftharpoons BL \qquad (29\text{-}1)$$

$$HB^+ + L \rightleftharpoons HBL^+ \qquad (29\text{-}2)$$

$$BL + L \rightleftharpoons BL_2 \qquad (29\text{-}3)$$

$$HBL^+ + L \rightleftharpoons HBL_2^+ \qquad (29\text{-}4)$$

Their corresponding stability constants can be similarly defined as those in Eqs. (2)-(5). The general relationship between [L] and L_t as shown in Eq. (20) will be derived. The electroneutrality equation becomes

$$[HB^+] + [HBL^+] + [HBL_2^+] + [H^+] = [Cl^-] + [OH^-] \quad (30)$$

where $[Cl^-]$ is the concentration of the acidic neutralizing agent (hydrochloric solution, for example) which is the counter ion to the conjugate acid form of the substrate. The apparent acid dissociation constant is then defined as

$$K_a' = \frac{[H^+]([Cl^-] + [H^+] - [OH^-])}{S_t - ([Cl^-] + [H^+] - [OH^-])} \quad (31)$$

The further development leading to (26) and its interpretation is identical with the earlier treatment.

2. Graphical Techniques for Evaluating Complexation Constants

In order to extract stability constants from the $\Delta pK_a'$ and L_t data, the free ligand concentration [L] in Eq. (27) must be known. Eq. (20) is the equation to solve for [L], but this requires the stability constants. A non-linear regression analysis was developed by Wong (115), treating the stability constants as adjustable parameters to curve-fit the data using Eqs. (20) and (27). Although it is possible to achieve good fits to the experimental

points, this technique does not always yield a unique solution, in part because $\Delta pK_a'$ is a ratio of two polynomials of like degree, and therefore is not highly sensitive to the absolute values of the parameters. The curve-fitting approach has therefore been abandoned and graphical techniques leading to unique solutions are developed here.

The experimental data consist of $\Delta pK_a'$ values measured as a function of L_t, at constant S_t and reaction conditions. Since $\Delta pK_a' = C$, the quantity C is available. This is related to the stability constants by Eq. (32)

$$C = \frac{1 + K_{11a}[L] + K_{11a}K_{12a}[L]^2}{1 + K_{11b}[L] + K_{11b}K_{12b}[L]^2} \qquad (32)$$

It has been observed that for such systems it is very seldom necessary to retain all four of the constants for a satisfactory description of the potentiometric data, and some important special cases of Eq. (32) suffice to account for most of these systems. These special cases are described in the following section.

To solve for [L], the following approach is effective. In this work, the substrate is exactly half-neutralized, therefore $[Na^+] = S_t/2$, if the substrate is a weak acid. Then $[H^+] = K_a'$, to a level of accuracy acceptable for the present purpose. Since $C = K_a/K_a'$, this gives $[H^+] = K_a/C$ which is equivalent to

$$A[H^+] = BK_a \tag{33}$$

Substituting this into Eq. (20) gives

$$L_t = [L] + S_t\left[\frac{M}{2A} + \frac{N}{2B}\right] \tag{34}$$

The value of [L] is estimated by combining Eq. (34) with the appropriate special case of Eq. (32). The important features of this approach are: first, since the experimental quantity C is incorporated into the expression for [L], the correct stability constants are used in Eq. (34) to estimate [L]; second, solution of the equation for [L] is usually simplified, since much of the algebraic complexity is possessed by the numerical C values, and the special case can be identified by the form of the dependence on [L]. The particular equations for [L] are given in the individual special cases when discussed, and their derivations are shown in Appendix A.

The following treatment considers systems in which C > 1 or $\Delta pK_a'$ is positive. If C < 1 or $\Delta pK_a'$ is negative, define C' = 1/C; then the same equations apply with the subscripts a and b interchanged.

Case I. $K_{12a} = 0$, $K_{12b} = 0$. Then Eq. (32) becomes

$$C = \frac{1 + K_{11a}[L]}{1 + K_{11b}[L]} \tag{35}$$

A plot of C vs. [L] or L_t will approach a limiting value at high ligand concentration. Diagnosis of Case I behavior is

tentative, because Eq. (32) also results in this type of curve. The value [L] is found from Eq. (36),

$$[L] = L_t - \frac{S_t}{X + 1} \tag{36}$$

where $X = \frac{(C + 1)(R - C)}{(C - 1)(R + C)}$

and $R = K_{11a}/K_{11b}$. R is estimated by extrapolation to $1/L_t = 0$ on a plot of log C vs. $1/L_t$, since C approaches R as L_t approaches infinity. The stability constants are obtained from a linear form of Eq. (35):

$$\frac{C - 1}{[L]} = K_{11a} - CK_{11b} \tag{37}$$

The calculated R is compared with the initial estimate; if they differ significantly, the process is repeated. Usually 2 iterations are sufficient.

Case II. $K_{11b} = 0$, $K_{12b} = 0$, $K_{12a} = 0$. Then, from Eq. (32)

$$C = 1 + K_{11a}[L] \tag{38}$$

C is a linear function of ligand concentration. Obviously, any system will approach linearity at sufficiently low ligand concentration, therefore a wide range in L_t should be studied to detect curvature if it exists. The [L] is obtained with Eq. (39). No estimation is made in this case, therefore [L] and K_{11a} are obtained directly.

$$[L] = L_t - \frac{(C - 1)}{2C} \cdot S_t \tag{39}$$

Case III. $K_{11b} = 0$, $K_{12b} = 0$. Eq. (32) becomes

$$C = 1 + K_{11a}[L] + K_{11a}K_{12a}[L]^2 \tag{40}$$

This case is diagnosed by the positive curvature in the C vs. L_t plot. [L] is calculated with Eq. (41).

$$[L] = \frac{2C(L_t - S_t) + 2S_t}{2C - S_t K_{11a}} \tag{41}$$

The linear form of Eq. (40) is

$$\frac{C - 1}{[L]} = K_{11a} + K_{11a}K_{12a}[L] \tag{42}$$

A preliminary estimate of K_{11a} is calculated from the intercept of the plot of $(C - 1)/L_t$ vs. L_t according to Eq. (42). Iteration is carried out until K_{11a} does not change.

The plot of Eq. (42) is useful for confirming Case II systems, which should yield a slope equal to zero.

Case IV. $K_{12b} = 0$. Then Eq. (32) becomes

$$C = \frac{1 + K_{11a}[L] + K_{11a}K_{12a}[L]^2}{1 + K_{11b}[L]} \tag{43}$$

The plot of C vs. L_t will approach a linear segment of positive slope at high L_t. The equation of this line is

$$C = R + RK_{12a}[L] \tag{44}$$

where $R = K_{11a}/K_{11b}$ and can be estimated from the intercept of the line. K_{12a} can also be estimated by Eq. (44). The concentration [L] is given by

$$K_{11b}[L]^2 + [1 + S_t K_{11b}(\frac{3}{2} - \frac{R}{2C}) - L_t K_{11b}][L] - [L_t - \frac{S_t(C - 1)}{C}] = 0 \quad (45)$$

To find K_{11a} and K_{11b} several techniques have been devised. It is a general result, from Eq. (32), that

$$\frac{dC}{d[L]} = \frac{MB - AN}{B^2[L]} \quad (46)$$

Where A, B, M, and N are defined in Eq. (15). Thus the slope at [L] = 0 is equal to $K_{11a} - K_{11b}$ since A = 1, B = 1, and

$$\left(\frac{dC}{d[L]}\right)_{[L]=0} = \left[\frac{M - N}{[L]}\right]_{[L]=0} = K_{11a} - K_{11b} \quad (47)$$

This result together with the value of R from Eq. (44) gives K_{11a} and K_{11b} values. Another method constructs, on the curved C vs. [L] plot, lines such that quantity $[L]_x$ is found as the value of [L] when C = R. Substitution into Eq. (43) gives

$$K_{11b} = \frac{R - 1}{RK_{12a}[L]_x^2} \quad (48)$$

However, both of these approaches rely on data at low L_t, where the relative error in [L] is large. A better

procedure is to measure K_{11b} by a different, independent, experimental method. This usually is straightforward, since the Case IV diagnosis shows that $K_{12b} = 0$. The simple 1:1 complex stability constant K_{11b} (when $C > 1$) or K_{11a} (when $C < 1$) can be determined by spectrophotometric methods which will be described in later sections.

Then the linear plot according to Eq. (49) is made.

$$\frac{C - 1}{[L]} + CK_{11b} = K_{11a} + K_{11a}K_{12a}[L] \qquad (49)$$

This plot is also useful for confirming Case I systems, which should yield a slope of zero.

These graphical methods are simple in application, the linear plotting forms allowing routine statistical treatments. If the general case [Eq. (32)] should be required, as with cinnamic acid (79), the preferred approach is to combine the potentiometric data with information from independent experimental techniques such as solubility and spectral methods.

8. Methyl Orange Competitive Spectrophotometric Method

For Case IV systems, it was suggested earlier that K_{11a} (for amines or phenols) or K_{11b} (for carboxylic acids) be determined independently to provide best accuracy. The conventional Benesi-Hildebrand method (73,117), measuring the absorbance changes at a fixed wavelength as a function

of ligand concentration, is one of the methods of choice. However, some substrates may not show significant spectral change upon complexation. Broser et al. (75) developed a methyl orange (MO) competitive spectrophotometric method to determine K_{11a} of adrenalin:α-cyclodextrin complexation. The theory was based on the competition of the substrate (adrenalin) and the indicator (MO) for the binding sites on α-cyclodextrin, and 1:1 stoichiometry was assumed in each complex formation. Casu and Rava applied this method to the study of the complexation stability of benzoic acids with α-cyclodextrin (76). In this section, the theory of the competitive method is extended and a graphical technique to determine K_{11a} is developed.

Broser (118) in 1953 described the 1:1 inclusion complex of methyl orange (I) and α-cyclodextrin (L) in acid solutions as the following:

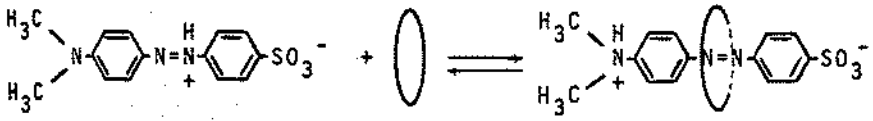

$$I + L \rightleftharpoons IL \qquad (50)$$

The corresponding stability constant is

$$K_{11I} = \frac{[IL]}{[I][L]} \qquad (51)$$

The absorptivities of the free and complexed forms of the

indicator in 0.08 N HCl solution at 508 nm are $\epsilon_I = 4.82 \times 10^4$ (lit. 5.7×10^4*) and $\epsilon_{IL} = 8.72 \times 10^2$ (lit. 4×10^3*), therefore it is easy to measure K_{11I} from the Benesi-Hildebrand double-reciprocal plot. (Detailed derivatives are described in Appendix B.) If a substrate (S), which is known to form 1:1 complex with cyclodextrin, is added to a solution of α-cyclodextrin and methyl orange, the formation of substrate-ligand complex (SL) will displace some indicator (I) from the complex form, thus increasing the absorbance. By measuring the absorbance changes at fixed wavelength, the complex formation constant for the substrate K_{11S} (K_{11a}) can be calculated according to the following derivation.

For 1:1 stoichiometry

$$S + L \rightleftharpoons SL \tag{52}$$

and the stability constant is

$$K_{11S} = \frac{[SL]}{[S][L]} \tag{53}$$

The competitive complexation equilibrium is

$$IL + S \rightleftharpoons SL + I \tag{54}$$

with the corresponding equilibrium constant

*Exact concentration was not given in literature; these are graphical estimates.

$$K = \frac{[SL][I]}{[IL][S]} = \frac{K_{11S}}{K_{11I}} \quad (55)$$

Mass balance equations on the substrate, ligand and indicator are

$$S_t = [S] + [SL] \quad (56)$$

$$L_t = [L] + [SL] + [IL] \quad (57)$$

$$I_t = [I] + [IL] \quad (58)$$

The [IL] term in Equation (57) is taken into consideration to be general; it can be neglected only when $L_t >> I_t$. Let

$$R = \frac{[I]}{[IL]} \quad (59)$$

Eq. (51) then becomes

$$K_{11I} = \frac{1}{R[L]} \quad (60)$$

Combining Eq. (56) and Eq. (53) gives

$$S_t = [S] + K_{11S}[S][L] \quad (61)$$

or

$$\frac{[S]}{S_t} = \frac{1}{1 + K_{11S}[L]} \quad (62)$$

therefore

$$\frac{[SL]}{S_t} = \frac{K_{11S}[L]}{1 + K_{11S}[L]} \tag{63}$$

Similarly,

$$\frac{[I]}{I_t} = \frac{1}{1 + K_{11I}[L]} \tag{64}$$

and

$$\frac{[IL]}{I_t} = \frac{K_{11I}[L]}{1 + K_{11I}[L]} \tag{65}$$

Combining Eqs. (57), (63) and (65):

$$L_t = [L] + \frac{K_{11S}[L]S_t}{1 + K_{11S}[L]} + \frac{K_{11I}[L]I_t}{1 + K_{11I}[L]} \tag{66}$$

Substituting into Eq. (66) from Eq. (60) for [L]

$$L_t = \frac{1}{RK_{11I}} + \frac{S_t K_{11S}}{RK_{11I} + K_{11S}} + \frac{I_t}{R + 1} \tag{67}$$

Define $P = L_t - \frac{1}{RK_{11I}} - \frac{I_t}{R + 1}$. Then

$$P = \frac{S_t K_{11S}}{RK_{11I} + K_{11S}} \tag{68}$$

Rearrangement of Eq. (68) gives

$$\frac{S_t}{P} = \frac{K_{11I}}{K_{11S}} \cdot R + 1 \tag{69}$$

where S_t is an independent variable, K_{11I} can be determined separately, and P and R can be measured (which will be discussed in the following), therefore K_{11S} is determinable graphically from Eq. (69).

R is defined in Eq. (59), and can be calculated from a

series of absorbance measurements: Suppose the substrate does not absorb at 508 nm, then the absorbance of a sample solution containing cyclodextrin, the acid form of methyl orange, and the substrate is contributed by the free and complexed forms of the indicator.

$$A = \varepsilon_I[I] + \varepsilon_{IL}[IL] \qquad \text{(1-cm cells)} \tag{70}$$

Combining Eq. (70) and Eq. (58) gives:

$$A - \varepsilon_{IL}I_t = (\varepsilon_I - \varepsilon_{IL})[I] \tag{71}$$

and setting $A_{IL} = \varepsilon_{IL}I_t$, which is the absorbance when all the indicator is in the complexed form, gives

$$A - A_{IL} = (\varepsilon_I - \varepsilon_{IL})[I] \tag{72}$$

Similarly,

$$A_I - A = (\varepsilon_I - \varepsilon_{IL})[IL] \tag{73}$$

where $A_I = \varepsilon_I I_t$ is the absorbance of indicator, with no cyclodextrin present. From Eqs. (59), (72) and (73),

$$R = \frac{A - A_{IL}}{A_I - A} \tag{74}$$

where A is the apparent absorbance of the sample solution; A_I can be determined easily. A_{IL} is obtained from an extrapolation of a plot of $1/\Delta A$ vs. $1/[L]$, where ΔA is the absorbance change due to the presence of cyclodextrin. At

$1/[L] = 0$ (the derivation to calculate [L] is in Appendix B), i.e., when free ligand concentration is infinite, it is assumed that the indicator is in the complexed form. Therefore

$$A_{IL} = A_I + (\Delta A)_{1/[L]=0} \tag{75}$$

R is experimentally determinable according to Eq. (74). It is important in using Eq. (74) that I_t be the same in all the solutions. If I_t is not exactly the same in solutions to determine A, A_{IL}, and A_I, this approach can correct for this. The observed absorbance is given by

$$A_{obs} = A_I + A_{IL} = \varepsilon_I[I] + \varepsilon_{IL}[IL] \quad \text{(1-cm cells)} \tag{76}$$

where A_I and A_{IL} merely refer to the absorbance contributed by these forms in the mixture. Define the apparent absorptivity ε_{obs} by

$$A_{obs} = \varepsilon_{obs}([I] + [IL]) \tag{77}$$

Setting Eq. (76) and Eq. (77) equal, then

$$(\varepsilon_{obs} - \varepsilon_{IL})[IL] = (\varepsilon_I - \varepsilon_{obs})[I] \tag{78}$$

and

$$R = \frac{\varepsilon_{obs} - \varepsilon_{IL}}{\varepsilon_I - \varepsilon_{obs}} \tag{79}$$

Following Eq. (69) to determine K_{11S}, we can measure P and R either at constant S_t with varying L_t, or at constant L_t with varying S_t. K_{11S} can be calculated from the slope of the plot of S_t/P vs. R.

Eq. (69) is a more exact description of the system than that derived by Casu and Ravà (76), who omitted the [IL] term in Eq. (57). This can be done only when $L_t >> I_t$ and $R >> 1$.

Further analysis of the system by taking into account the possible formation of substrate-indicator complex, which may occur for rigid, planar interactants (119-124,81, 83), supposes substrate and indicator form a 1:1 complex.

$$S + I \rightleftharpoons SI \tag{80}$$

The stability constant is

$$K_{SI} = \frac{[SI]}{[S][I]} \tag{81}$$

Let R_c be the measured ratio as defined in Eq. (74)

$$R_c = \frac{A - A_{IL}}{A_I - A} \tag{82}$$

and the true R is defined in Eq. (59). Consider the effect of the presence of (SI) on R_c. We define ε_{SI} as the molar absorptivity of (SI) complex. In any solution of this system, the apparent absorbance A is

$$A = \varepsilon_I[I] + \varepsilon_{IL}[IL] + \varepsilon_{SI}[SI] \tag{83}$$

and mass balance on I gives

$$I_t = [I] + [IL] + [SI] \tag{84}$$

For a special case that $\varepsilon_I = \varepsilon_{SI}$, i.e., SI forms but there is no change in spectrum when S is added to I, Eq. (83) becomes

$$A = \varepsilon_I([I] + [SI]) + \varepsilon_{IL}[IL] \tag{85}$$

Substituting into Eq. (85) from Eq. (84) gives

$$A = \varepsilon_I I_t - [\varepsilon_I - \varepsilon_{IL}][IL] \tag{86-1}$$

or $$A_I - A = [\varepsilon_I - \varepsilon_{IL}][IL] \tag{86-2}$$

Similarly, substituting [IL] in Eq. (84) into Eq. (85) gives

$$A - A_{IL} = (\varepsilon_I - \varepsilon_{IL})([I] + [SI]) \tag{87}$$

Combining Eqs. (82), (86-2) and (87),

$$R_c = \frac{[I] + [SI]}{[IL]} \tag{88}$$

or $$R_c = R + \frac{[SI]}{[IL]} \tag{89}$$

Eq. (89) shows that even in the special case, R_c is not equal to R.

$$L_t - \frac{1}{RK_{11I}} - \frac{I_t}{1 + R(1 + K_{SI}[I])} =$$

$$\frac{S_t K_{11S}}{K_{11S} + RK_{11I}(1 + K_{SI}[I])} \qquad (97)$$

Set left hand side = P'. Then Eq. (97) becomes

$$\frac{S_t}{P'} = 1 + \frac{RK_{11I}(1 + K_{SI}[I])}{K_{11S}} \qquad (98)$$

In order to determine K_{11S} in Eq. (98), R, K_{11I}, K_{SI}, [I] and P' must be solved. K_{11I} can be determined easily; R can be related to the experimental R_c by combining Eqs. (89), (93) and (95),

$$R_c = R + \frac{S_t K_{SI}[I]}{I_t K_{11I}[L]} \qquad (99)$$

Substituting for R in the P' expression and neglecting the $[I]^2$ term, which is extremely small as compared with other terms, P' can be described in Eq. (100)

$$P' = L_t - \frac{1}{R_c K_{11I} - \frac{S_t K_{SI}[I]}{I_t[L]}} -$$

$$\frac{I_t}{1 + R_c(1 + K_{SI}[I]) - \frac{S_t K_{SI}[I]}{I_t K_{11I}[L]}} \qquad (100)$$

Actually the entire last term in P' probably is negligible. Describe Eq. (98) in terms of R_c instead of R by substitution and rearrangement, the $[I]^2$ term again being

neglected,

$$\frac{S_t}{P'} - \frac{S_t K_{SI}[I]}{I_t K_{11S}[L]} = 1 + \frac{R_c K_{11I}(1 + K_{SI}[I])}{K_{11S}} \qquad (101)$$

Eq. (101), as compared with Eq. (69), shows that a plot of S_t/P vs. R_c is not exactly linear if (SI) is present, and K_{SI}, [I] and [L] in Eq. (100) must be known beforehand to generate a linear plot.

Cohen and Connors (120) studied a series of organic complexes in aqueous solution and found that the stability of the complex is roughly dependent on the maximal overlap area, which is an estimate of the surface area change upon complexation. The complexes were treated as stacked complexes. K_{SI}, therefore, can be roughly estimated from that correlation.

To estimate [L] and [I], several reasonable approximations were made. Assume the $K_{SI}[I]$ term in Eqs. (92) and (95) is small enough to be neglected. Combining Eqs. (92), (95) and (57) gives

$$L_t = [L] + \frac{K_{11S} S_t [L]}{1 + K_{11S}[L]} + \frac{K_{11I} I_t [L]}{1 + K_{11I}[L]} \qquad (102)$$

Usually I_t is small as compared with S_t and L_t, therefore the I_t term in Eq. (102) can be neglected and the equation becomes

$$L_t = [L](1 + \frac{K_{11S}S_t}{1 + K_{11S}[L]}) \quad (103)$$

L_t and S_t are independent variables. A preliminary determination will give an approximation of K_{11S}. Then [L] can be calculated from the quadratic solution of Eq. (103), and [I] with Eq. (104)

$$[I] = \frac{I_t}{1 + K_{11I}[L]} \quad (104)$$

Therefore, P' in Eq. (100) can be calculated. According to Eq. (101), K_{11S} can be estimated from the slope of a plot of the left hand side of Eq. (101) vs. $(1 + K_{SI}[I])R_c$. Iteration is carried out till K_{11S} does not change.

The calculations including the substrate-indicator complexation (SI) are rather complicated. However, the (SI) complex can be minimized if, according to Eq. (99), S_t and [I] are kept small. There are two ways to make [I] small: (1) use a lower I_t or make L_t large so that most of the indicator is in the (IL) form; (2) use the lower R_c values which are obtained experimentally by using lower S_t while L_t is kept constant or using higher L_t while S_t is kept constant. Then R_c can be an approximation of R. Eq. (69) can be applied to determine K_{11S}.

Recently, DeVylder and co-worker observed self-association of methyl orange in pH 2.2 aqueous solution at a concentration higher than 10^{-4} M (125). In our research,

the concentration of methyl orange used was 1.67×10^{-5} M and the absorbances of several indicator solutions of different concentrations on the order of 10^{-5} M followed Beer's Law perfectly. Therefore, self-aggregation of methyl orange in the systems studied here was justifiably neglected.

III. EXPERIMENTAL

A. Materials

Benzoic acid and its para-substituted derivatives were recrystallized from water and dried under reduced pressure over P_2O_5 at room temperature for 12 hours. The melting points were: 4-methylaminobenzoic acid (Aldrich), 162.8° [lit. (126): 163°]; 4-methoxybenzoic acid (Aldrich), 184° [lit. (127): 184°]; 4-acetylbenzoic acid (Aldrich), 209.5° [lit. (128): 210°]. The following compounds were purified by Wong (115): 4-aminobenzoic acid, 4-hydroxybenzoic acid, 4-toluic acid, benzoic acid, 4-fluorobenzoic acid, 4-cyanobenzoic acid, and 4-nitrobenzoic acid.

4-Methoxyphenol (Aldrich) was distilled under reduced pressure, b.p. 111°/2mm; m.p. 55° [lit. (129): 54-55°]. 4-Methylphenol, phenol, 4-fluorophenol, 4-iodophenol, 4-chlorophenol, 4-bromophenol, 4-cyanophenol and 4-nitrophenol were previously purified by Wong (115).

4-Phenylenediamine (Aldrich) was recrystallized from benzene and dried under reduced pressure over P_2O_5, m.p. 141° [lit. (129): 140°]; 4-anisidine (Aldrich) was distilled under reduced pressure, b.p. 98°/2mm, m.p. 56.5-57° [lit. (129): 57°]; 4-toluidine (Aldrich) was distilled under reduced pressure, b.p. 61.5°/2 mm, m.p. 44.5-45° [lit. (130): 44.8°]; aniline (Mallinckrodt) was purified

by fractional distillation, b.p. 181° [lit. (131): 184°]; 4-chloroaniline (Aldrich), 4-cyanoaniline (Aldrich), and 4-nitroaniline (Eastman) were recrystallized from water and dried under reduced pressure over P_2O_5. The melting points were: 72° [lit. (132): 72.5°], 86-86.5° [lit. (129): 85-87°], and 148-149° [lit. (129): 148-148.5°], respectively.

The purification of benzylamine, phenethylamine, imidazole, N-methylimidazole, 4-nitroimidazole, quinoline, isoquinoline, and t-butylaniline were also described by Wong (115)

α-Cyclodextrin (Sigma Lot 29C-0425 was used in benzoic acids and phenols studies; Lot 20F-0507 was used in amine studies) was dried at 95° for 48 hours. Samples from different Lots gave the same pH changes upon complexation when 4-cyanophenol was used as substrate. A sample of α-cyclodextrin recrystallized from water and dried under reduced pressure over P_2O_5 at room temperature for 12 hrs (70) had identical pH changes with that of freshly dried α-cyclodextrin without further purification; 4-methylbenzoic acid was used as substrate in this test.

Methyl orange (Eastman) was recrystallized from water, then washed with a little ethanol followed by ethyl ether (129). The molar absorptivity (ε) in 0.08 N HCl solution at 508 nm was 4.821×10^4.

All the solutions were prepared with ion-exchanged

water redistilled from alkaline permanganate.

B. Equipment

Potentiometric studies were carried out in a Haake E52 constant temperature water bath. pH measurements were made with an Orion 701A pH meter in conjunction with a Sargent-Welch S30072-15 combination electrode. Spectrophotometric measurements were made on Cary 14, Cary 16 and Perkin-Elmer Model 559 UV-VIS spectrophotometers fitted with jacketted cell compartments for temperature control at 25.0 ± 0.1°C. TI-59 (Texas Instrument) programmable calculator was used to calculate free ligand concentration [L]. The digital computer, Minitab Ver. 3.2, at the Academic Computing Center of Madison was used for linear regression and error analysis.

C. Procedures

1. Potentiometric Studies

A stock solution of the substrate was prepared such that its final concentration would be 0.004-0.005 M. First, the compound was accurately weighed out and then half-neutralized with a standard 0.1 N NaOH solution or a 0.1 N HCl solution. A 0.1 N NaCl solution was used to bring the solution to the mark.

Increasing amounts of α-cyclodextrin were accurately

weighed into a series of 5-ml volumetric flasks such that the resulting solutions would cover the full range of the solubility of α-cyclodextrin. (Maximum solubility is about 0.14 M.) 4.0-ml portions of the substrate stock solution were pipetted into each flask. Gentle heating on a water bath was required to dissolve all the α-cyclodextrin. The solutions were allowed to cool to 25°C and the 0.1 N NaCl solution was used to bring the solution to volume (substrate concentration 0.003 ∿ 0.004 M*). Then they were equilibrated at 25.0°C for at least 15 minutes; to ensure adequate mixing, a 10-mm stirring bar was added and was driven by a submerged water-driven magnetic stirrer. The solutions were then transferred to 5-ml test tubes together with the stirring bar, and the combination pH electrode was lowered into the solution, which was covered by a rubber stopper to protect it from contact with the atmosphere. Discoloration occurred in solutions of 4-methoxyphenol, aniline and p-phenylenediamine upon standing. Aluminum foil was used to cover each flask to improve the stability of the sample solution. The solutions were prepared just before measurement and no discoloration was observed during

*Studies of the effect of various substrate concentrations (S_t) on pH measurements showed that S_t should be at least 0.002 M to give reproducible results. At lower concentrations the reproducibility was poor because of the low buffer capacity.

the studies. Reproducibility of the duplicate solutions was 0.003 pH unit or better.

2. UV-VIS Spectrophotometric Studies

Increasing amounts of α-cyclodextrin were weighed into a series of 5-ml volumetric flasks. For K_{11b} determinations of benzoate anions, 4-cyanoaniline and 4-nitroaniline, the substrate was dissolved in pH 9.18 tris(hydroxymethyl)-aminomethane (TRIS) buffer. Sodium chloride was added to adjust ionic strength to 0.1 M. This pH ensured that the substrate was in the base form and the α-cyclodextrin was not appreciably ionized [pK_a = 12.3 (13)]. A potentiometric experiment showed that TRIS does not significantly complex with α-cyclodextrin (115). 4.0-ml portions of the substrate stock solution were pipetted into each flask. Gentle warming to dissolve the α-cyclodextrin was required. The TRIS buffer was then added to the mark. Reference solutions were prepared for each sample solution with identical α-cyclodextrin in TRIS buffer but no substrate. Spectra of complexed and uncomplexed substrate were obtained in order to select a wavelength at which the substrate absorptivity changes substantially upon complexation. Absorbance measurements were made at those selected wavelengths using Cary 16 spectrophotometer with 1.0-cm quartz cells. All the sample

solutions were equilibrated at 25.0°C for at least 15 minutes before the measurements. Reproducibility of the duplicate solutions was 0.003 absorbance unit.

K_{11a} of 4-nitrophenol was studied in the same manner, except that the substrate was dissolved in a solution of 0.01 N HCl with ionic strength 0.1 M.

3. Methyl Orange Competitive Spectrophotometric Studies

4.0-ml portions of a stock solution containing 4.185×10^{-5} M methyl orange (MO) in 0.2 N HCl were pipetted into 10.0-ml volumetric flasks containing 2.0 mls of 0.01 M α-cyclodextrin aqueous solution. The substrate solution at variable concentrations such that the final diluted concentrations were from 2.0×10^{-3} M to 1.38×10^{-2} M was then added to each flask. Water was used to bring the solution to volume. The reference solution was prepared by using the same concentration of α-cyclodextrin as the sample measured in 0.08 N HCl solution. The final solutions were equilibrated at 25.0°C for at least 15 minutes and the absorbance was read at 508 nm in 1-cm cells.

K_{11I} was determined in this same manner except that the concentration of α-cyclodextrin in the final solutions varied from 4.78×10^{-4} M to 2.0×10^{-2} M and no substrate

was present. Reference solutions were prepared for each sample solution having equal amounts of α-cyclodextrin in 0.08 N HCl solutions.

All stability constants reported here at 25°C and ionic strength 0.10 M.

IV. TREATMENT OF EXPERIMENTAL DATA

A. Potentiometric Data

For each potentiometric run, the pH was measured as a function of L_t and pK_a' was calculated according to Eq. (28). Experimentally we half-neutralized the substrate, so the counter-ion concentration in Eq. (28) equals $S_t/2$ and the equation becomes

$$K_a' = \frac{[H^+][\frac{1}{2}S_t + [H^+] - [OH^-]]}{\frac{1}{2}S_t - [H^+] + [OH^-]} \tag{105}$$

If $\frac{1}{2}S_t >> |[H^+] - [OH^-]|$, i.e., pH was within 5 to 9, since S_t was usually about 4×10^{-3} M, then the measured pH could be interpreted as pK_a'.

If the pH of the sample solution was less than 5, Eq. (106) was used to obtain the apparent dissociation constant pK_a'.

$$pK_a' = pH - \log \frac{\frac{1}{2}S_t + [H^+]}{\frac{1}{2}S_t - [H^+]} \tag{106}$$

If the pH of the sample solution was higher than 9, Eq. (107) was used to calculate pK_a'.

$$pK_a' = pH - \log \frac{\frac{1}{2}S_t - [OH^-]}{\frac{1}{2}S_t + [OH^-]} \tag{107}$$

The changes in apparent dissociation constant ($\Delta pK_a'$) as a function of L_t were obtained by subtracting the pK_a'

when L_t = 0 (usually this is an average of four independent measurements) from the pK_a' values at different L_t.

C is the inverse logarithm of $\Delta pK_a'$. If C was greater than unity ($\Delta pK_a'$ was positive), the equations described in the four special Cases were applicable. If C was less than unity ($\Delta pK_a'$ was negative), we defined C' = 1/C; then all the equations to extract stability constants were used with the subscripts a and b interchanged.

The general approach was to make a plot of C vs. L_t. From the shape of the curve, the system was tentatively assigned to one of the special cases. Free ligand concentration [L] was calculated and stability constants were evaluated from the appropriate linear plot. Iterations were carried out until the final determinations of either R, the ratio of K_{11a}/K_{11b}, or stability constants agreed with those of the preceding estimates within 0.5%. Usually two iterations sufficed to yield final estimates of the stability constants.

The accuracy of the assignment to Case I and Case II systems could be tested. For Case I systems K_{12a} = 0; if we treated it as if it were Case IV, according to Eq. (49), the $(C - 1/[L]) + CK_{11b}$ values should be constant, and zero slope is expected when making this plot. Statistical analysis can be carried out for the significance of K_{12a}. For Case II systems, K_{12a} = 0. If we treat it as if it

were Case III according to Eq. (42), the (C - 1)/[L] values should be constant. Making a plot according to this equation, the intercept is K_{11a} with zero slope.

B. Spectrophotometric Data

A spectrophotometric method was applied to study simple 1:1 complex systems. The absorbance changes at a single wavelength as a function of ligand concentration were analyzed to construct a "double reciprocal" plot based on the Benesi-Hildebrand relationship and readily derived (73,117) as shown in Eq. (108). (Derivations are shown in Appendix B.)

$$\frac{b}{\Delta A} = 1/K_{11}S_t\Delta\epsilon[L] + 1/S_t\Delta\epsilon \qquad (108)$$

where $$\Delta A = A_L' - A_0 \qquad (109)$$

A_L' is the absorbance in presence of cyclodextrin, A_0 is the absorbance of substrate only at the same concentration. K_{11} is the ratio of intercept/slope from the linear plot of $1/\Delta A$ vs. $1/[L]$.

When the cyclodextrin concentration is much larger than the substrate concentration, it seems adequate to assume $[L] = L_t$. In this work, the substrate concentration was in the range of $3.17 \sim 8.43 \times 10^{-5}$ M while cyclodextrin concentration was $1.12 \times 10^{-3} \sim 10^{-1}$ M. The ligand consumed by substrate is negligible. However, if substrate

concentration and ligand concentration are comparable, free ligand concentration must be used in Eq. (108). The derivation to obtain [L] is in Appendix B.

In placing a "least squares" line through the observed points on the plot of $b/\Delta A$ vs. $1/L_t$, we must note that the value of $b/\Delta A$ generally becomes less precise as the ligand concentration decreases and the absorbance differences being measured decrease. Therefore the variance in $b/\Delta A$ increases as $b/\Delta A$ increases. In this least square analysis of a reciprocal plot a weighting factor ω_i, which was defined (121) as

$$\omega_i = \frac{(\Delta A)_i^2}{\sum_1 (\Delta A)_i^2} \qquad (110)$$

must be multiplied into each point to account for its variable precision. The greater the absorbance change the larger the weighting factor is, which implies a higher degree of precision. The intercept and slope for K_{11} calculation were obtained from the weighted least squares analyses (133-135).

C. Error Analysis

To estimate the uncertainties in stability constants determined, error propagation was carried out as described by Perrin (136).

Let Q be a function of x and y. If

$$Q = x \pm y \tag{111}$$

then

$$\sigma_Q^2 = \sigma_x^2 + \sigma_y^2 \tag{112}$$

If $Q = \frac{x}{y}$ (113)

then $$\sigma_Q^2 = \frac{x^2}{y^2}\left(\frac{\sigma_x^2}{x^2} + \frac{\sigma_y^2}{y^2}\right) \tag{114}$$

where σ_Q^2, σ_x^2, and σ_y^2 are the variances of function Q and x and y. Using these basic forms, the standard deviations of K_{12a}'s (when C > 1) or K_{12b}'s (when C < 1) in Case III and IV systems were calculated.

V. RESULTS

A. Methyl Orange:α-Cyclodextrin System

Methyl orange (MO) forms a 1:1 cyclodextrin complex as reported by Broser (118). Fig. 3 shows the spectral changes of MO as a function of cyclodextrin concentration over the range of 4.78×10^{-4} M to 2.0×10^{-2} M. The concentration of MO in these solutions was constant. An isosbestic point was observed at 414 nm, indicating 1:1 complex formation in acidic solutions. Table III gives spectral data for the MO:α-cyclodextrin system in 0.08 N HCl solutions (pH 1.19). At low L_t, the concentration was comparable with the indicator concentration (I_t), therefore free ligand concentration, [L], was calculated according to Eq. (B-13) in Appendix B. Fig. 4 is the linear plot of $1/\Delta A$ vs. $1/[L]$. The stability constant for this system (K_{111}), calculated from the ratio of intercept/slope, was 672.9 M^{-1} with standard deviation 5.0 M^{-1}. Broser (118) reported the dissociation constant of MO:α-cyclodextrin complexes in 0.08 N HCl solution as 1.3×10^{-3} M, which is in reasonable agreement with 1.49×10^{-3} M from this work.

The absorbance of MO (A_I) at 1.67×10^{-5} M in 0.08 N HCl solution was 0.807 (std. dev. 0.003) and A_{IL} in Eq. (75) was 0.015 (std. dev. 0.006) at this concentration.

Figure 3. Spectra of methyl orange:α-cyclodextrin system. I_t = 1.67 x 10^{-5} M in 0.08 N HCl solutions. α-Cyclodextrin concentrations: 1, 0.00 M; 2, 4.78 x 10^{-4} M; 3, 9.72 x 10^{-4} M; 4, 1.94 x 10^{-3} M; 5, 4.00 x 10^{-3} M; 6, 2.00 x 10^{-2} M.

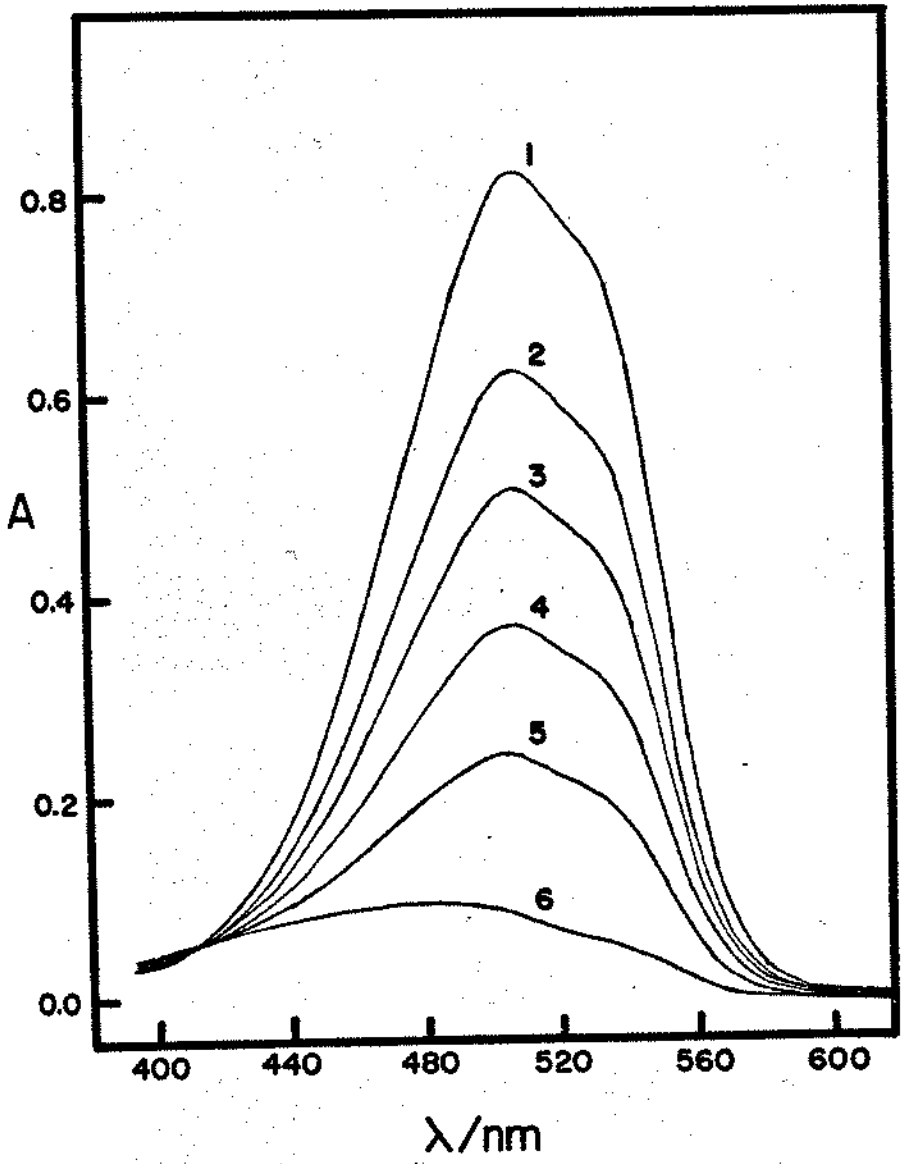
0.8
0.6
A
0.4
0.2
0.0
1
2
3
4
5
6
400
440
480
520
560
600
λ/nm

Table III. Spectral data of methyl orange:α-cyclodextrin system at 25.0 ± 0.1°.[a]

10^3 L_t/M	$-\Delta A$[b]	10^3 [L]
0.478	0.190	0.474
0.637	0.236	0.632
0.972	0.312	0.965
1.944	0.447	1.935
3.999	0.573	3.987
20.000	0.730	19.980

[a] $I_t = 1.67 \times 10^{-5}$ M in 0.08 N HCl; L_t represents cyclodextrin concentration.

[b] $\lambda = 508$ nm, $A_I = 0.807$.

Figure 4. Benesi-Hildebrand plot for the methyl orange:α-cyclodextrin system at 25.0°C. Substrate concentration: 1.67×10^{-5} M in 0.08 N HCl solutions.

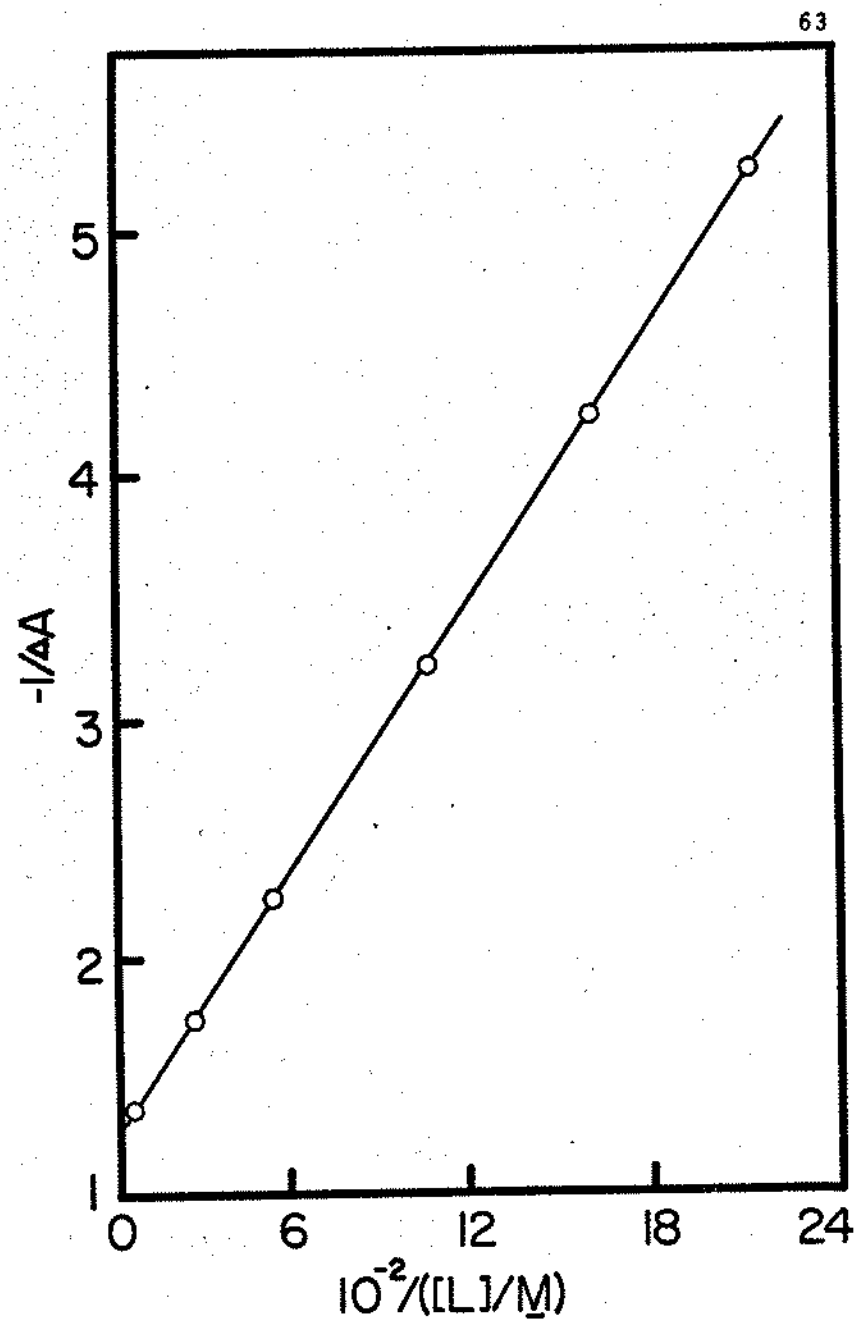
-1/ΔA
1
2
3
4
5
0
6
12
18
24
10⁻²/([L]/M)

B. Benzoic Acids

Benzoic acid and nine of its para-substituted derivatives were investigated. Substrates with ionizable para-substituents, namely 4-$NHCH_3$-C_6H_4COOH, $pK_{a\ CH_3\overset{+}{N}H_2}$ = 2.22 and $pK_{a\ COOH}$ = 5.04 (137); 4-NH_2-C_6H_4COOH, $pK_{a\ NH_3^+}$ = 2.41 and $pK_{a\ COOH}$ = 4.85 (138); and 4-HO-C_6H_4COOH, $pK_{a\ OH}$ = 9.31 and $pK_{a\ COOH}$ = 4.61 (139), have pK_a values separated sufficiently that the measurement of pK_a' for the carboxylic acid group leaves the para-substituent in its unionized state. The potentiometric data and further analysis to calculate [L] are listed in Tables IV to XIII. All of these compounds have positive $\Delta pK_a'$ values, indicating that carboxylic acids form complexes more strongly in acid forms than in their conjugate base forms according to Eq. (27).

A typical Case I system plot of C vs. L_t for 4-hydroxybenzoic acid is shown in Fig. 5. Fig. 6 shows the extrapolation of a plot of log C vs. $1/L_t$ for 4-hydroxybenzoic acid to obtain first estimate of R. Fig. 7 is the corresponding linear plot of Case I system, according to Eq. (37), for 4-hydroxybenzoic acid.

The potentiometric data for 4-acetylbenzoic acid, 4-cyanobenzoic acid and 4-nitrobenzoic acid indicated that they were Case IV systems. An Independent method to determine K_{11b} was necessary.

The ultraviolet spectra of these three substrates in

Table IV. Potentiometric data for 4-methylaminobenzoic acid:α-cyclodextrin system at 25.0 ± 0.1°C.[a]

L_t/M	$\Delta pK_a'$[b]	[L]/M
0.0100	1.041	0.0081
0.0201	1.347	0.0179
0.0300	1.497	0.0277
0.0400	1.611	0.0377
0.0500	1.676	0.0476
0.0600	1.762	0.0575
0.0700	1.792	0.0674
0.0799	1.845	0.0773
0.0900	1.873	0.0874
0.100	1.907	0.0973
0.110	1.923	0.1073
0.120	1.956	0.1172

[a] S_t = 0.00400 M.

[b] pK_a' = 4.881.

Table V. Potentiometric data for 4-aminobenzoic acid: α-cyclodextrin system at 25.0 ± 0.1°C.[a]

L_t/M	$\Delta pK_a'$[b]	[L]/M
0.0129	1.147	0.0108
0.0149	1.216	0.0128
0.0319	1.502	0.0294
0.0202	1.335	0.0179
0.0408	1.588	0.0383
0.0506	1.658	0.0479
0.0596	1.716	0.0568
0.0698	1.760	0.0669
0.0830	1.797	0.0801
0.0910	1.830	0.0880
0.1005	1.841	0.0975
0.1208	1.885	0.1177

[a] S_t = 0.00412 M.

[b] pK_a' = 4.711.

Table VI. Potentiometric data for 4-hydroxybenzoic acid: α-cyclodextrin system at 25.0 ± 0.1°C.[a]

L_t/M	$\Delta pK_a'$[b]	[L]/M
0.0100	0.944	0.0080
0.0201	1.210	0.0177
0.0301	1.346	0.0275
0.0400	1.427	0.0373
0.0500	1.486	0.0472
0.0601	1.531	0.0571
0.0700	1.566	0.0670
0.0799	1.589	0.0768
0.0900	1.606	0.0868
0.1001	1.627	0.0969
0.1100	1.639	0.1068
0.1200	1.654	0.1167

[a] S_t = 0.00400 M.

[b] pK_a' = 4.458.

Table VII. Potentiometric data for 4-methoxybenzoic acid: α-cyclodextrin system at 25.0 ± 0.1°C.[a]

L_t/M	$\Delta pK_a'$[b]	[L]/M
0.0201	1.223	0.0188
0.0300	1.377	0.0287
0.0400	1.490	0.0387
0.0500	1.572	0.0486
0.0600	1.640	0.0586
0.0700	1.696	0.0685
0.0800	1.744	0.0785
0.1000	1.813	0.0985
0.1100	1.847	0.1084
0.1200	1.877	0.1184

[a] S_t = 0.00250 M.

[b] pK_a' = 4.387.

Table VIII. Potentiometric data for 4-toluic acid: α-cyclodextrin system at 25.0 ± 0.1°C.[a]

L_t/M	$\Delta pK_a'$[b]	[L]/M
0.0100	0.969	0.0081
0.0201	1.266	0.0179
0.0299	1.423	0.0277
0.0401	1.529	0.0377
0.0501	1.602	0.0476
0.0600	1.664	0.0575
0.0701	1.700	0.0675
0.0801	1.753	0.0774
0.0899	1.786	0.0872
0.1001	1.817	0.0973
0.1099	1.843	0.1071
0.1200	1.858	0.1171
0.1300	1.880	0.1270

[a] S_t = 0.00400 M.

[b] pK_a' = 4.229.

Table IX. Potentiometric data for benzoic acid: α-cyclodextrin system at 25.0 ± 0.1°C.[a]

L_t/M	$\Delta pK_a'$[b]	[L]/M
0.0101	0.801	0.0083
0.0200	1.067	0.0178
0.0300	1.217	0.0276
0.0400	1.289	0.0375
0.0499	1.347	0.0473
0.0598	1.417	0.0571
0.0701	1.454	0.0673
0.0801	1.482	0.0772
0.0900	1.503	0.0871
0.0999	1.531	0.0969
0.1099	1.556	0.1069
0.1200	1.569	0.1169
0.1300	1.583	0.1269

[a] S_t = 0.00398 M.

[b] pK_a' = 4.084.

Table X. Potentiometric data for 4-fluorobenzoic acid: α-cyclodextrin system at 25.0 ± 0.1°C.[a]

L_t/M	$\Delta pK_a'$,[b]	[L]/M
0.0304	1.034	0.0281
0.0405	1.115	0.0381
0.0497	1.168	0.0471
0.0596	1.211	0.0569
0.0706	1.250	0.0679
0.0815	1.283	0.0787
0.0905	1.304	0.0876
0.0983	1.324	0.0953
0.1105	1.334	0.1075
0.1304	1.369	0.1273

[a] S_t = 0.00378 M.

[b] pK_a' = 4.017.

Table XI. Potentiometric data for 4-acetylbenzoic acid: α-cyclodextrin system at 25.0 ± 0.1°C.[a]

L_t/M	$\Delta pK_a'$[b]	[L]/M
0.0100	0.758	0.0075
0.0200	1.039	0.0165
0.0299	1.203	0.0259
0.0400	1.328	0.0356
0.0500	1.419	0.0454
0.0600	1.479	0.0552
0.0700	1.532	0.0651
0.0799	1.605	0.0749
0.0899	1.636	0.0848
0.1000	1.669	0.0948
0.1100	1.703	0.1047
0.1201	1.735	0.1148

[a] S_t = 0.00401 M.

[b] pK_a' = 3.675.

Table XII. Potentiometric data for 4-cyanobenzoic acid: α-cyclodextrin system at 25.0 ± 0.1°C.[a]

L_t/M	$\Delta pK_a'$[b]	[L]/M
0.0102	0.507	0.0076
0.0208	0.727	0.0174
0.0306	0.855	0.0267
0.0408	0.944	0.0366
0.0499	1.013	0.0455
0.0602	1.063	0.0556
0.0699	1.124	0.0652
0.0799	1.166	0.0751
0.0911	1.216	0.0861
0.1004	1.255	0.0954
0.1051	1.274	0.1000
0.1108	1.284	0.1057

[a] S_t = 0.00388 M.

[b] pK_a' = 3.405.

Table XIII. Potentiometric data for 4-nitrobenzoic acid: α-cyclodextrin system at 25.0 ± 0.1°C.[a]

L_t/M	$\Delta pK_a'$[b]	[L]/M
0.0100	0.383	0.0084
0.0200	0.575	0.0177
0.0300	0.691	0.0274
0.0401	0.794	0.0372
0.0501	0.865	0.0471
0.0600	0.900	0.0568
0.0700	0.947	0.0668
0.0800	0.989	0.0767
0.0900	1.020	0.0866
0.1000	1.063	0.0966
0.1100	1.091	0.1065
0.1200	1.106	0.1165

[a] S_t = 0.00270 M.

[b] pK_a' = 3.431.

Figure 5. Plot of C vs. L_t for the 4-hydroxybenzoic acid: α-cyclodextrin system.

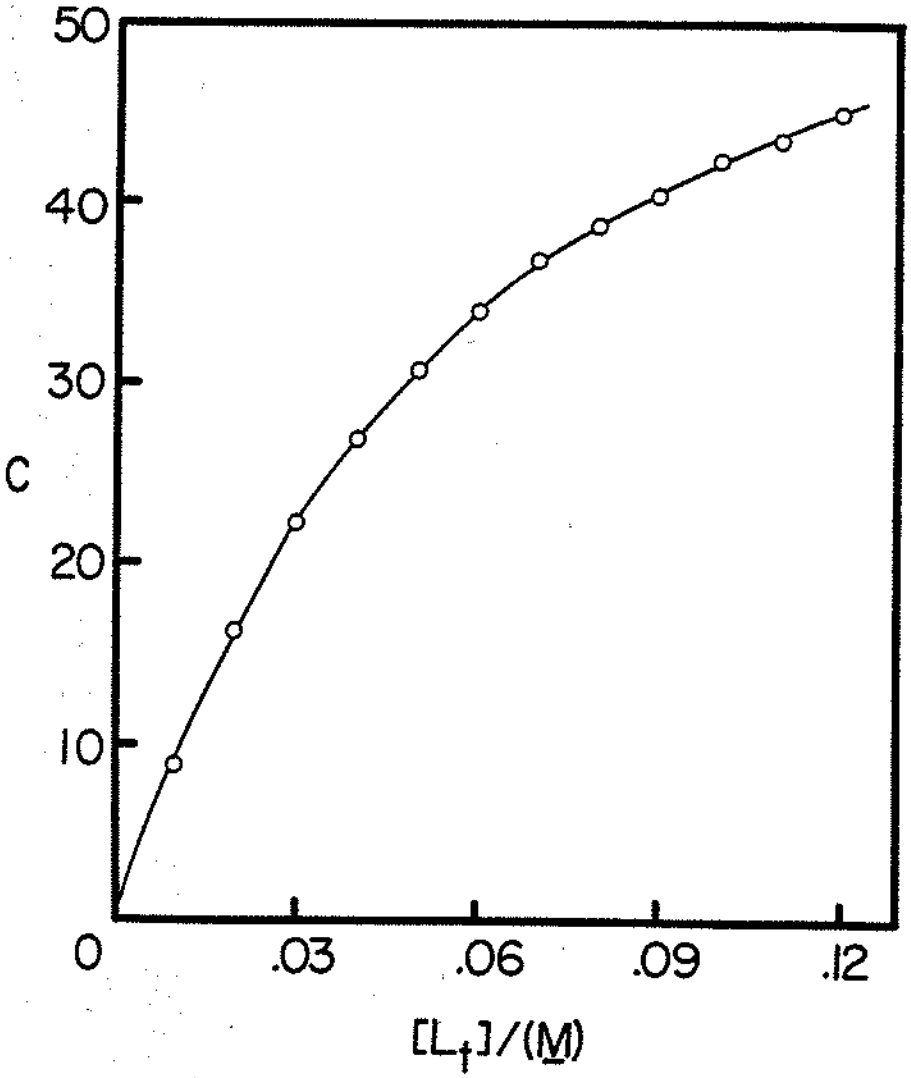
50
40
30
20
10
0
C
.03
.06
.09
.12
[L_t]/(M)

Figure 6. Plot of log C vs. $1/L_t$ for the 4-hydroxybenzoic acid:α-cyclodextrin system.

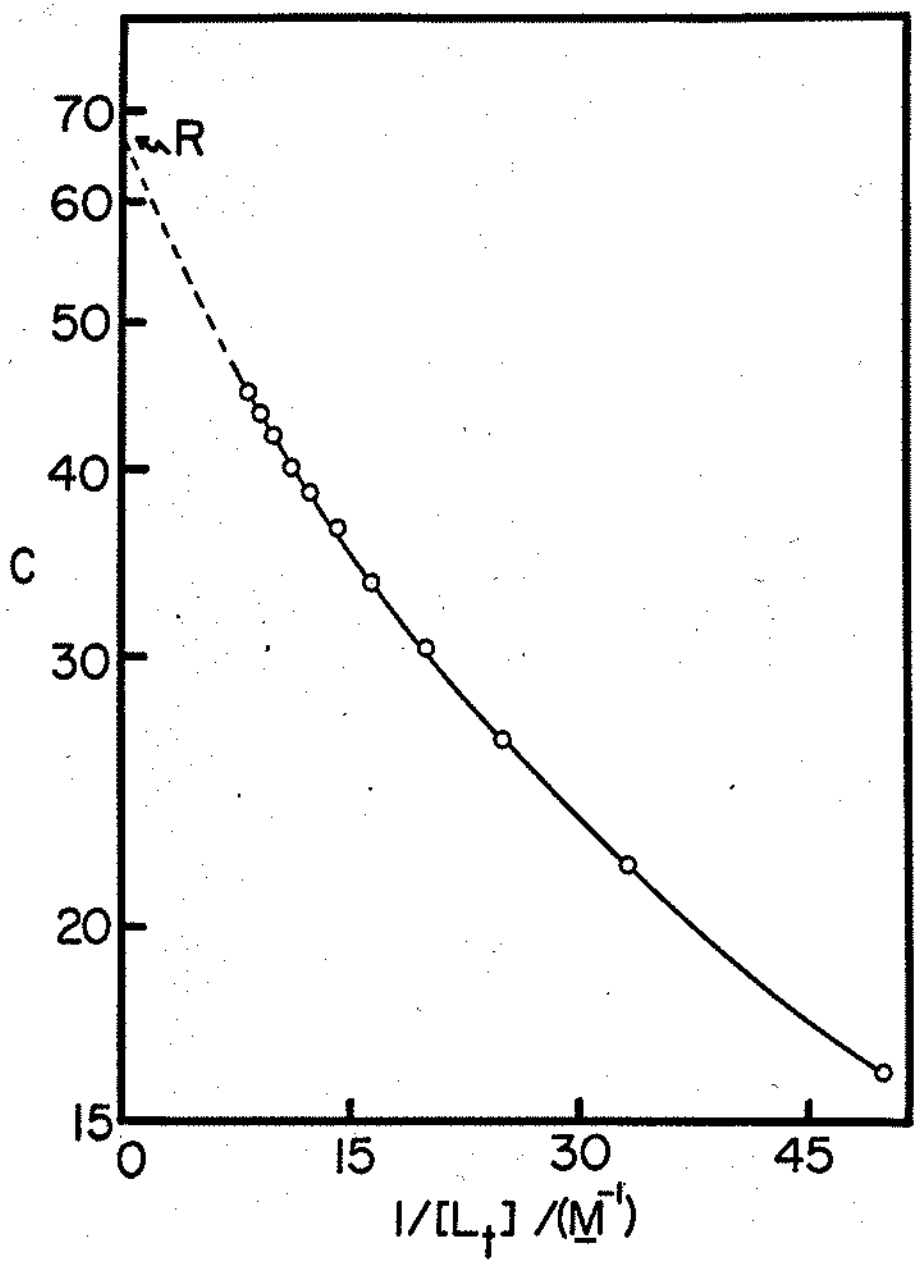
70
60
50
40
30
20
15
C
R
0
15
30
45
1/[L_t] /(M̄¹)

Figure 7. Plot of Eq. (37) for the 4-hydroxybenzoic acid: α-cyclodextrin system.

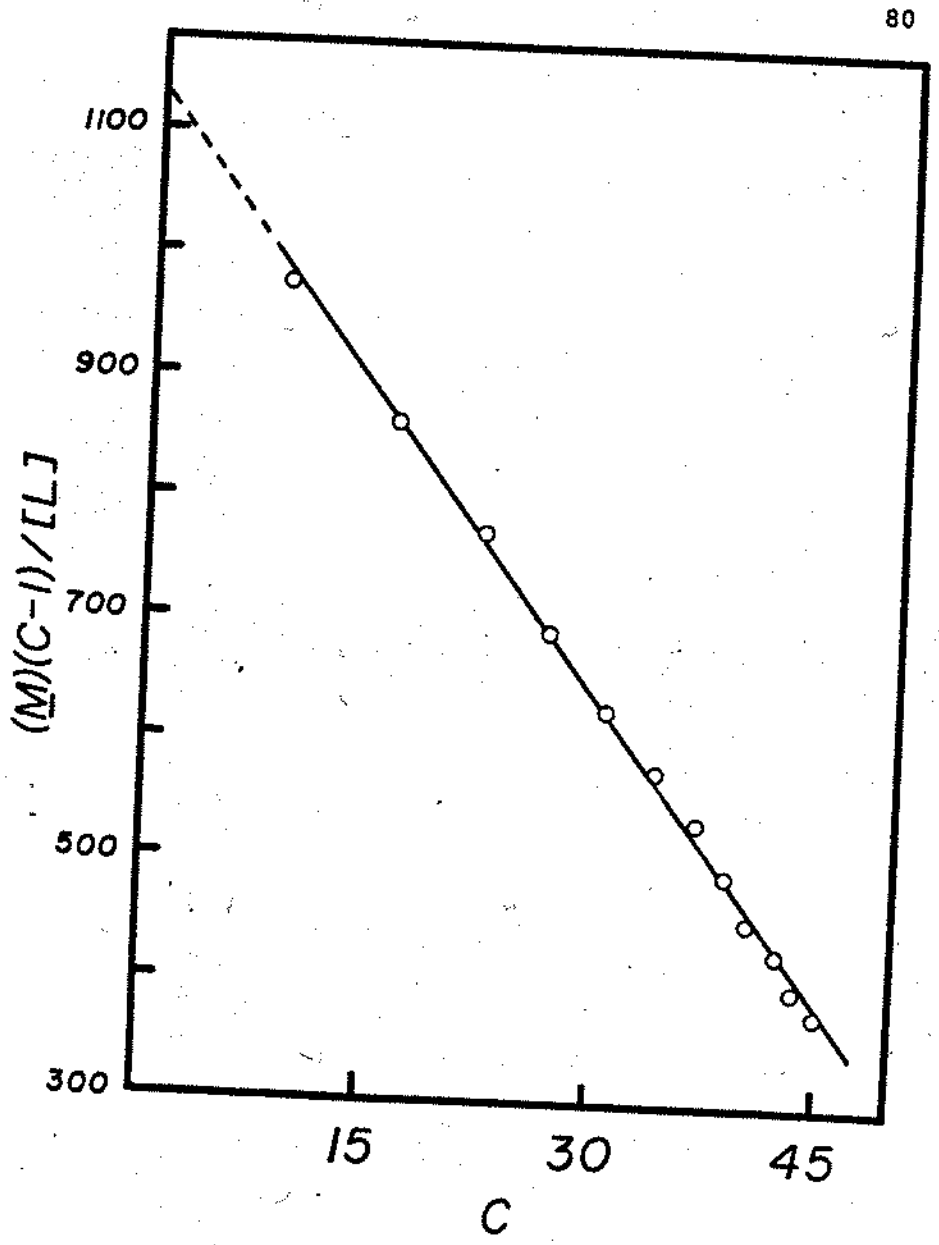
1100
900
700
500
300
(M)(C-1)/[L]
15
30
45
C

their conjugate base forms were significantly altered by the presence of cyclodextrin. Fig. 8 shows the spectral changes of 4-acetylbenzoate anion as a function of cyclodextrin concentration in TRIS buffer (pH 9.18) solutions. The spectral data obtained at 253 nm for 4-acetylbenzoate anion:cyclodextrin system are given in Table XIV. Fig. 9 is the weighted least-squares linear plot of $1/\Delta A$ vs. $1/L_t$. The K_{11b} value calculated from the ratio of intercept/slope is 60.3 $\underline{M}^{-1}$ at 25.0°C.

The spectral data obtained at 237 nm and 231 nm for 4-cyanobenzoate anion:cyclodextrin system at 25.0°C are collected in Table XV. The linear Benesi-Hildebrand "double reciprocal" plots of $1/\Delta A$ vs. $1/L_t$ were characteristic of simple 1:1 complexing. The K_{11b} values determined at 237 nm and 231 nm were 78.12 $\underline{M}^{-1}$ (std. dev. 3.69 $\underline{M}^{-1}$) and 80.28 $\underline{M}^{-1}$ (std. dev. 5.43 $\underline{M}^{-1}$), respectively. The results indicated that the stability constants were wavelength independent.

The spectrum of 4-nitrobenzoate anion was altered in the presence of cyclodextrin, as shown in Fig. 10. Over the range of cyclodextrin concentration studied, an isosbestic point is observed at 286 nm and the spectra are bathochromically shifted. The presence of the isosbestic point is evidence for 1:1 stoichiometry.

The spectral data for 4-nitrobenzoate anion:

Figure 8. Ultraviolet spectra of 4-acetylbenzoate anion at various α-cyclodextrin concentrations; S_t = 5.62×10^{-5} M; pH = 9.18; ionic strength = 0.1 M. Cyclodextrin concentrations: 1, 0.00 M; 2, 5.33×10^{-3} M; 3, 3.02×10^{-2} M; 4, 6.99×10^{-2} M.

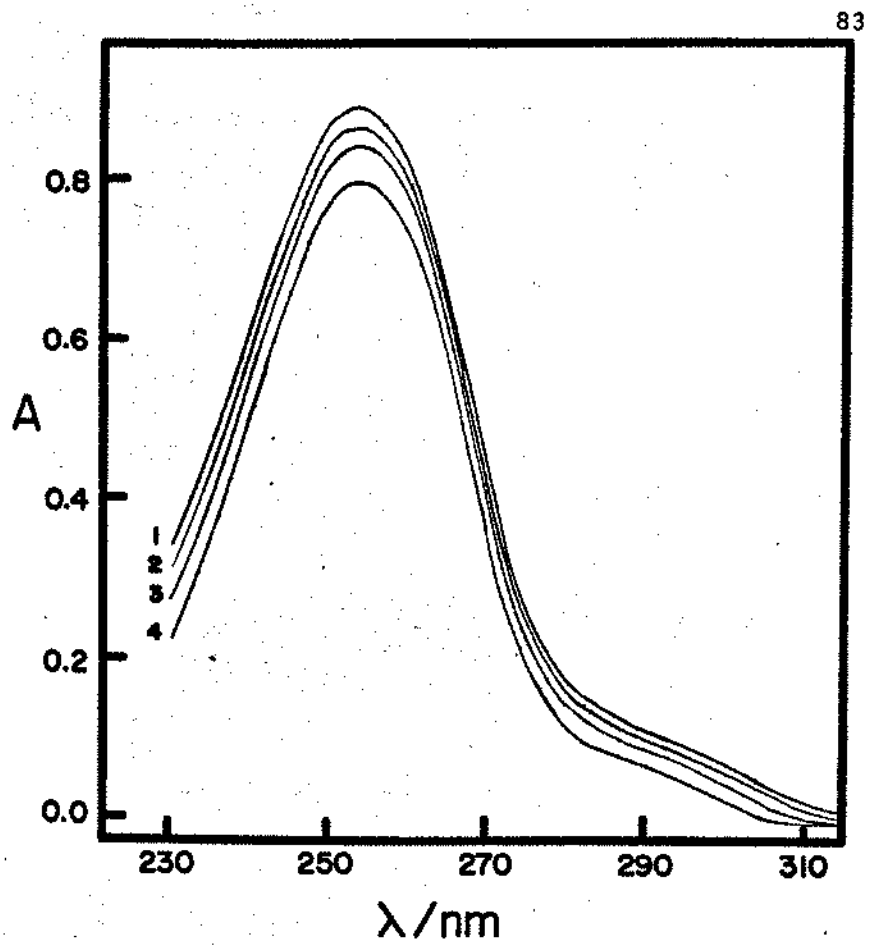
0.8
0.6
A
0.4
0.2
0.0
1
2
3
4
230
250
270
290
310
λ/nm

Table XIV. Spectral data for 4-acetylbenzoate anion: α-cyclodextrin system at 25.0 ± 0.1°C.[a]

$10^2 L_t/M$	$-\Delta A^b$
0.201	0.011
0.346	0.019
0.533	0.027
1.004	0.040
3.023	0.050
6.993	0.096

[a] $S_t = 5.62 \times 10^{-5}$ M; pH = 9.18 TRIS buffer.

[b] λ = 253 nm; A_0 = 0.897.

Figure 9. Benesi-Hildebrand plot for the 4-acetylbenzoate anion:α-cyclodextrin system at 25.0°C. Substrate concentration = 5.62×10^{-5} M in TRIS (pH 9.18) buffer solutions.

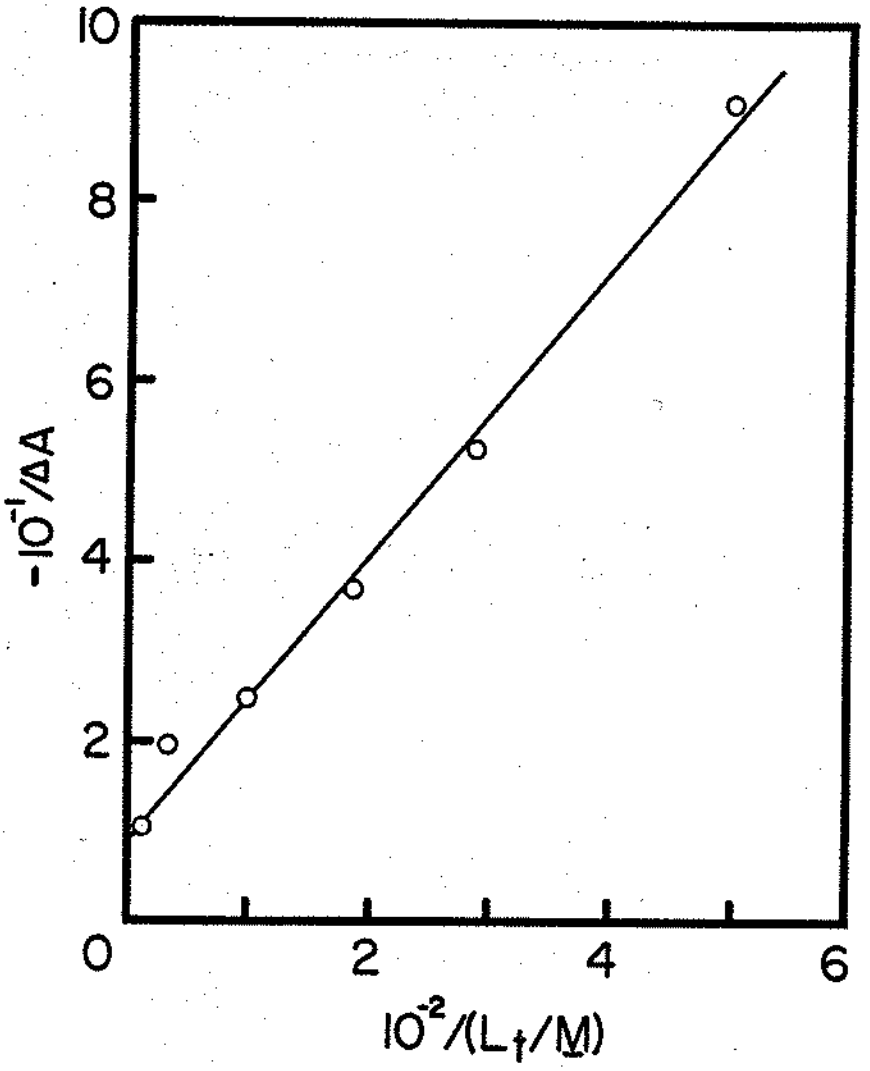
10
8
6
4
2
0
2
4
6
$-10^{-1}/\Delta A$
$10^{-2}/(L_t/M)$

Table XV. Spectral data for 4-cyanobenzoate anion: α-cyclodextrin system at 25.0 ± 0.1°C.[a]

$10^2 L_t/M$	$-\Delta A^b$	$-\Delta A^c$
0.112	0.019	- - -
0.343	0.050	0.057
0.532	0.067	0.076
0.727	0.088	0.097
1.003	0.100	0.110
3.021	0.167	0.186

[a] $S_t = 8.43 \times 10^{-5}$ M; pH = 9.18.

[b] λ = 237 nm; A_0 = 1.460.

[c] λ = 231 nm; A_0 = 1.314.

Figure 10. Ultraviolet spectra of 4-nitrobenzoate anion at various α-cyclodextrin concentrations; S_t = 8.43×10^{-5} M; pH = 9.18; ionic strength = 0.1 M. Cyclodextrin concentrations: 1, 0.00 M; 2, 3.44×10^{-3} M; 3, 1.00×10^{-2} M; 4, 0.1 M.

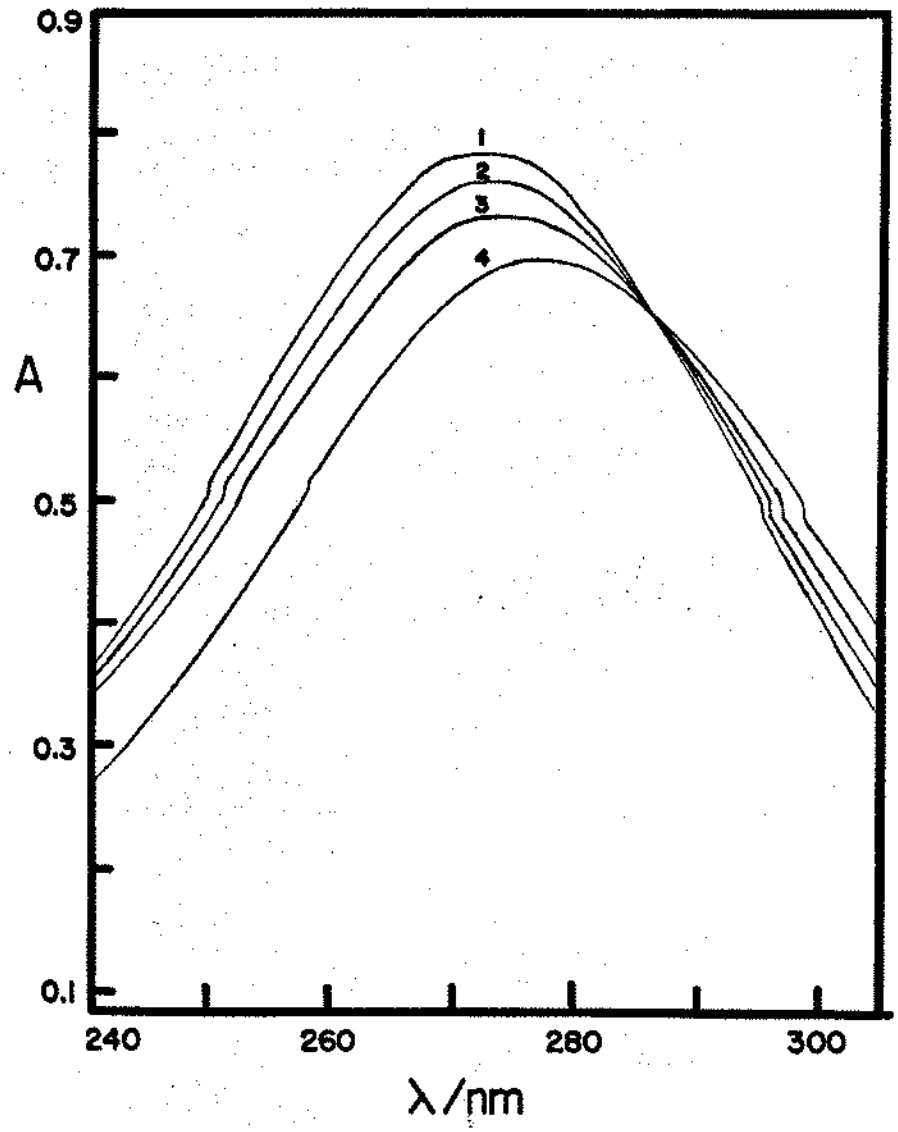
0.9
0.7
0.5
0.3
0.1
A
1
2
3
4
240
260
280
300
λ/nm

cyclodextrin system studied at 265 nm and 315 nm are given in Table XVI. The results of K_{11b} determinations were 85.5 $\underline{M}^{-1}$ (std. dev. 8.1) at 265 nm and 76.5 $\underline{M}^{-1}$ (std. dev. 10.4) at 315 nm.

For Case IV systems, Fig. 11 shows a typical plot of C vs. L_t for 4-cyanobenzoic acid. R is estimated from the extrapolation of the linear portion at high ligand concentration. Fig. 12 is the corresponding linear plot according to Eq. (49) for 4-cyanobenzoic acid.

The stability constants of the ten benzoic acid derivatives are collected in Table XVII. These systems were adequately described by either Case I or Case IV. Therefore, by definition $K_{12b} = 0$ for all these complexes. For compounds 1-7, the potentiometric data were interpreted as Case I systems, $K_{12a} = 0$. However, the assignment to this system was tested by treating it as if it were Case IV. The K_{12a} values in Table XVII were evaluated from the ratio of slope/intercept according to Eq. (49). It is clear that these values are not significantly different from zero. Compounds 8-10 are Case IV systems and possess significant K_{12a} values. The relative standard deviations of K_{11a} range from 0.6% to 1.3% and of K_{11b} from 1.4% to 4.3%. The precision of Case IV systems is poorer, which seems reasonable, for these are 3-parameter systems.

Table XVI. Spectral data for 4-nitrobenzoate anion: α-cyclodextrin system at 25.0 ± 0.1°C.[a]

$10^2 L_t/M$	$-\Delta A^b$	ΔA^c
0.344	0.031	0.019
0.532	0.047	0.026
0.720	0.060	0.029
1.003	0.065	0.040
3.021	0.092	0.074
6.984	0.124	0.076
10.000	0.138	0.068

[a] $S_t = 8.43 \times 10^{-5}$ M; pH = 9.18.

[b] λ = 265 nm; A_0 = 0.738.

[c] λ = 315 nm; A_0 = 0.192.

Figure 11. Plot of C vs. L_t for 4-cyanobenzoic acid:α-cyclodextrin system.

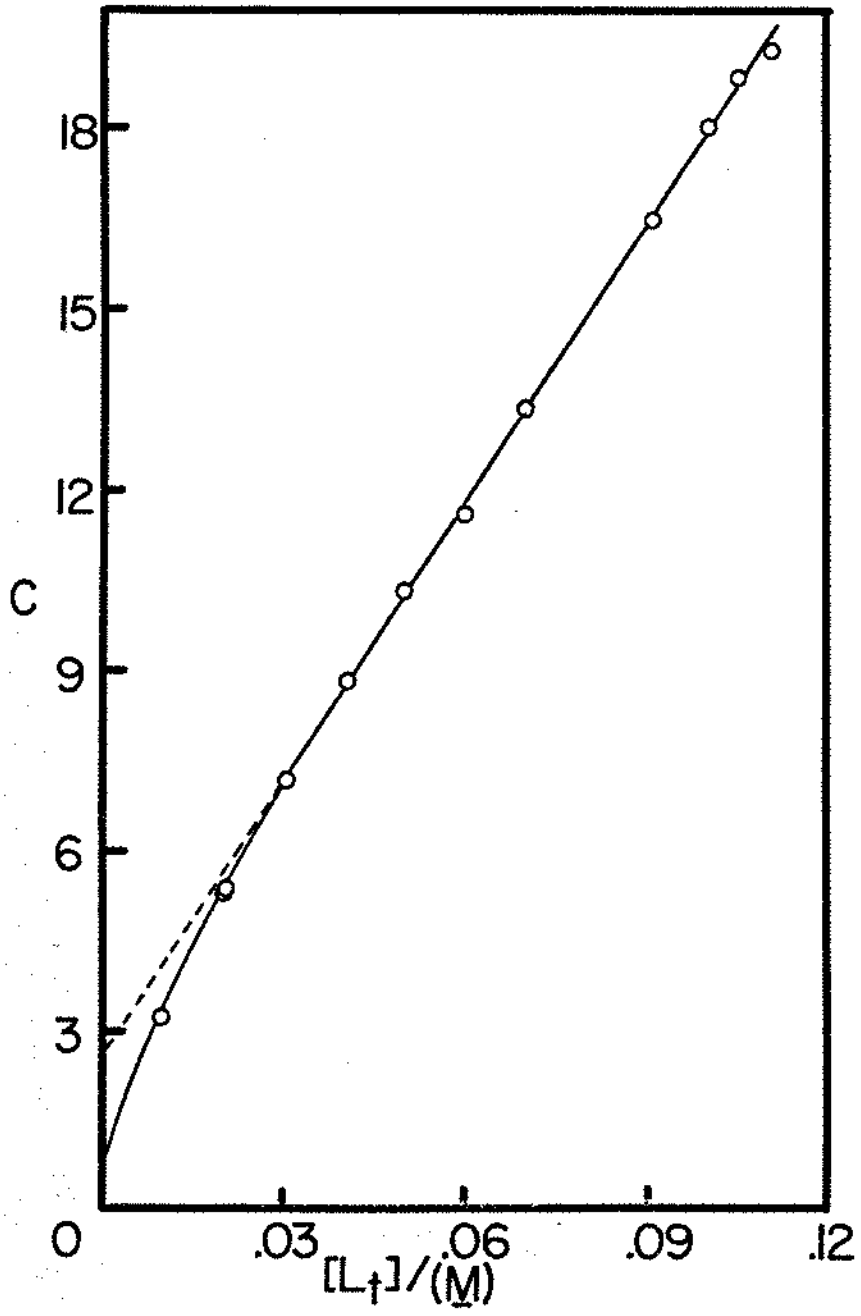
18
15
12
C
9
6
3
0
.03
.06
.09
.12
[L_t]/(M)

Figure 12. Plot of Eq. (49) for the 4-cyanobenzoic acid: α-cyclodextrin system.

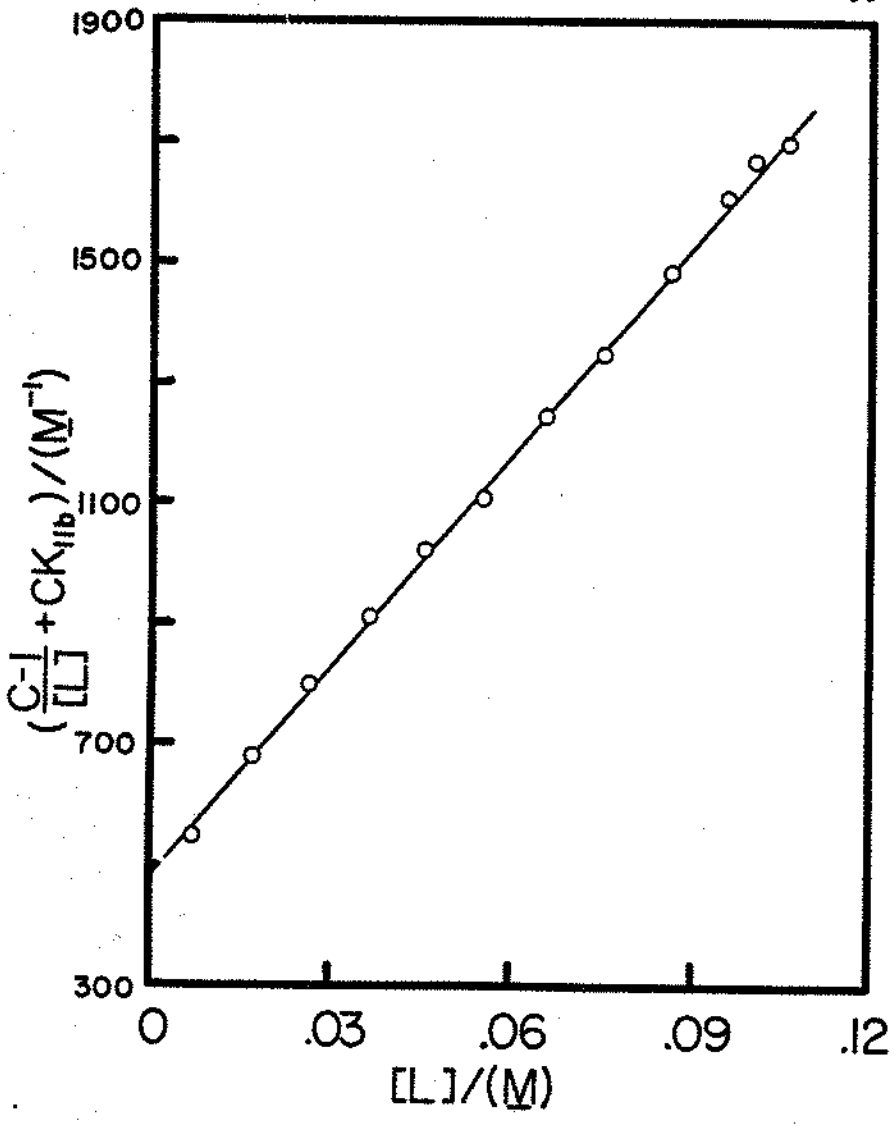
1900
1500
1100
700
300
0
.03
.06
.09
.12
[L]/(M)
$(\frac{C-I}{[L]} + CK_{11b})/(M^{-1})$

Table XVII. Stability constants for α-cyclodextrin complexes of *para*-substituted benzoic acids at 25°.

No.	σ[a]	X[b]	K^c_{11a}/M^{-1}	K^c_{11b}/M^{-1}	K^c_{12a}/M^{-1}
1	-0.84	$NHCH_3$	1301 (15.9)	6.1 (0.26)	-0.010 (0.14)
2	-0.66	NH_2	1341 (11.1)	9.0 (0.22)	-0.024 (0.10)
3	-0.37	OH	1130 (7.7)	16.6 (0.23)	-0.048 (0.063)
4	-0.27	OCH_3	884 (5.1)	3.5 (0.10)	0.0064 (0.067)
5	-0.17	CH_3	1091 (7.4)	6.6 (0.14)	0.0026 (0.071)
6	0.00	H	722 (9.7)	11.2 (0.35)	-0.0047 (0.13)
7	+0.06	F	504 (4.4)	14.2 (0.26)	0.020 (0.081)
8	+0.50	CH_3CO	889 (45.0)	60.3 (11.7)	28.8 (1.63)
9	+0.66	CN	471 (7.5)	79.2 (4.6)	25.0 (0.47)
10	+0.78	NO_2	350 (16.2)	81.0 (9.3)	20.2 (1.14)

[a] Hammett substituent constant.

[b] X in X-C_6H_4-COOH.

[c] Standard deviation in parentheses.

C. Phenols

The potentiometric data and the calculated [L] values for phenol and para-substituted phenols are collected in Tables XVIII to XXVI. 4-Hydroxyquinone is rapidly oxidized in aqueous solution, so the study of this compound was not pursued. All of these systems have negative $\Delta pK_a'$ values, indicating that the base forms of phenols complex more strongly than their conjugate acid forms, according to Eq. (27). (Note that when $\Delta pK_a'$ was negative, C was less than unity, we defined $C' = 1/C$, and the subscripts a and b in all the equations derived were interchanged.)

The potentiometric data of 4-cyanophenol and 4-nitrophenol were interpreted as Case I systems. Fig. 13 shows the C' vs. L_t plot for 4-cyanophenol. Fig. 14 is the corresponding linear plot for Case I system. 4-Methylphenol, phenol and 4-fluorophenol were described as Case II systems. The linear plot of C' vs. L_t for 4-methylphenol, as shown in Fig. 15, is characteristic of Case II. Fig. 16 is the plot of C' vs. [L] for 4-methylphenol to obtain K_{11b}. 4-Methoxyphenol fell in the Case III system. A typical plot of C' vs. L_t for the Case III system is shown in Fig. 17. Fig. 18 is the corresponding linear plot. The C' vs. L_t plots for 4-iodophenol, 4-chlorophenol and 4-bromophenol indicated that they were Case IV systems. Fig. 19 is an example plot of C' vs. L_t for 4-chlorophenol.

Table XVIII. Potentiometric data for 4-methoxyphenol: α-cyclodextrin system at 25.0 ± 0.1°C.[a]

L_t/M	$\Delta pK_a'$[b]	[L]/M
0.0100	-0.013	0.0099
0.0302	-0.046	0.0299
0.0400	-0.065	0.0396
0.0502	-0.091	0.0496
0.0601	-0.111	0.0594
0.0700	-0.133	0.0692
0.0800	-0.161	0.0791
0.0901	-0.177	0.0890
0.1000	-0.214	0.0988
0.1100	-0.234	0.1087
0.1201	-0.265	0.1186

[a] S_t = 0.00403 M.

[b] pK_a' = 10.018.

Table XIX. Potentiometric data for 4-methylphenol: α-cyclodextrin system at 25.0 ± 0.1°C.[a]

L_t/M	$\Delta pK_a'$[b]	[L]/M
0.0100	-0.069	0.0097
0.0203	-0.109	0.0199
0.0301	-0.152	0.0294
0.0401	-0.191	0.0393
0.0501	-0.229	0.0493
0.0600	-0.249	0.0590
0.0701	-0.293	0.0690
0.0799	-0.339	0.0789
0.0900	-0.349	0.0888
0.1001	-0.366	0.0988
0.1101	-0.403	0.1088
0.1200	-0.433	0.1187

[a] S_t = 0.00426 M.

[b] pK_a' = 10.075.

Table XX. Potentiometric data for phenol: α-cyclodextrin system at 25.0 ± 0.1°C.[a]

L_t/M	$\Delta pK_a'$[b]	$[L]/M$
0.0105	-0.047	0.0103
0.0200	-0.084	0.0196
0.0300	-0.122	0.0295
0.0400	-0.150	0.0394
0.0503	-0.187	0.0496
0.0602	-0.214	0.0594
0.0701	-0.243	0.0692
0.0799	-0.273	0.0790
0.0900	-0.293	0.0890
0.1000	-0.324	0.0989
0.1101	-0.343	0.1090
0.1200	-0.378	0.1189
0.1299	-0.398	0.1288

[a] S_t = 0.00402 M.

[b] pK_a' = 9.826.

Table XXI. Potentiometric data for 4-fluorophenol: α-cyclodextrin system at 25.0 ± 0.1°C.[a]

L_t/M	$\Delta pK_a'$[b]	[L]/M
0.0090	-0.062	0.0088
0.0212	-0.142	0.0207
0.0318	-0.192	0.0311
0.0423	-0.186	0.0415
0.0497	-0.233	0.0488
0.0597	-0.257	0.0587
0.0695	-0.296	0.0684
0.0806	-0.318	0.0794
0.0877	-0.379	0.0865
0.1019	-0.415	0.1007
0.1090	-0.431	0.1078
0.1226	-0.465	0.1213

[a] S_t = 0.00407 M.

[b] pK_a' = 9.729.

Table XXII. Potentiometric data for 4-iodophenol: α-cyclodextrin system at 25.0 ± 0.1°C.[a]

L_t/M	$\Delta pK_a'$[b]	[L]/M
0.0201	-0.243	0.0161
0.0304	-0.258	0.0263
0.0400	-0.263	0.0358
0.0500	-0.276	0.0458
0.0599	-0.290	0.0556
0.0701	-0.291	0.0658
0.0796	-0.301	0.0753
0.0906	-0.308	0.0862
0.0923	-0.320	0.0879
0.1120	-0.327	0.1076
0.1186	-0.339	0.1141
0.1304	-0.346	0.1259

[a] S_t = 0.00406 M.

[b] pK_a' = 9.111.

Table XXIII. Potentiometric data for 4-chlorophenol: α-cyclodextrin system at 25.0 ± 0.1°C.[a]

L_t/M	$\Delta pK_a'$[b]	$[L]/M$
0.0100	-0.190	0.0071
0.0149	-0.218	0.0116
0.0201	-0.240	0.0166
0.0300	-0.261	0.0262
0.0401	-0.277	0.0362
0.0500	-0.296	0.0460
0.0600	-0.307	0.0559
0.0700	-0.319	0.0658
0.0799	-0.335	0.0757
0.0900	-0.344	0.0857
0.1000	-0.359	0.0956

[a] S_t = 0.00402 M.

[b] pK_a' = 9.263.

Table XXIV. Potentiometric data for 4-bromophenol: α-cyclodextrin system at 25.0 ± 0.1°C.[a]

L_t/M	$\Delta pK_a'$[b]	[L]/M
0.0104	-0.223	0.0068
0.0205	-0.256	0.0166
0.0303	-0.278	0.0262
0.0401	-0.298	0.0359
0.0506	-0.315	0.0463
0.0612	-0.329	0.0568
0.0715	-0.357	0.0670
0.0798	-0.361	0.0753
0.0903	-0.381	0.0858
0.1001	-0.396	0.0955
0.1103	-0.410	0.1056
0.1192	-0.424	0.1145

[a] S_t = 0.00404 M.

[b] pK_a' = 9.222.

Table XXV. Potentiometric data for 4-cyanophenol: α-cyclodextrin system at 25.0 ± 0.1°C.

L_t/M	$\Delta pK_a'$[b]	[L]/M
0.0075	-0.383	0.0051
0.0101	-0.431	0.0073
0.0152	-0.493	0.0120
0.0200	-0.517	0.0167
0.0249	-0.541	0.0214
0.0300	-0.554	0.0265
0.0399	-0.568	0.0363
0.0501	-0.578	0.0464
0.0600	-0.586	0.0562

[a] S_t = 0.00401 M.

[b] pK_a' = 7.814.

Table XXVI. Potentiometric data for 4-nitrophenol: α-cyclodextrin system at 25.0 ± 0.1°C.[a]

L_t/M	$\Delta pK_a'$[b]	[L]/M
0.0120	-0.844	0.0087
0.0150	-0.876	0.0116
0.0251	-0.929	0.0214
0.0301	-0.941	0.0264
0.0400	-0.951	0.0363
0.0500	-0.962	0.0462
0.0600	-0.960	0.0562
0.0700	-0.964	0.0662

[a] S_t = 0.00399 M.

[b] pK_a' = 7.004.

Figure 13. Plot of C' vs. L_t for the 4-cyanophenol:α-cyclodextrin system.

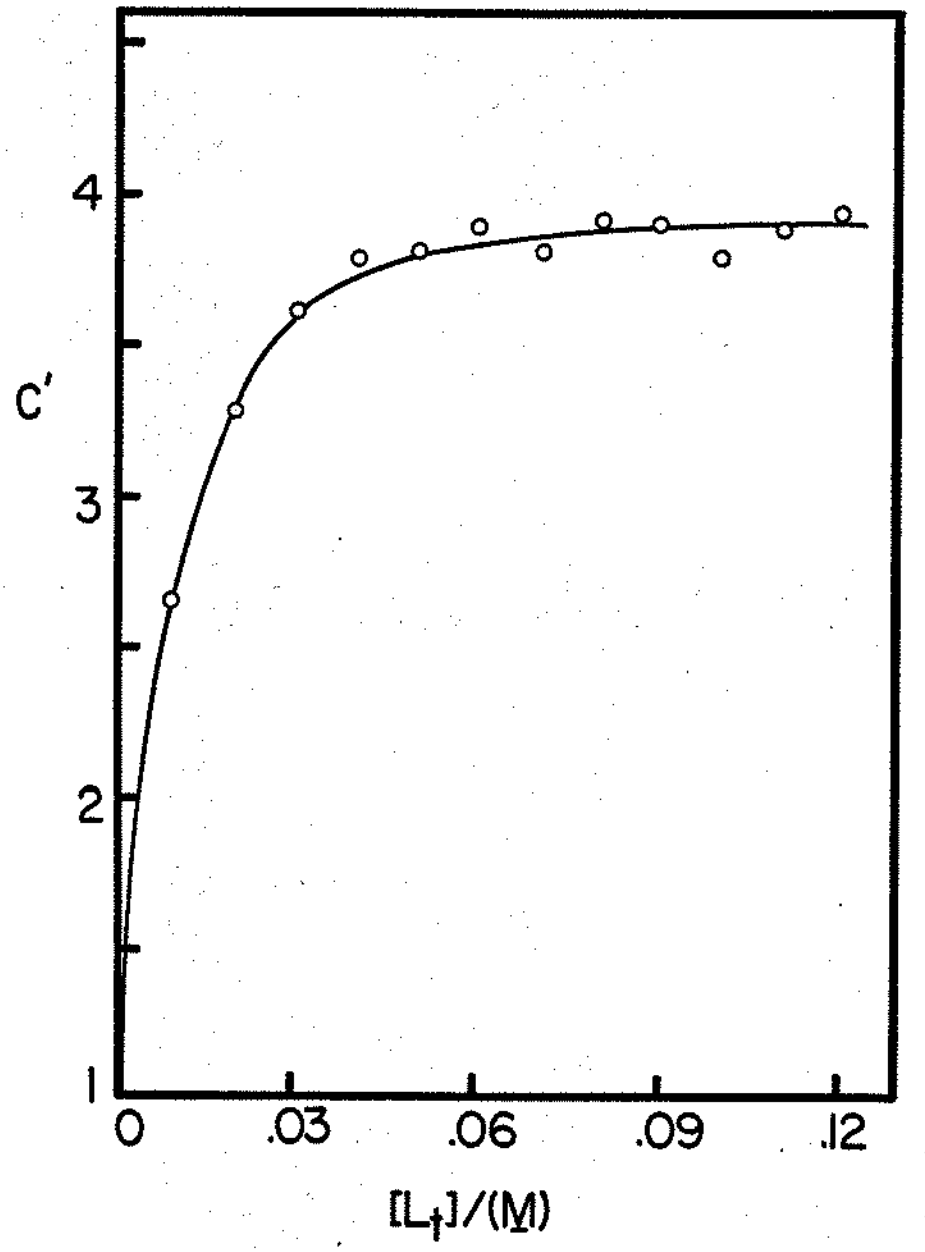
C'
4
3
2
1
0
.03
.06
.09
.12
[L_t]/(M)

Figure 14. Plot of Eq. (37), with subscripts a and b interchanged, for the 4-cyanophenol:α-cyclodextrin system.

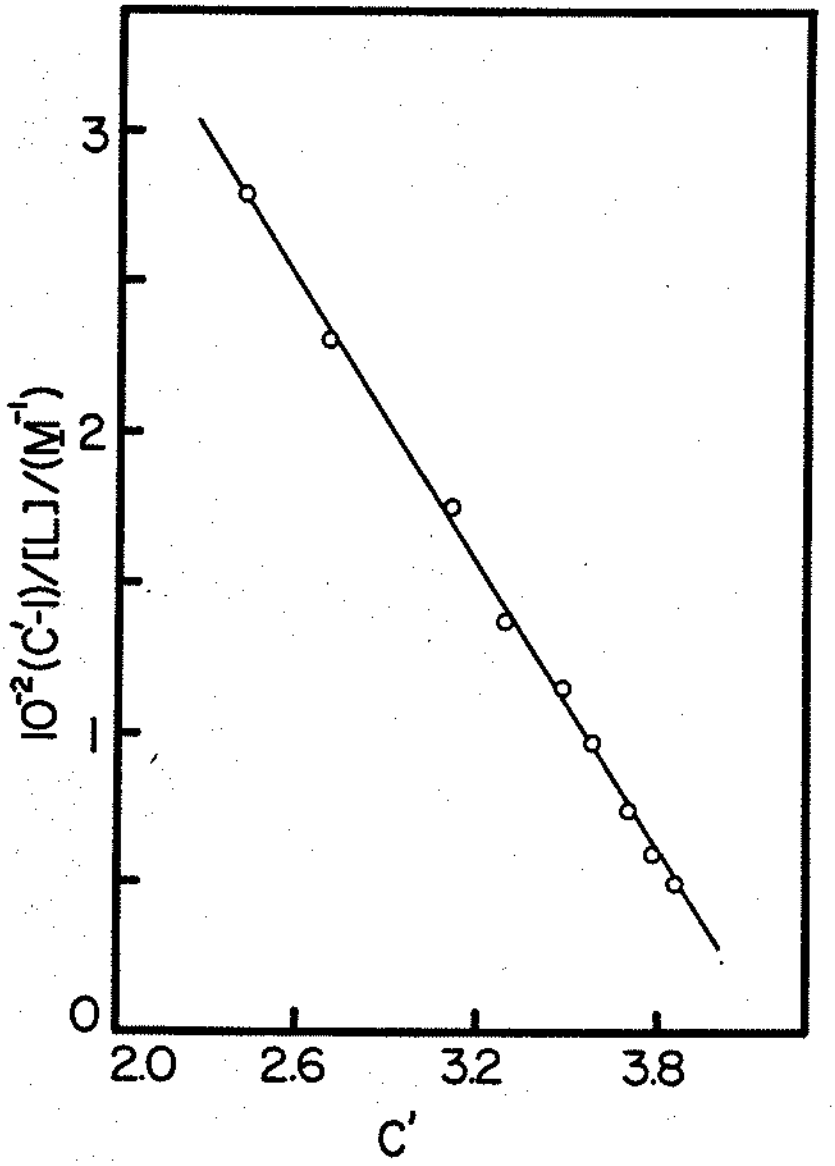
$10^{-2}(C'-1)/[L]/(M^{-1})$
3
2
1
0
2.0
2.6
3.2
3.8
C'

Figure 15. Plot of C' vs. L_t for the 4-methylphenol:α-cyclodextrin system.

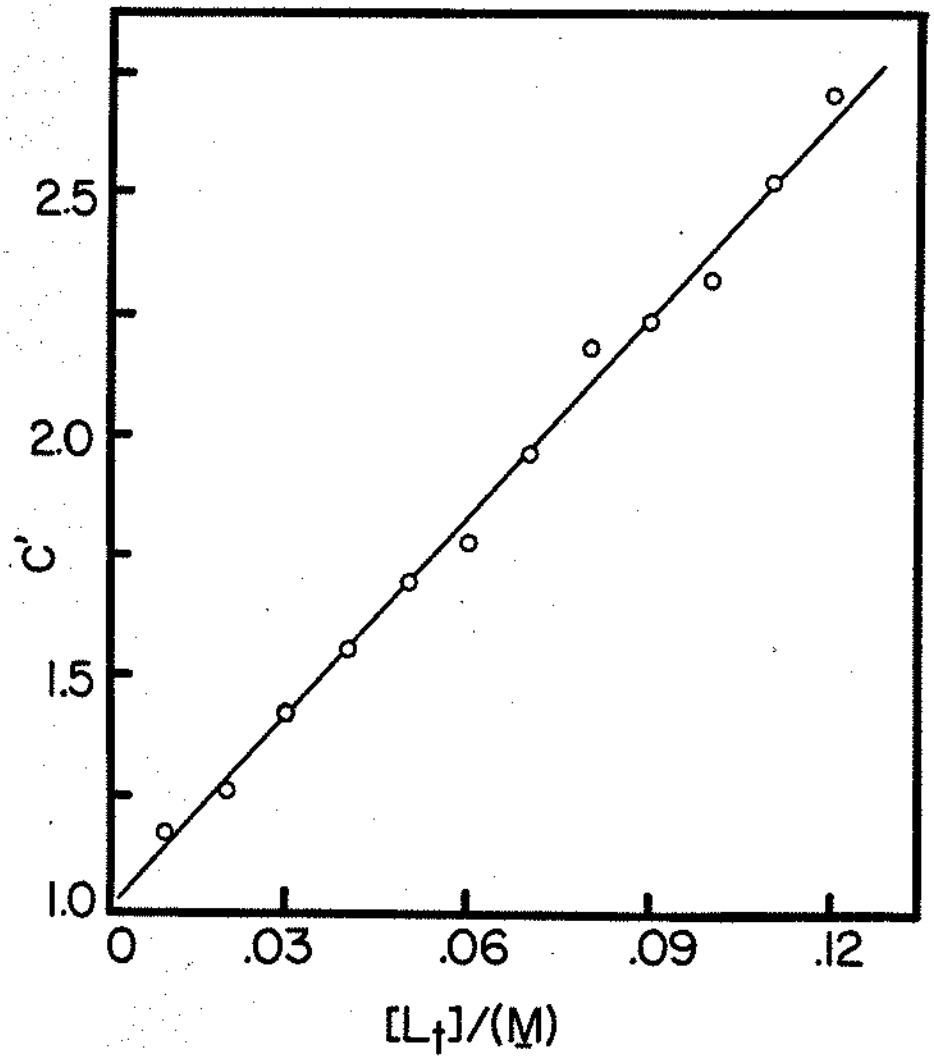
2.5
2.0
1.5
1.0
ν̄
0
.03
.06
.09
.12
[L_f]/(M)

Figure 16. Plot of C' vs. [L] for the 4-methylphenol:α-cyclodextrin system.

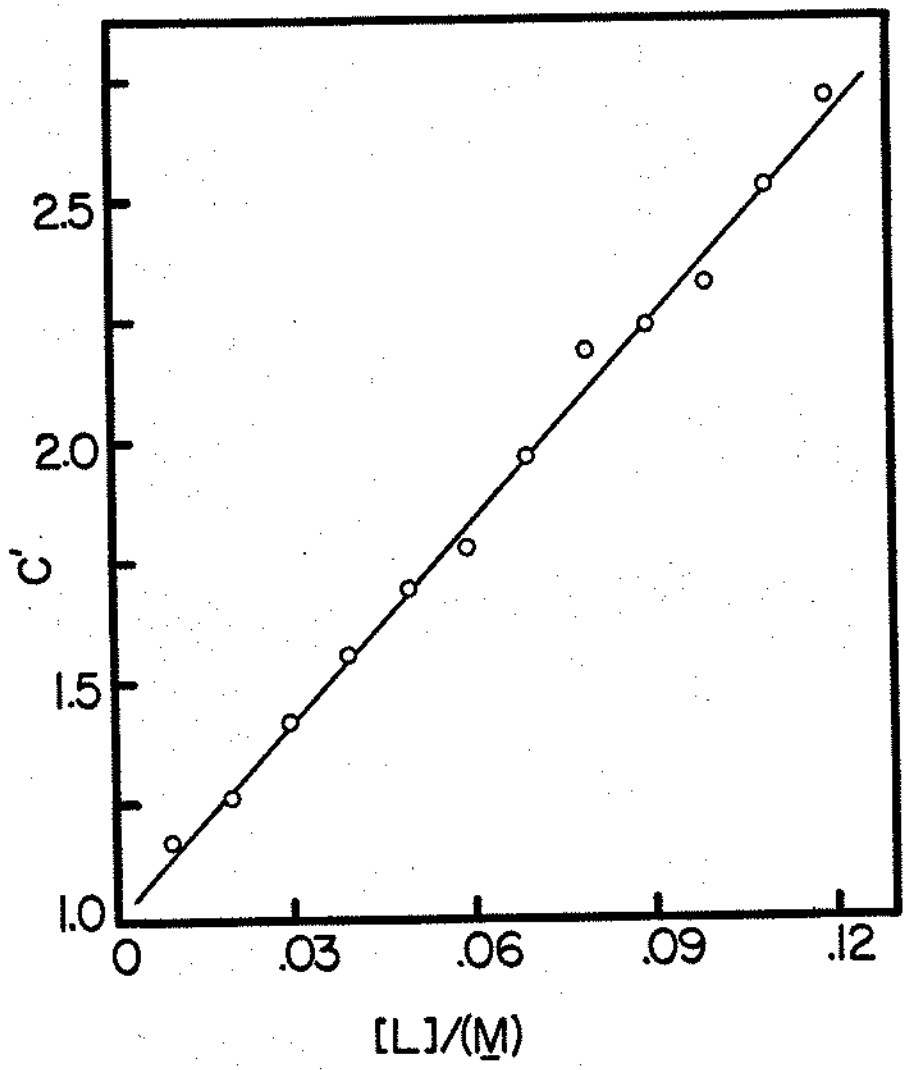
2.5
2.0
1.5
1.0
C'
0
.03
.06
.09
.12
[L]/(M)

Figure 17. Plot of C' vs. L_t for the 4-methoxyphenol:α-cyclodextrin system.

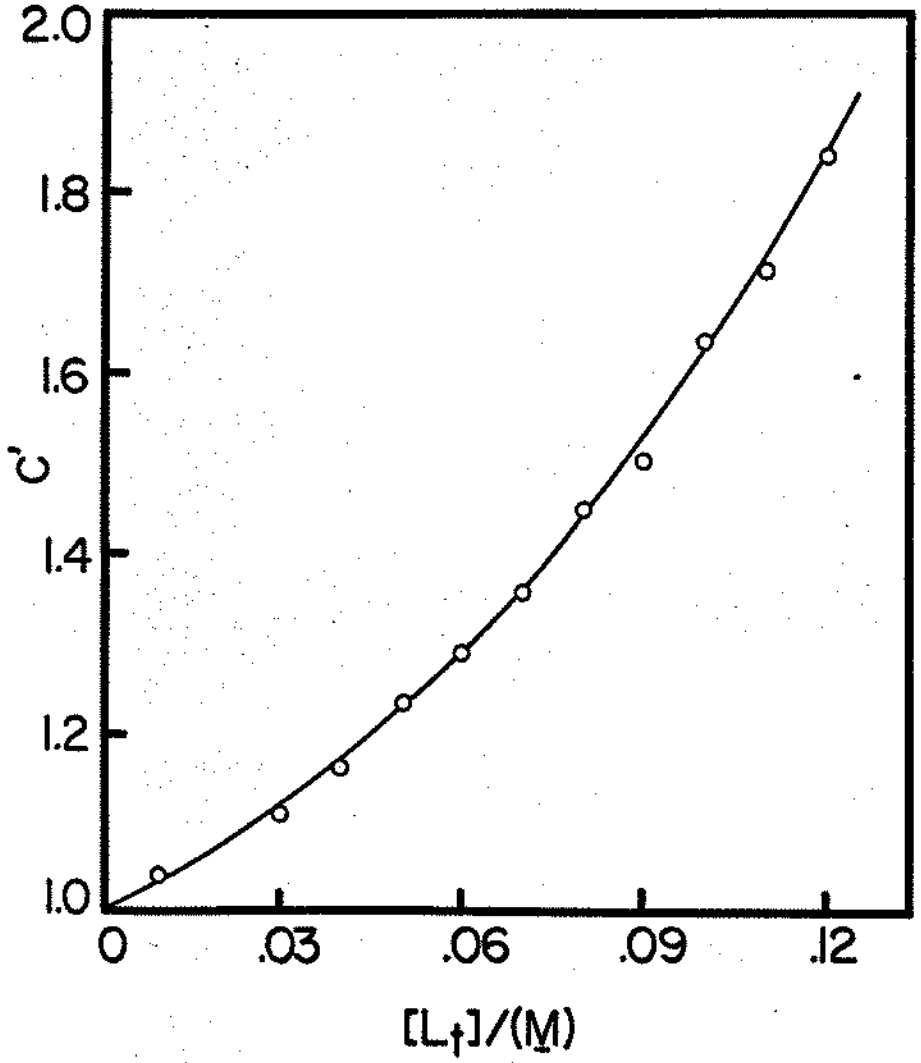
2.0
1.8
1.6
1.4
1.2
1.0
$\bar{\nu}$
0
.03
.06
.09
.12
$[L_f]/(M)$

Figure 18. Plot of Eq. (42), with subscripts a and b interchanged, for 4-methoxyphenol:α-cyclodextrin system.

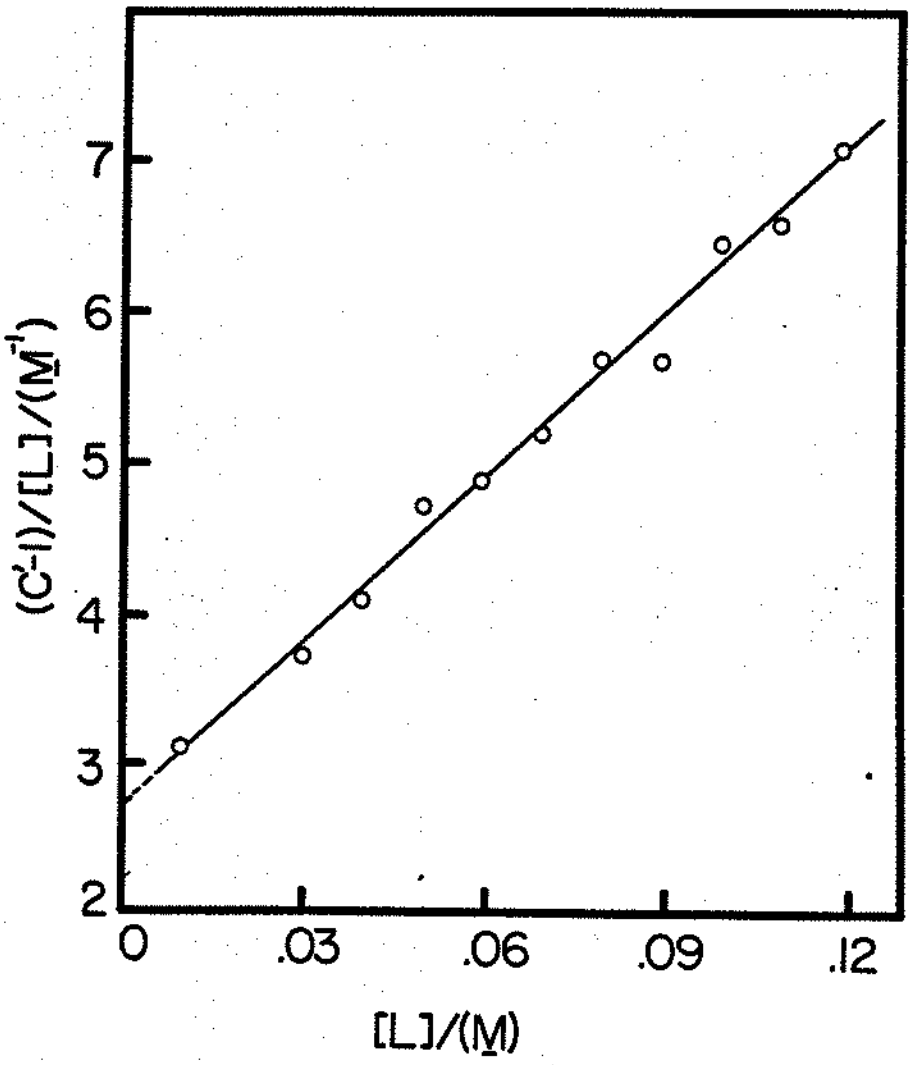
(C'-1)/[L]/(M⁻¹)
7
6
5
4
3
2
0
.03
.06
.09
.12
[L]/(M)

Figure 19. Plot of C' vs. L_t for 4-chlorophenol:α-cyclodextrin system.

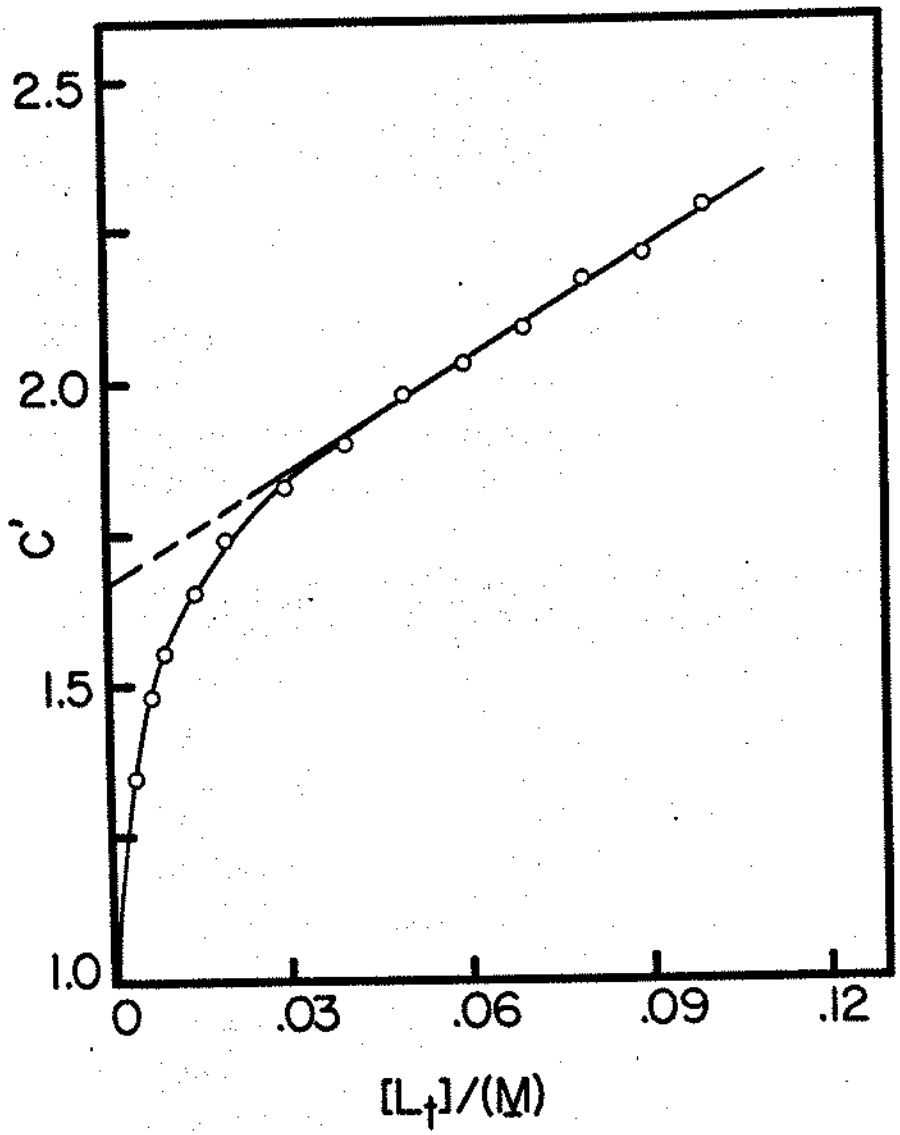
2.5
2.0
1.5
1.0
$\bar{c}$
0
.03
.06
.09
.12
$[L_t]/(M)$

For Case IV systems, an independent study to determine K_{11a} was carried out as suggested previously. The UV spectra of these three substrates were not significantly altered by the presence of α-cyclodextrin. The MO competitive spectrophotometry was used as the independent experimental approach. According to Eq. (69), the absorbance change of MO can be followed either at constant S_t with varying L_t or at constant L_t with varying S_t. For experimental convenience, the studies were carried out at constant L_t with varying S_t. Table XXVII gives the spectral data of 4-iodophenol:methyl orange:α-cyclodextrin system at 508 nm. R was calculated according to Eq. (74) and P from Eq. (67) as defined, where $A_{IL} = 0.015$, $A_I = 0.807$, $I_t = 1.67 \times 10^{-5}$ M and K_{11I} was 672.9 M^{-1}. L_t was kept constant at 2.0×10^{-3} M. Fig. 20 is the linear plot according to Eq. (69) for 4-chlorophenol. The spectral data for 4-chlorophenol and 4-bromophenol are collected in Tables XXVIII and XXIX, respectively. Fig. 21 is the linear plot for 4-chlorophenol to determine K_{11b} and K_{12b} after K_{11a} was measured.

4-Nitrophenol, a simple Case I system, was also studied by this competitive spectrophotometric method, so that the K_{11a} determined could be compared with those from other techniques. The spectral data are shown in Table XXX, and the corresponding linear plot is in Fig. 22.

Table XXVII. Spectral data for 4-iodophenol:methyl orange:α-cyclodextrin system at 25.0 ± 0.1°C.[a]

10^3 S_t/M	A[b]	R	S_t/P
3.50	0.647	3.95	2.16
3.00	0.619	3.22	1.95
2.50	0.584	2.55	1.77
2.00	0.544	2.01	1.59

[a] $L_t = 2.0 \times 10^{-3}$ M; $I_t = 1.67 \times 10^{-5}$ M.

[b] λ = 508 nm.

Table XXVIII. Spectral data for 4-chlorophenol:methyl orange:α-cyclodextrin system at 25.0 ± 0.1°C.[a]

10^3 S_t/M	A[b]	R	S_t/P
2.00	0.419	1.04	3.55
2.00	0.419	1.04	3.55
4.00	0.472	1.36	4.43
5.00	0.494	1.53	4.90
6.00	0.516	1.72	5.30
8.00	0.546	2.04	6.32
8.00	0.550	2.08	6.25
11.01	0.595	2.72	7.59

[a] $L_t = 2.00 \times 10^{-3}$ M; $I_t = 1.67 \times 10^{-5}$ M.

[b] λ = 508 nm.

Table XXIX. Spectral data for 4-bromophenol:methyl orange:α-cyclodextrin system at 25.0 ± 0.1°C.[a]

10^3 S_t/M	A[b]	R	S_t/P
2.01	0.469	1.33	2.28
3.01	0.520	1.76	2.62
4.01	0.558	2.18	3.05
5.01	0.590	2.62	3.50

[a] $L_t = 2.00 \times 10^{-3}$ M; $I_t = 1.67 \times 10^{-5}$ M.

[b] λ = 508 nm.

Figure 20. Plot of Eq. (69) for 4-chlorophenol:methyl orange:α-cyclodextrin system.

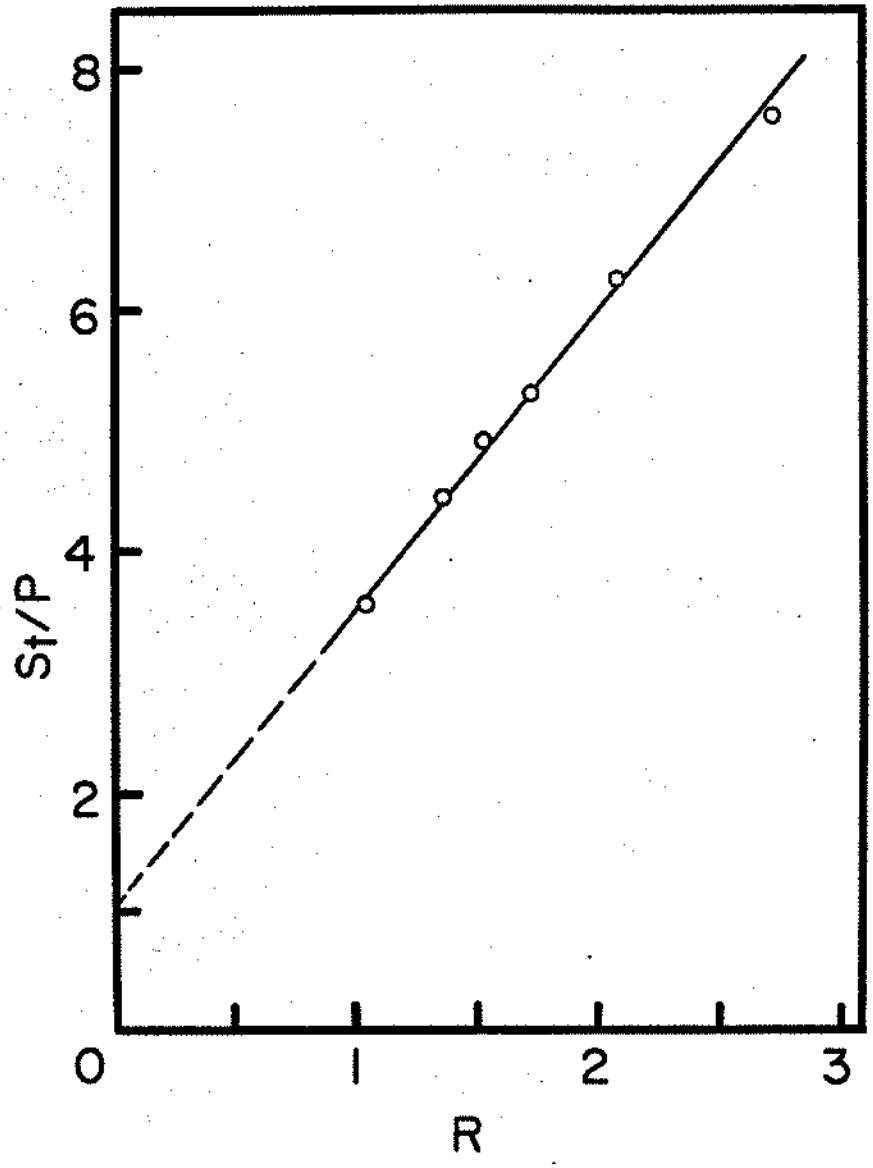
8
6
4
2
0
1
2
3
S_t/P
R

Figure 21. Plot of Eq. (49), with subscripts a and b interchanged, for 4-chlorophenol:α-cyclodextrin system.

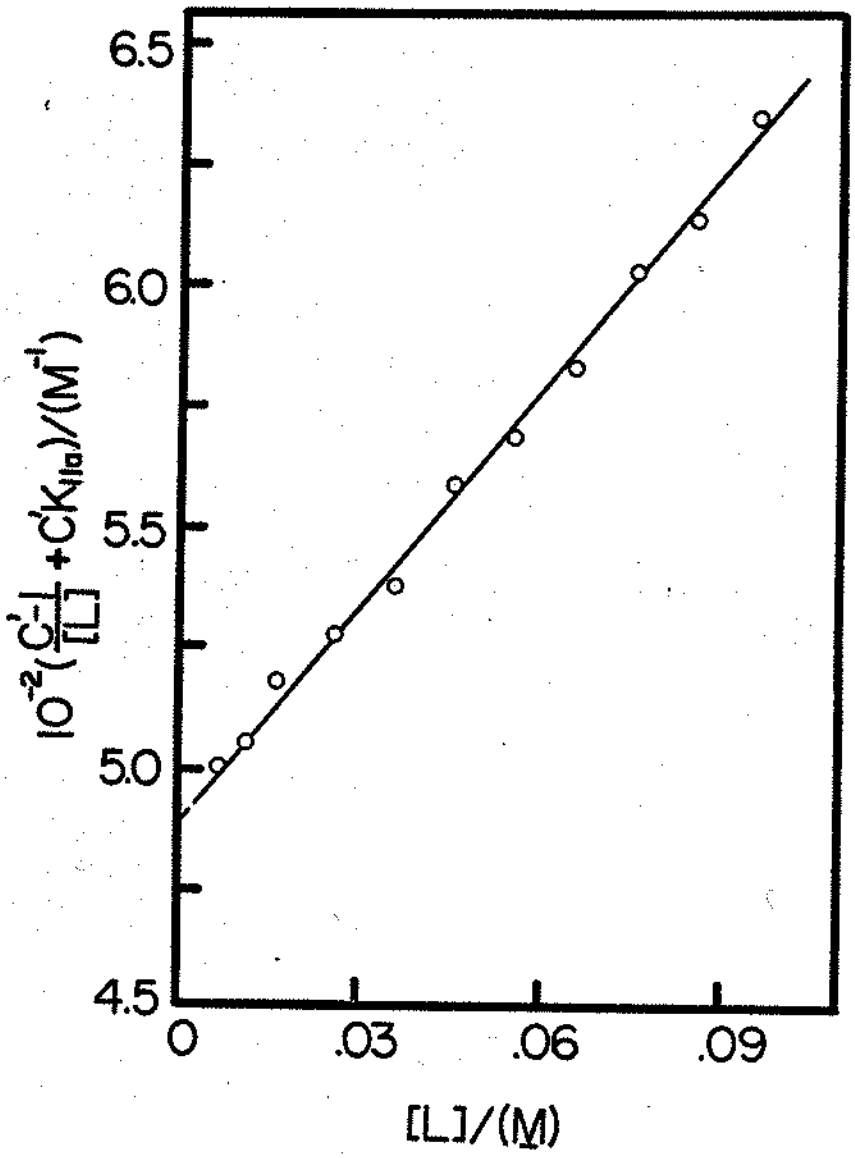
6.5
6.0
5.5
5.0
4.5
0
.03
.06
.09
$10^{-2}(\frac{C'_{-1}}{[L]} + C'K_{11a})/(M^{-1})$
[L]/(M)

Table XXX. Spectral data of p-nitrophenol:methyl orange:α-cyclodextrin system at 25.0 ± 0.1°C.[a]

10^3 S_t	A[b]	R	S_t/P
1.98	0.414	1.01	3.74
4.94	0.485	1.46	5.05
7.91	0.539	1.96	6.39
10.87	0.581	2.51	7.74
13.83	0.609	3.00	9.20

[a] $L_t = 2.00 \times 10^{-3}$ M.

[b] $I_t = 1.67 \times 10^{-5}$ M. λ = 508 nm.

Figure 22. Plot of Eq. (69) for 4-nitrophenol:methyl orange:α-cyclodextrin system.

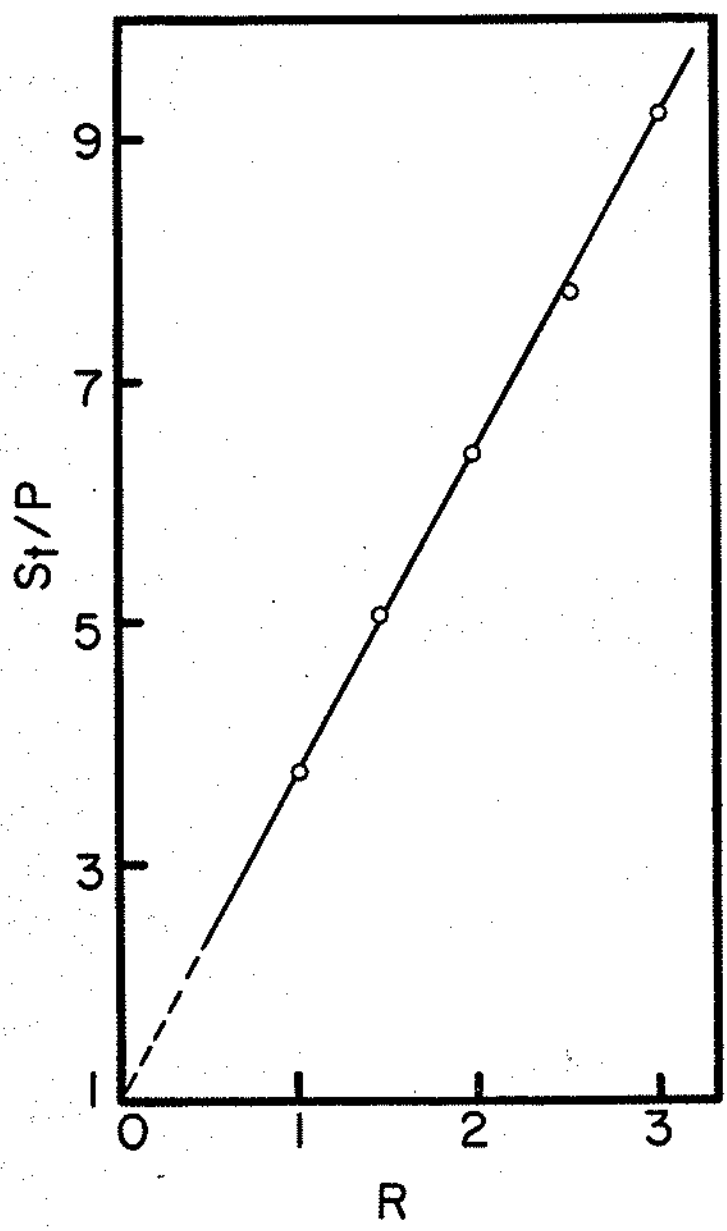
9
7
5
3
1
St/P
0
1
2
3
R

The compound could also be studied by direct UV-spectrophotometric method using the Benesi-Hildebrand double reciprocal plot. The spectral data are shown in Table XXXI, where [L] was calculated according to Eq. (B-13) in Appendix B.

The stability constants for the nine phenolic derivatives are summarized in Table XXXII. For all these systems, $K_{12a} = 0$ since they could be described by the four cases adequately.

Again, the assignment to Case I systems of compounds 18 and 19 was tested by treating them as if they were Case IV systems. K_{12b} values in Table XXXII were calculated according to Eq. (49). The assignment to Case II of compounds 12, 13 and 14 was tested by treating them as if they were Case III systems. K_{12b} values were obtained from Eq. (42). Student's t-test at 95% confidence level was carried out to test the significance of K_{12b} values. It is clear that K_{12b} values for Case IV systems (compounds 15-17) and for Case III system (compound 11) are finite. The K_{12b}'s for Case I and II systems are not significantly different from zero except for compound 13 (phenol). However, the correlation coefficient (R^2) of linear least squares regression for phenol data was 99.7% for the Case II assignment, but 30.6% for Case III assignment. This indicates that the potentiometric data for phenol are more

Table XXXI. Spectral data of p-nitrophenol: α-cyclodextrin system at 25.0 ± 0.1°C.[a]

10^3 L_t/M	$-\Delta A$[b]	10^3 [L]/M
0.443	0.027	0.425
0.707	0.042	0.680
1.039	0.053	1.001
1.768	0.080	1.712
3.409	0.122	3.326
5.482	0.157	5.378
11.16	0.204	11.03
20.22	0.235	20.07

[a] $S_t = 1.749 \times 10^{-4}$ M.

[b] $\lambda = 317$ nm; $A_o = 1.731$.

Table XXXII. Stability constants for α-cyclodextrin complexes of *para*-substituted phenols at 25.0 ± 0.1°C.

No.	X[a]	K^{b}_{11b}/M^{-1}	K^{b}_{12b}/M^{-1}	K^{b}_{11a}/M^{-1}
11	OCH_3	2.7 (0.10)	13.3 (0.68)	0
12	CH_3	13.9 (0.34)	-0.083(0.36)	0
13	H	10.9 (0.19)	0.46 (0.21)	0
3	COO^-[c]	-	-	16.6 (0.23)
14	F	15.6 (0.70)	-1.00 (0.95)	0
15	I	3955.0 (26.3)	2.4 (0.09)	2315.8 (65.5)
16	Cl	487.9 (1.6)	3.1 (0.06)	271.7 (9.9)
17	Br	1221.1 (7.4)	4.7 (0.09)	703.7 (31.8)
3	COOH[c]	-	-	1130.3 (7.7)
18	CN	661.5 (9.0)	0.093 (0.083)	158.3 (2.7)
19	NO_2	2408.0 (87.6)	-0.14 (0.16)	245.3 (10.2)
				249.0[d] (4.8)
				249.2[e] (9.0)

[a] X in X-C_6H_4-OH.

[b] Standard deviation in parentheses.

[c] Data from Table XVII.

[d] Obtained from MO competitive spectrophotometry.

[e] UV-spectrophotometric method.

appropriately interpreted as a Case II system.

According to Eq. (38) for Case II system and Eq. (69), in the methyl orange competitive spectrophotometric method, the linear plots to determine stability constants should result in an intercept of 1. Table XXXIII lists the intercepts obtained from least squares linear regression following Eqs. (38) and (69) for compounds 12, 13 and 14, and for compounds 15, 16 and 17. Student's t-values, as shown in Table XXXIII, indicate that the intercepts are not significantly different from unity at 95% confidence level.

The relative standard deviations in K_{11b} determination ranged from 0.3% to 4.5% and K_{11a} from 0.7% to 4.2%.

D. Anilines

Aniline and four para-substituted aniline derivatives were studied potentiometrically. The conjugate acid of p-phenylenediamine has $pK_{a1} = 6.16$ and $pK_{a2} = 2.89$ (140), so that the measurement of the first pK_a' for one amine group leaves the other amino group in its base form. The potentiometric data and calculated [L] are shown in Tables XXXIV to XXXVIII. It was found that all the $\Delta pK_a'$ values were negative and relatively small.

4-Chloroaniline was described by the Case I system. Fig. 23 shows the plot of C' vs. L_t, and Fig. 24 is the corresponding linear plot for this compound at 25°.

Table XXXIII. Student's t-test for the significance of intercept = 1 in least squares regression of some phenols.

X[a]	Intercept[b]	t[c]	$t_{(n-2,\ 0.025)}$[d]
CH_3	1.009 (0.024)	0.375	2.228
H	0.972 (0.015)	1.898	2.201
F	0.981 (0.051)	0.369	2.228
I	1.014 (0.024)	0.583	4.303
Cl	1.050 (0.157)	0.318	2.447
Br	0.979 (0.086)	0.249	4.303

[a] X in $X\text{-}C_6H_4\text{-}OH$.

[b] First three intercepts obtained from Eq. (38). Last three intercepts obtained from Eq. (69). Standard deviation in parentheses.

[c] $t = \dfrac{\text{intercept} - 1}{\text{standard deviation of intercept}}$

[d] Student's t-values at n-2 degrees of freedom, 95% confidence interval.

Table XXXIV. Potentiometric data for p-phenylenediamine: α-cyclodextrin System at 25.0 ± 0.1°C.[a]

L_t/M	$\Delta pK_a'$[b]	[L]/M
0.0301	-0.025	0.0299
0.0400	-0.027	0.0398
0.0500	-0.041	0.0498
0.0600	-0.042	0.0598
0.0701	-0.058	0.0698
0.0802	-0.069	0.0799
0.0901	-0.073	0.0897
0.1001	-0.078	0.0997
0.1100	-0.092	0.1096
0.1201	-0.098	0.1197

[a] S_t = 0.00401 M.

[b] pK_a' = 6.236.

Table XXXV. Potentiometric data for 4-anisidine: α-cyclodextrin system at 25.0 ± 0.1°C.[a]

L_t/M	$\Delta pK_a'$[b]	[L]/M
0.0101	-0.029	0.0100
0.0201	-0.057	0.0198
0.0300	-0.085	0.0297
0.0402	-0.104	0.0398
0.0501	-0.132	0.0496
0.0602	-0.150	0.0596
0.0700	-0.165	0.0694
0.0800	-0.181	0.0793
0.0900	-0.214	0.0893
0.1000	-0.224	0.0992
0.1100	-0.240	0.1091

[a] S_t = 0.00405 M.

[b] pK_a' = 5.368.

Table XXXVI. Potentiometric data for 4-toluidine: α-cyclodextrin system at 25.0 ± 0.1°C.[a]

L_t/M	$\Delta pK_a'$[b]	[L]/M
0.0100	-0.059	0.0088
0.0201	-0.103	0.0181
0.0300	-0.135	0.0276
0.0401	-0.166	0.0373
0.0502	-0.184	0.0472
0.0601	-0.208	0.0568
0.0701	-0.225	0.0667
0.0800	-0.245	0.0764
0.0901	-0.262	0.0863
0.1000	-0.279	0.0962
0.1100	-0.293	0.1060
0.1200	-0.300	0.1160

[a] S_t = 0.00403 M.

[b] pK_a' = 5.116.

Table XXXVII. Potentiometric data for aniline: α-cyclodextrin system at 25.0 ± 0.1°C.[a]

L_t/M	$\Delta pK_a'$[b]	[L]/M
0.0100	-0.041	0.0098
0.0200	-0.079	0.0197
0.0301	-0.108	0.0297
0.0401	-0.126	0.0396
0.0501	-0.168	0.0495
0.0600	-0.192	0.0593
0.0701	-0.215	0.0693
0.0799	-0.235	0.0791
0.0900	-0.258	0.0891
0.1002	-0.276	0.0992
0.1101	-0.294	0.1091
0.1201	-0.316	0.1191
0.1301	-0.335	0.1291

[a] S_t = 0.00405 M.

[b] pK_a' = 4.646.

Table XXXVIII. Potentiometric data for 4-chloroaniline: α-cyclodextrin system at 25.0 ± 0.1°C.[a]

L_t/M	$\Delta pK_a'$[b]	[L]/M
0.0104	-0.299	0.0083
0.0201	-0.387	0.0174
0.0300	-0.432	0.0270
0.0401	-0.458	0.0368
0.0501	-0.475	0.0467
0.0600	-0.494	0.0565
0.0704	-0.496	0.0669
0.0800	-0.496	0.0765
0.0902	-0.515	0.0866
0.1002	-0.518	0.0966
0.1100	-0.536	0.1062
0.1201	-0.536	0.1163

[a] S_t = 0.00403 M.

[b] pK_a' = 4.042.

Figure 23. Plot of C' vs. L_t for the 4-chloroaniline:α-cyclodextrin system.

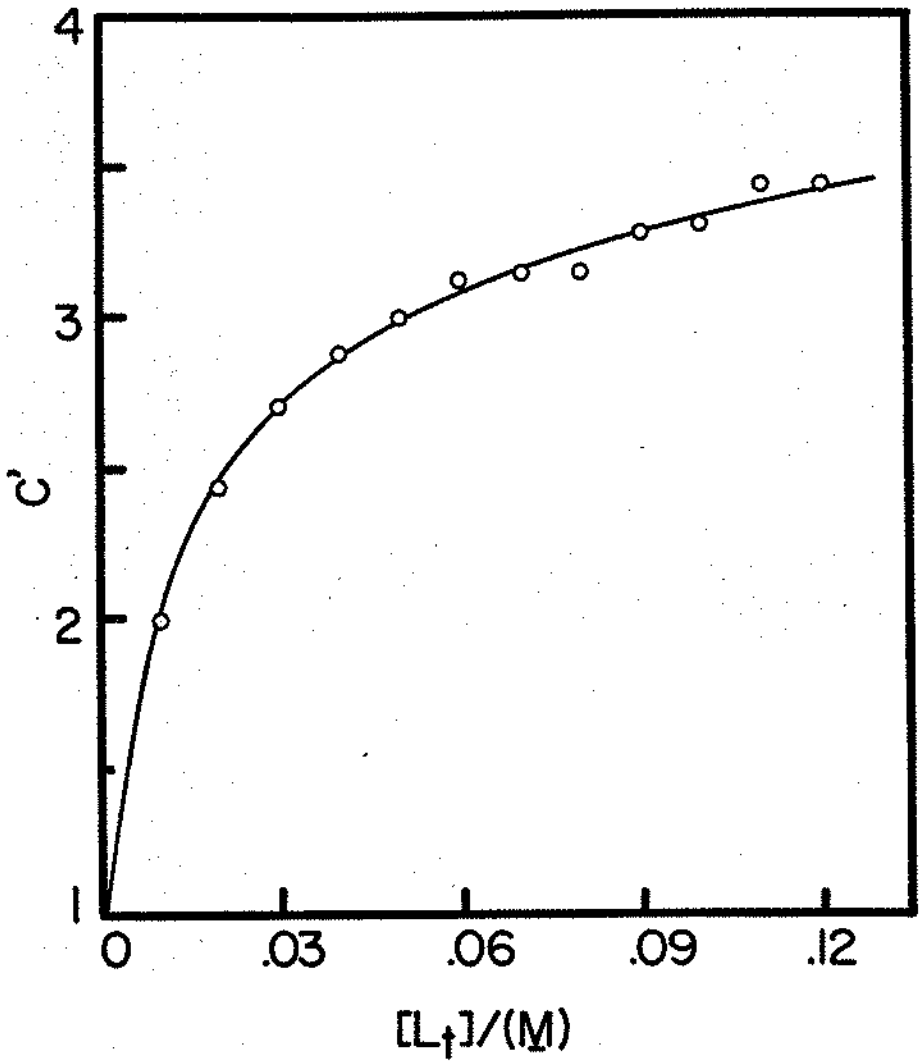
4
3
2
1
$\bar{C}$
0
.03
.06
.09
.12
$[L_f]/(M)$

Figure 24. Plot of Eq. (37), with subscripts a and b interchanged, for 4-chloroaniline:α-cyclodextrin system.

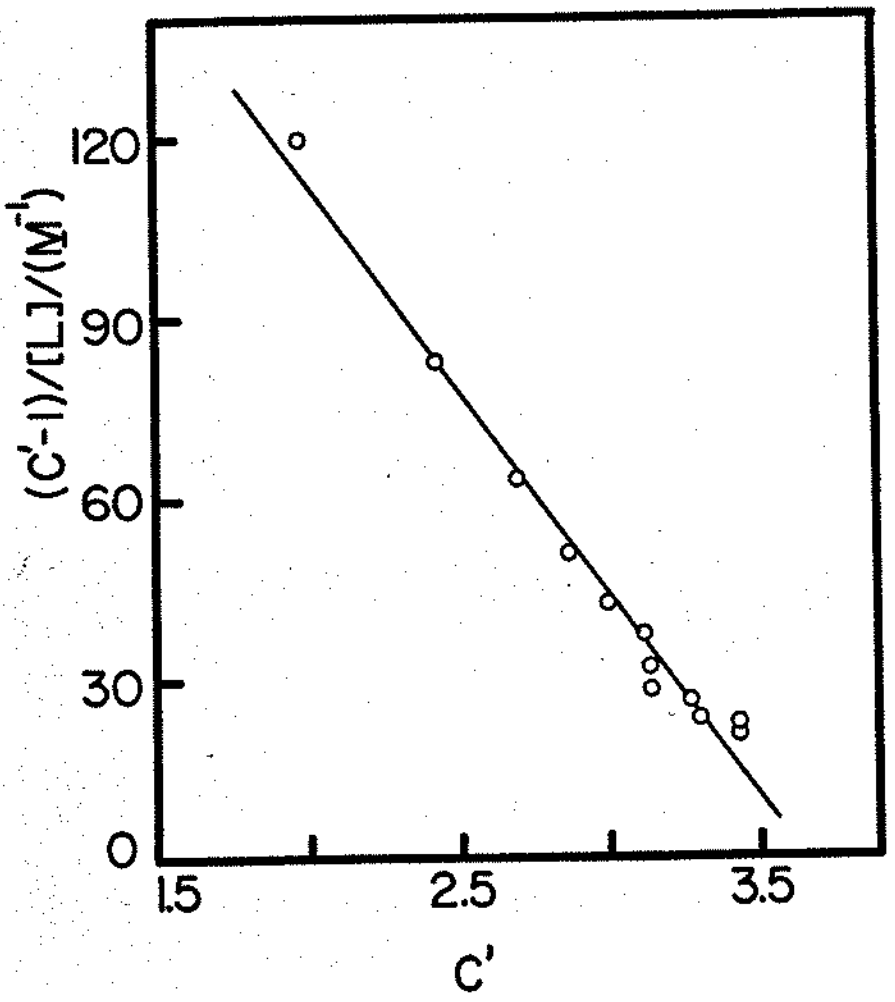
120
90
60
30
0
(C'-1)/[L]/(M⁻¹)
1.5
2.5
3.5
C'
8

Aniline, 4-anisidine and the symmetric compound, para-phenylenediamine, followed Case II systems. Fig. 25 is an example plot of C' vs. L_t for aniline in Case II system. The linear plot of C' vs. [L] is shown in Fig. 26. The potentiometric data of 4-toluidine was interpreted as Case IV. Fig. 27 is the diagnostic plot of C vs. L_t for this system. K_{11a} was determined by the MO competitive spectrophotometric method, since the ultraviolet spectrum of the substrate was not significantly altered by the presence of cyclodextrin in solution. The weak complex required higher concentration of substrate to displace methyl orange from cyclodextrin binding site. Alternatively, the concentration of cyclodextrin was reduced, while the substrate concentration was relatively high enough to compete with MO for binding sites. The spectral data for this 4-toluidine: MO:α-cyclodextrin competitive system studied at two concentration levels of cyclodextrin are shown in Table XXXIX. R and P were calculated according to Eq. (74) and as defined in Eq. (67), respectively, using $A_{IL} = 0.015$, $A_I = 0.807$ and $K_{11I} = 672.9\ \underline{M}^{-1}$. The potentiometric data then were analyzed according to Eq. (49). The linear plot for this Case IV system is shown in Fig. 28.

For 4-nitroaniline and 4-cyanoaniline, the pK_a's of their conjugate acid forms are 1.00 (141) and 1.74 (142), respectively. These are too low to be studied

Figure 25. Plot of C' vs. L_t for aniline:α-cyclodextrin system.

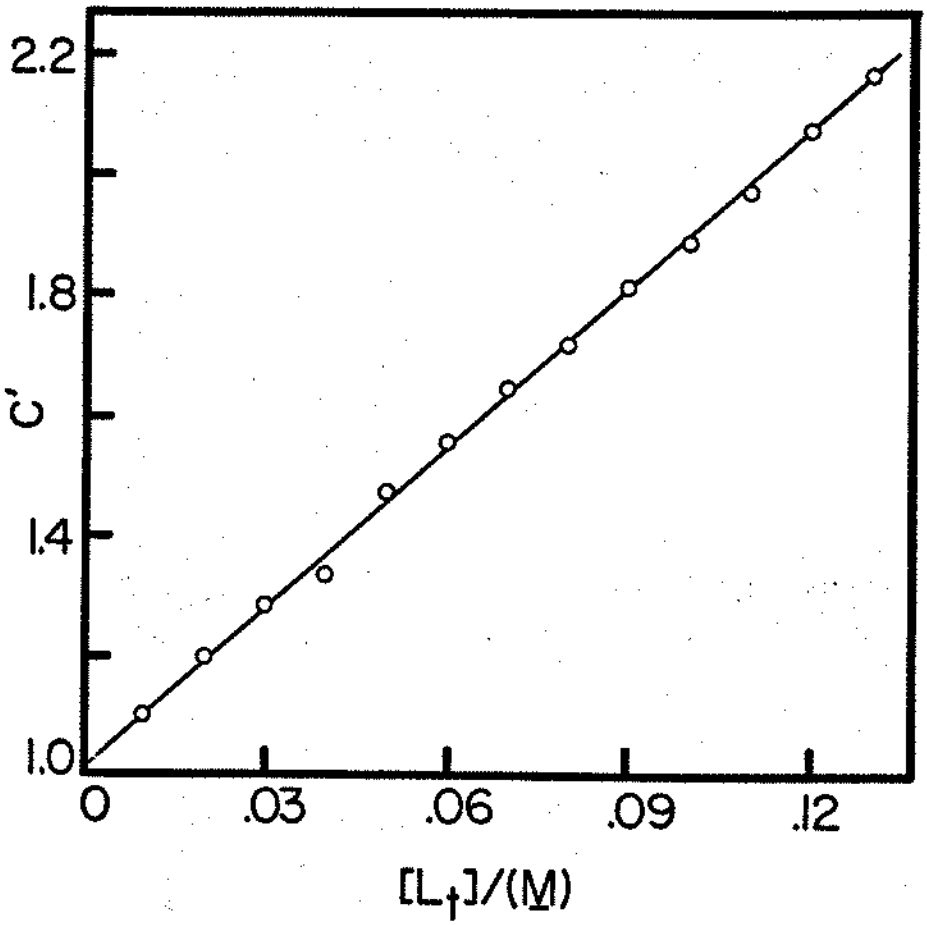
2.2
1.8
1.4
1.0
ĉ
0
.03
.06
.09
.12
[L_f]/(M)

Figure 26. Plot of C' vs. [L] for aniline:α-cyclodextrin system.

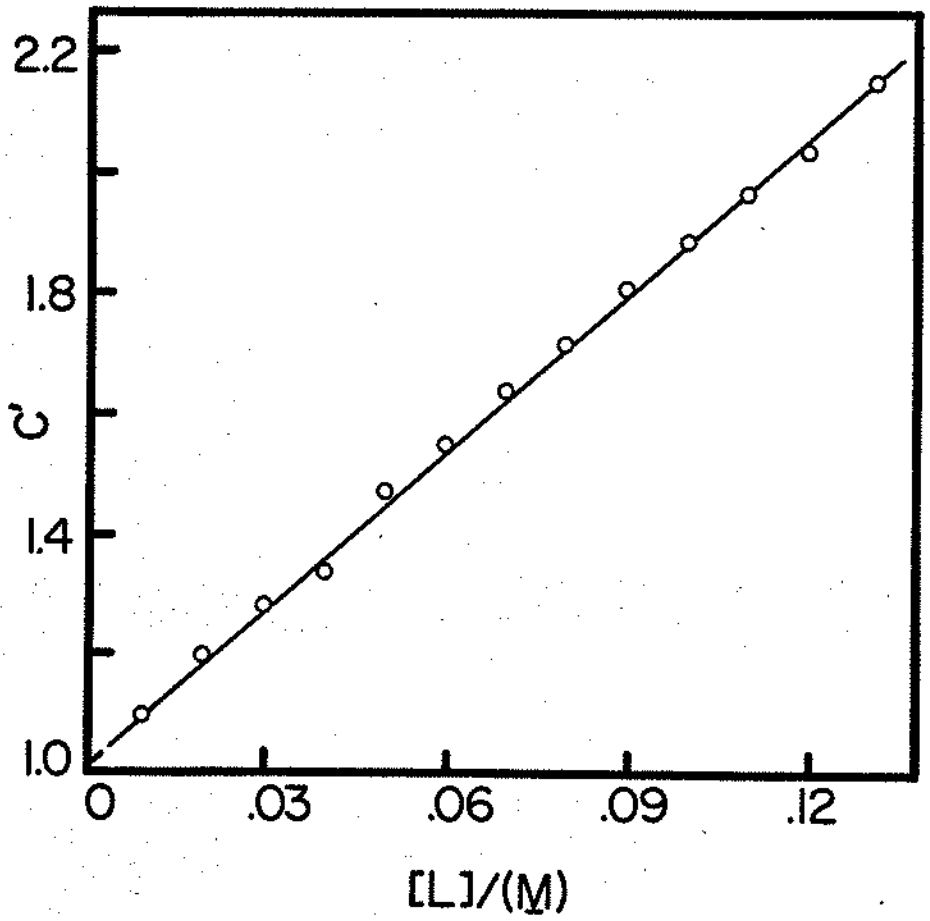
2.2
1.8
1.4
1.0
ν̄
0
.03
.06
.09
.12
[L]/(M)

Figure 27. Plot of C' vs. L_t for 4-toluidine:α-cyclodextrin system.

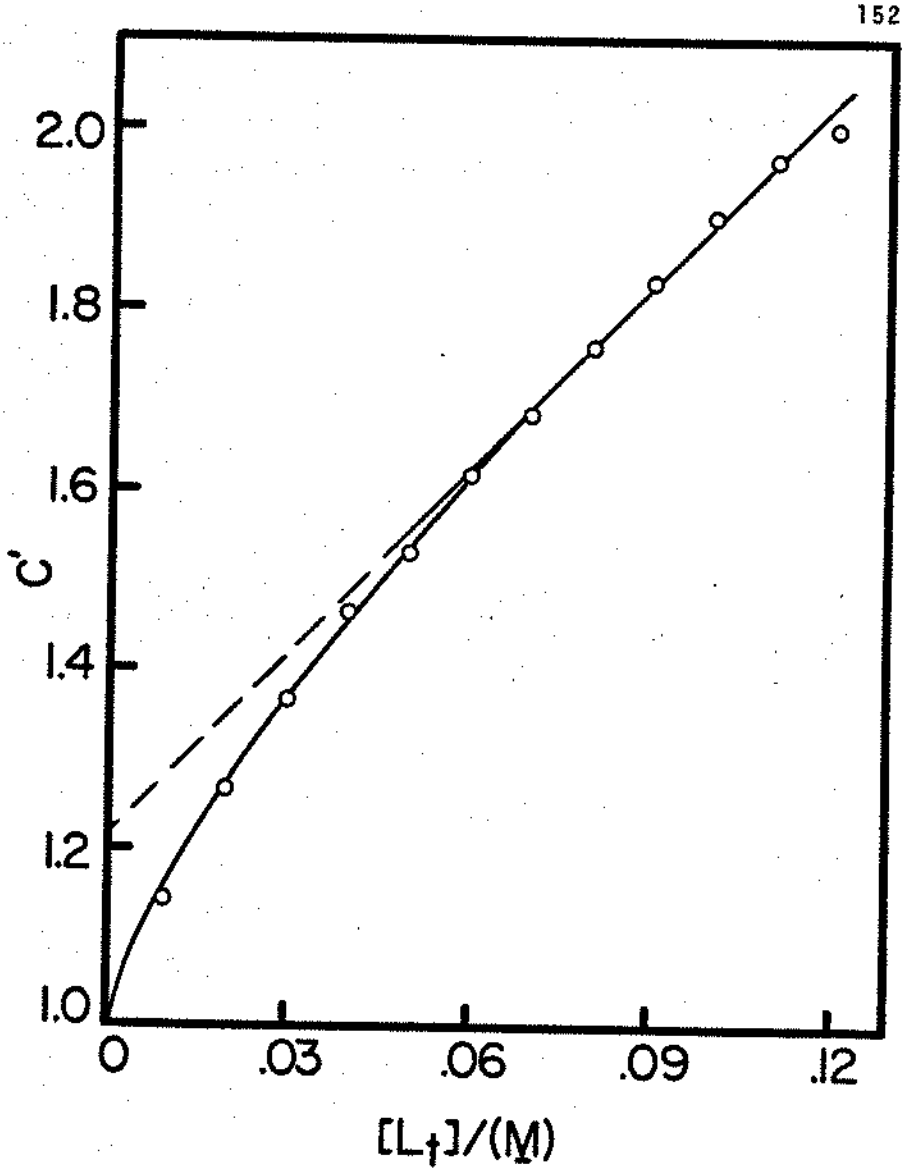
2.0
1.8
1.6
1.4
1.2
1.0
C'
0
.03
.06
.09
.12
[L_t]/(M)

Table XXXIX. Spectral data for 4-toluidine:methyl orange: α-cyclodextrin system at 25.0 ± 0.1°C.[a]

10^2 S_t/M	A[b]	R	S_t/P
$L_t = 1.00 \times 10^{-3}$ M			
0.90	0.542	1.98	36.39
1.20	0.556	2.15	39.15
1.50	0.567	2.29	42.91
1.80	0.578	2.44	46.17
2.10	0.587	2.58	49.65
$L_t = 2.00 \times 10^{-3}$ M			
1.00	0.413	1.02	18.82
1.30	0.424	1.08	21.29
1.50	0.432	1.12	22.54
1.80	0.445	1.20	23.94
2.00	0.455	1.26	24.61

[a] $I_t = 1.67 \times 10^{-5}$ M.

[b] $\lambda = 508$ nm.

Figure 28. Plot of Eq. (49), with subscripts a and b interchanged, for the 4-toluidine:α-cyclodextrin system.

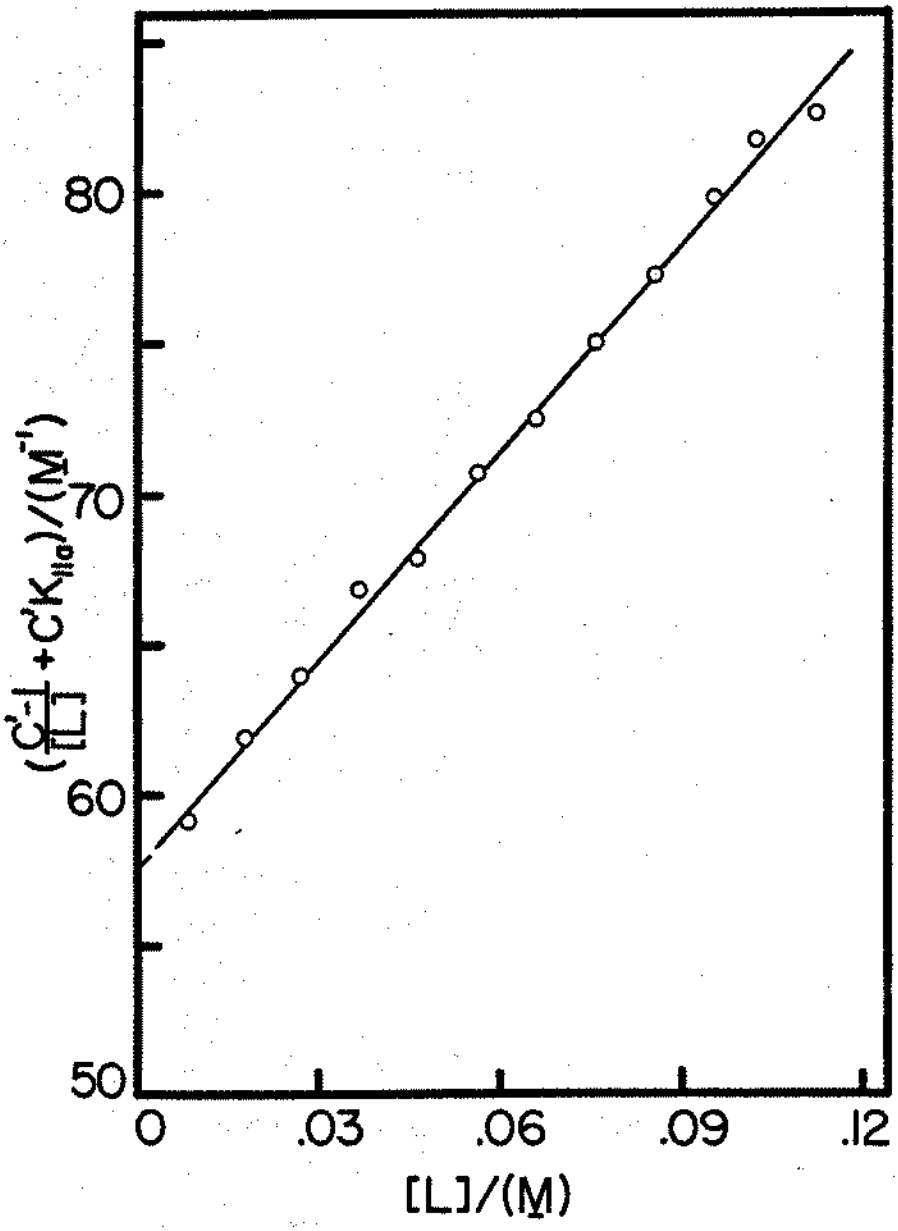
80
70
60
50
0
.03
.06
.09
.12
[L]/(M)
$(\frac{C'^{-1}}{[L]} + C'K_{110})/(M^{-1})$

potentiometrically. However, the complexation with cyclodextrin could be observed by ultraviolet spectrophotometry. The spectrum of 4-nitroaniline was bathochromically shifted with an increase in λ_{max} upon complexation. An isosbestic point observed at 382 nm, as shown in Fig. 29, is evidence for simple 1:1 complex formation. Fig. 30 is the Benesi-Hildebrand plot of $1/\Delta A$ vs. $1/L_t$ at 410 nm, K_{11b} determined was 638.2 $\underline{M}^{-1}$ (std. dev. 34.4 $\underline{M}^{-1}$). Spectral readings were also taken at 350 nm and the resulting K_{11b} was 631.6 $\underline{M}^{-1}$ (std. dev. 34.5 $\underline{M}^{-1}$), which was in excellent agreement with that determined at different wavelength.

Similarly, the spectral changes of 4-cyanoaniline were followed as a function of cyclodextrin concentration. An isosbestic point at 274 nm was characteristic for 1:1 complex formation. The spectral data for this system are recorded in Table XL.

The stability constants for the aniline derivatives are collected in Table XLI. The assignment to Case I and Case II systems were tested as described previously. Statistical analysis of K_{12b} values indicated that for 4-toluidine, assigned to Case IV, K_{12b} was significant by definition; for other compounds, the K_{12b} values were not significant within 95% confidence limits. The intercepts obtained from Case II system and MO spectrophotometric method were also analyzed as shown in Table XLII. At 95% confidence level, the intercepts were not different from unity. Therefore,

Figure 29. Ultraviolet spectra of 4-nitroaniline at various cyclodextrin concentrations; S_t = 7.11×10^{-5} M; pH = 9.18; ionic strength = 0.1 M. Cyclodextrin concentrations: 1, 0.00 M; 2, 3.39×10^{-3} M; 3, 5.68×10^{-3} M; 4, 1.67×10^{-2} M.

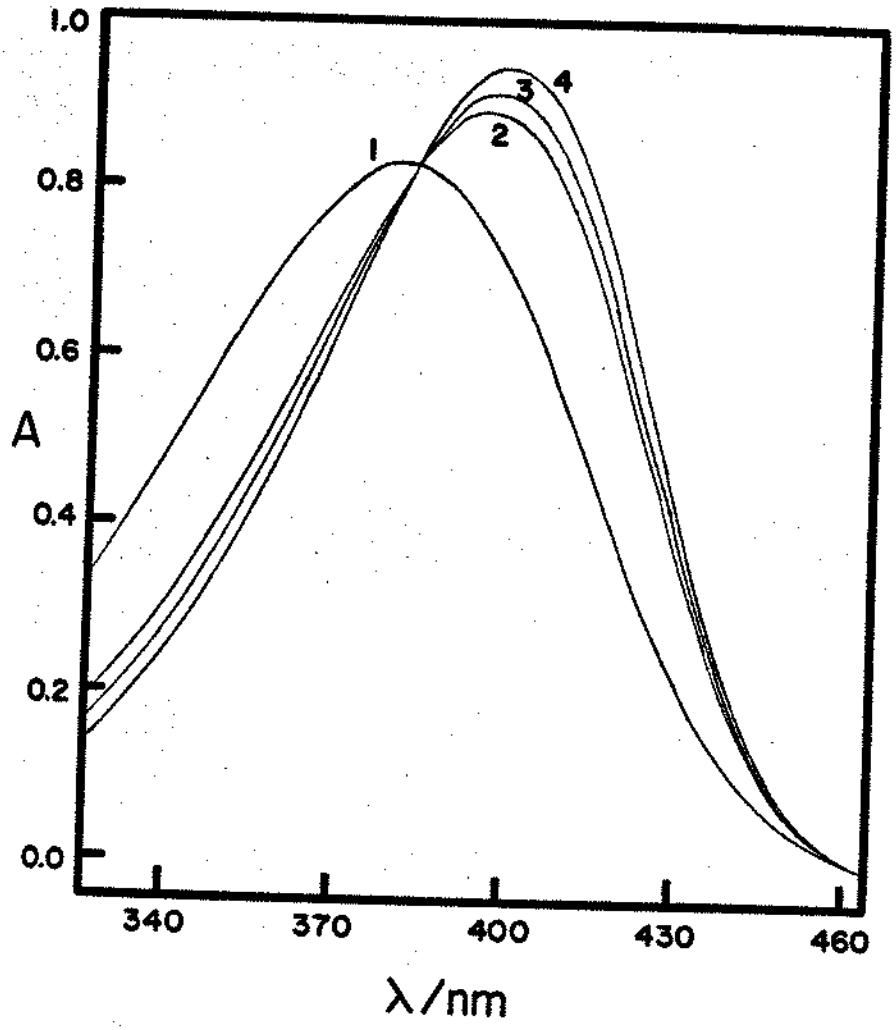
1.0
0.8
0.6
A
0.4
0.2
0.0
1
2
3
4
340
370
400
430
460
λ/nm

Figure 30. Benesi-Hildebrand plot for the 4-nitroaniline: α-cyclodextrin system at 25.0°C. S_t = 7.11 x 10^{-5} M, λ = 410 nm.

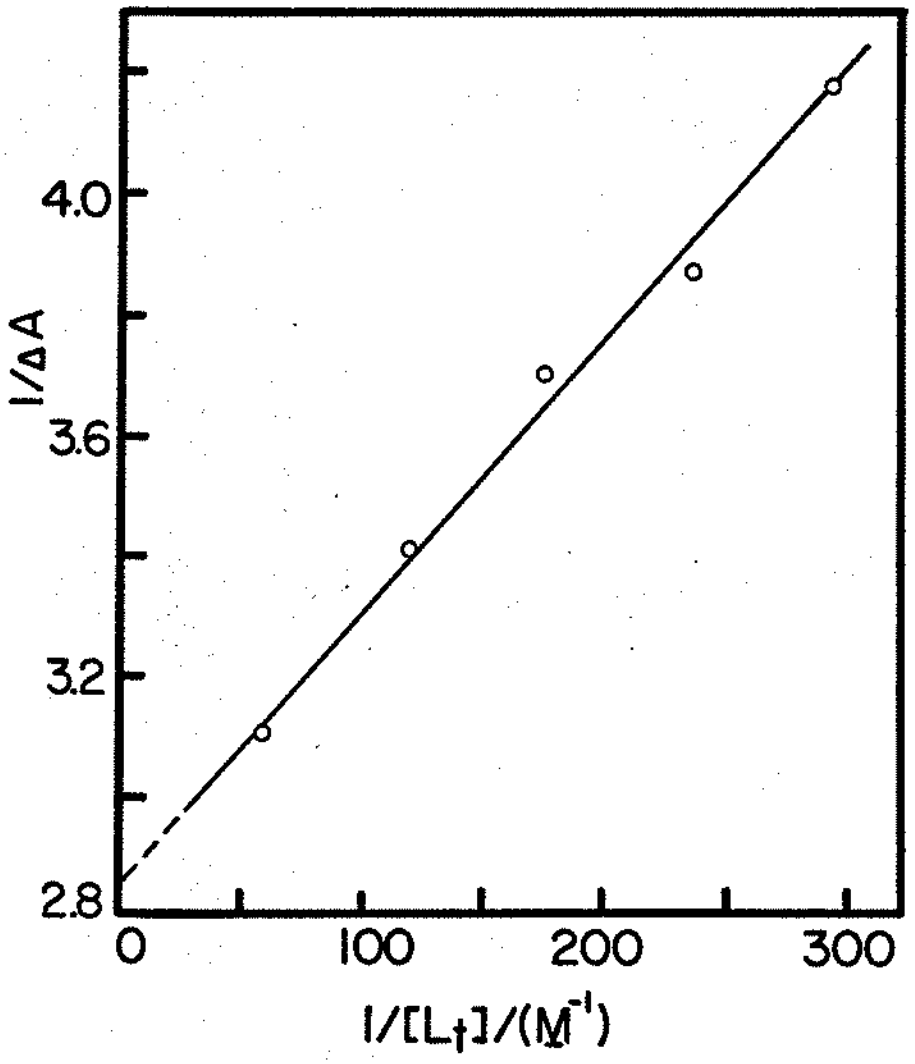
4.0
3.6
3.2
2.8
1/ΔA
0
100
200
300
1/[L_t]/(M^-1)

Table XL. Spectral data for 4-cyanoaniline: α-cyclodextrin system at 25.0 ± 0.1°C.[a]

$10^2 L_t/M$	ΔA[b]
0.333	-0.091
0.422	-0.103
0.556	-0.115
0.869	-0.121
1.671	-0.139
3.348	-0.144

[a] $S_t = 3.17 \times 10^{-5}$ M; pH = 9.18.

[b] λ = 260 nm; A_0 = 0.531.

Table XLI. Stability constants for α-cyclodextrin complexes of *para*-substituted anilines at 25.0 ± 0.1°C.

No.	X[a]	K^{b}_{11b}/M^{-1}	K^{b}_{12b}/M^{-1}	K^{b}_{11a}/M^{-1}
20	NH_2	2.3 (0.10)	2.11 (1.02)	0
21	OCH_3	6.7 (0.14)	-0.49 (0.31)	0
22	CH_3	57.6 (0.34)	3.91 (0.09)	37.1 (1.05)
23	H	8.8 (0.12)	-0.39 (0.39)	0
2	COO^-[c]	9.0 (0.22)	-	-
24	Cl	250.5 (10.0)	0.12 (0.16)	68.6 (3.32)
2	COOH[c]	1340.7 (11.1)	-	-
25	CN	451.2 (33.7)	-	-
26	NO_2	634.9[d] (34.4)	-	-

[a] X in X-C_6H_4-NH_2.

[b] Standard deviation in parentheses.

[c] Data from Table XVII.

[d] Average of two determinates at different wavelengths.

Table XLII. Student's t-test for the significance of intercept = 1 in least square regression of some anilines.

No.	X[a]	Intercept[b]	t[c]	$t^{d}_{(n-2,\ 0.025)}$
20	NH_2	0.983 (0.008)	2.131	2.306
21	OCH_3	1.009 (0.010)	0.907	2.262
22	CH_3	1.458 (0.905)	0.506	2.306
23	H	1.019 (0.009)	2.256	2.262

[a] X in $X\text{-}C_6H_4\text{-}NH_2$.

[b] The intercepts of compounds 20, 21, and 23 obtained from Eq. (38). The intercept of compound 22 obtained from Eq. (69). Standard deviation in parentheses.

[c] $t = \dfrac{\text{intercept} - 1}{\text{standard deviation of intercept}}$

[d] Student's t-values at n-2 degrees of freedom, 95% confidence limit.

it was concluded that the potentiometric data of these aniline derivatives were adequately assigned to individual special cases. For all these systems, $K_{12a} = 0$.

The relative standard deviation of K_{11b} ranged from 0.6% to 7.5% and of K_{11a} from 2.8% to 4.8%. The precision was poorer as compared with those of benzoic acids and phenols. This probably was a result of weak complexation. The relatively smaller $\Delta pK_a'$ values induced a larger error in estimation of the stability constants.

E. Benzylamine, Phenethylamine and Heterocyclic Amines

The amino compounds listed in Table LI were studied potentiometrically by Wong (115), who analyzed the data by a curve-fitting method. However, the stability constants reported were anomalously high. In this work, Wong's data were re-analyzed using the graphical techniques developed in this thesis. The potentiometric data and calculated [L] values are collected in Tables XLIII to L. Similar to the phenols and anilines, the $\Delta pK_a'$ values were negative, indicating the base forms form complexes more strongly than their conjugate acid forms.

The complexation of these compounds was simply described by Case I, II or III system. Fig. 31 is a plot of C' vs. L_t for compound 31 (4-nitroimidazole), a Case I system. Fig. 32 is the corresponding linear plot according

Table XLIII. Potentiometric data for benzylamine: α-cyclodextrin system at 25.0 ± 0.1°C.[a]

L_t/M	$\Delta pK_a'$[b]	[L]/M
0.0299	-0.193	0.0291
0.0396	-0.248	0.0386
0.0516	-0.312	0.0504
0.0591	-0.349	0.0578
0.0708	-0.406	0.0693
0.0829	-0.461	0.0813
0.0904	-0.487	0.0887
0.0980	-0.522	0.0962
0.1049	-0.559	0.1030
0.1102	-0.561	0.1084
0.1257	-0.619	0.1237

[a] S_t = 0.00392 M.

[b] pK_a' = 9.466.

Table XLIV. Potentiometric data for phenethylamine: α-cyclodextrin system at 25.0 ± 0.1°C.[a]

L_t/M	$\Delta pK_a'$[b]	[L]/M
0.0049	-0.067	0.0047
0.0086	-0.114	0.0083
0.0207	-0.205	0.0200
0.0303	-0.256	0.0294
0.0398	-0.322	0.0388
0.0499	-0.375	0.0488
0.0604	-0.419	0.0592
0.0701	-0.465	0.0689
0.0799	-0.501	0.0786
0.0898	-0.529	0.0884
0.1004	-0.565	0.0990
0.1100	-0.592	0.1085
0.1205	-0.625	0.1190

[a] S_t = 0.00405 M.

[b] pK_a' = 9.899.

Table XLV. Potentiometric data for imidazole: α-cyclodextrin system at 25.0 ± 0.1°C.[a]

L_t/M	$\Delta pK_a'$[b]	[L]/M
0.0049	-0.030	0.0047
0.0099	-0.054	0.0096
0.0199	-0.110	0.0194
0.0307	-0.167	0.0300
0.0398	-0.214	0.0390
0.0507	-0.257	0.0497
0.0604	-0.294	0.0594
0.0697	-0.325	0.0686
0.0810	-0.369	0.0798
0.0923	-0.388	0.0910
0.1023	-0.416	0.1010

[a] S_t = 0.00429.

[b] pK_a' = 7.112.

Table XLVI. Potentiometric data for N-methylimidazole: α-cyclodextrin system at 25.0 ± 0.1°C.[a]

L_t/M	$\Delta pK_a'$[b]	[L]/M
0.0051	-0.025	0.0050
0.0103	-0.048	0.0100
0.0208	-0.100	0.0203
0.0305	-0.136	0.0299
0.0407	-0.178	0.0399
0.0606	-0.251	0.0596
0.0500	-0.216	0.0491
0.0704	-0.281	0.0693
0.0815	-0.317	0.0804
0.0900	-0.335	0.0888
0.0999	-0.363	0.0987

[a] S_t = 0.00429 M.

[b] pK_a' = 7.327.

Table XLVII. Potentiometric data for 4-nitroimidazole: α-cyclodextrin system at 25.0 ± 0.1°C.[a]

L_t/M	$\Delta pK_a'$[b]	$[L]/M$
0.0204	-0.261	0.0194
0.0308	-0.345	0.0295
0.0397	-0.402	0.0383
0.0499	-0.451	0.0483
0.0553	-0.488	0.0536
0.0713	-0.541	0.0695
0.0798	-0.569	0.0779
0.0903	-0.599	0.0884
0.1003	-0.630	0.0983

[a] S_t = 0.00362 M.

[b] pK_a' = 9.239.

Table XLVIII. Potentiometric data for t-butylpyridine: α-cyclodextrin system at 25.0 ± 0.1°C.[a]

L_t/M	$\Delta pK_a'$[b]	[L]/M
0.0099	-0.275	0.0088
0.0208	-0.487	0.0191
0.0401	-0.796	0.0376
0.0502	-0.959	0.0474
0.0604	-1.063	0.0574
0.0699	-1.186	0.0667
0.0800	-1.250	0.0768
0.0900	-1.329	0.0867
0.0997	-1.401	0.0963
0.1210	-1.520	0.1175

[a] S_t = 0.00421 M.

[b] pK_a' = 6.251.

Table XLIX. Potentiometric data for quinoline: α-cyclodextrin system at 25.0 ± 0.1°C.[a]

L_t/M	$\Delta pK_a'$[b]	[L]/M
0.0049	-0.090	0.0047
0.0098	-0.101	0.0094
0.0207	-0.194	0.0200
0.0302	-0.236	0.0292
0.0403	-0.326	0.0392
0.0494	-0.359	0.0482
0.0603	-0.412	0.0590
0.0697	-0.458	0.0683
0.0803	-0.523	0.0789
0.0895	-0.539	0.0880
0.1009	-0.571	0.0993
0.1203	-0.655	0.1188

[a] S_t = 0.00408 M.

[b] pK_a' = 4.982.

Table L. Potentiometric data for isoquinoline: α-cyclodextrin system at 25.0 ± 0.1°C.[a]

L_t/M	$\Delta pK_a'$[b]	$[L]/M$
0.0125	-0.117	0.0120
0.0236	-0.218	0.0226
0.0314	-0.282	0.0302
0.0405	-0.332	0.0392
0.0494	-0.423	0.0477
0.0613	-0.506	0.0594
0.0713	-0.574	0.0692
0.0773	-0.628	0.0750
0.0910	-0.705	0.0885
0.1009	-0.736	0.0984
0.1226	-0.854	0.1199

[a] S_t = 0.00407 M.

[b] pK_a' = 5.480.

Figure 31. Plot of C' vs. L_t for 4-nitroimidazole:α-cyclodextrin system.

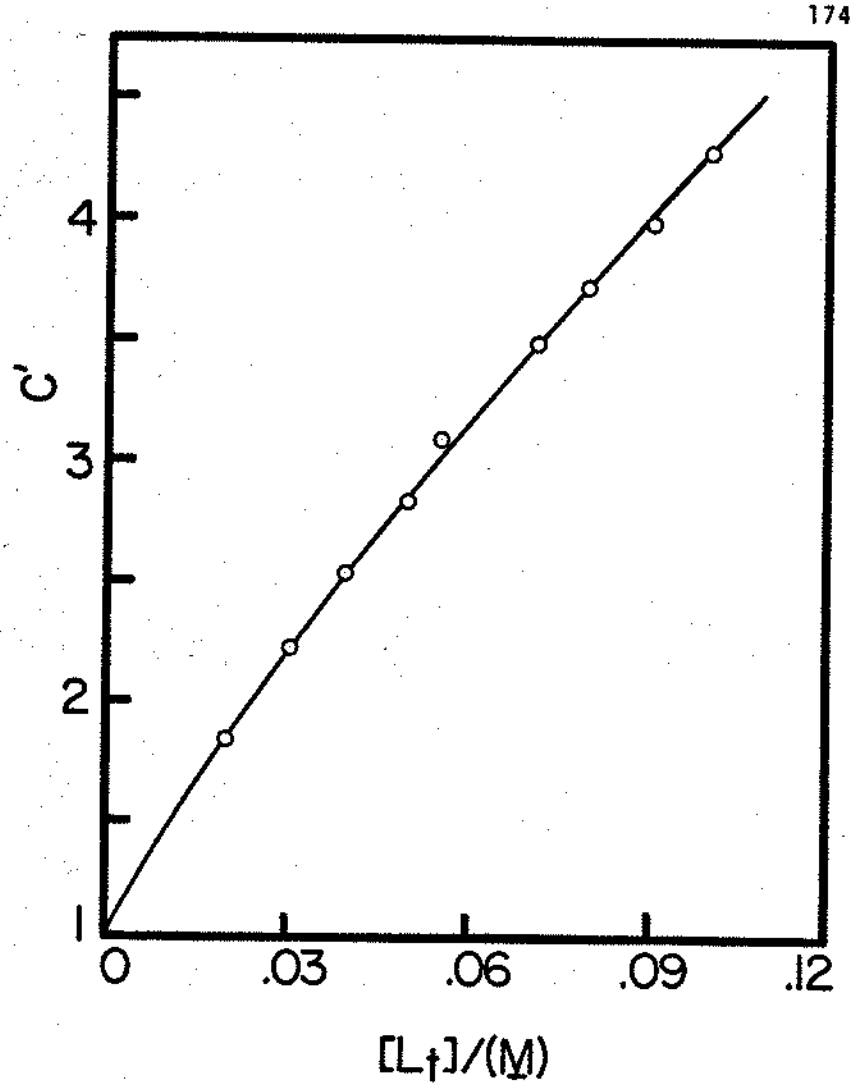
4
3
2
1
C̀
0
.03
.06
.09
.12
[L_f]/(M)

Figure 32. Plot of Eq. (37), with subscripts a and b interchanged, for 4-nitroimidazole:α-cyclodextrin system.

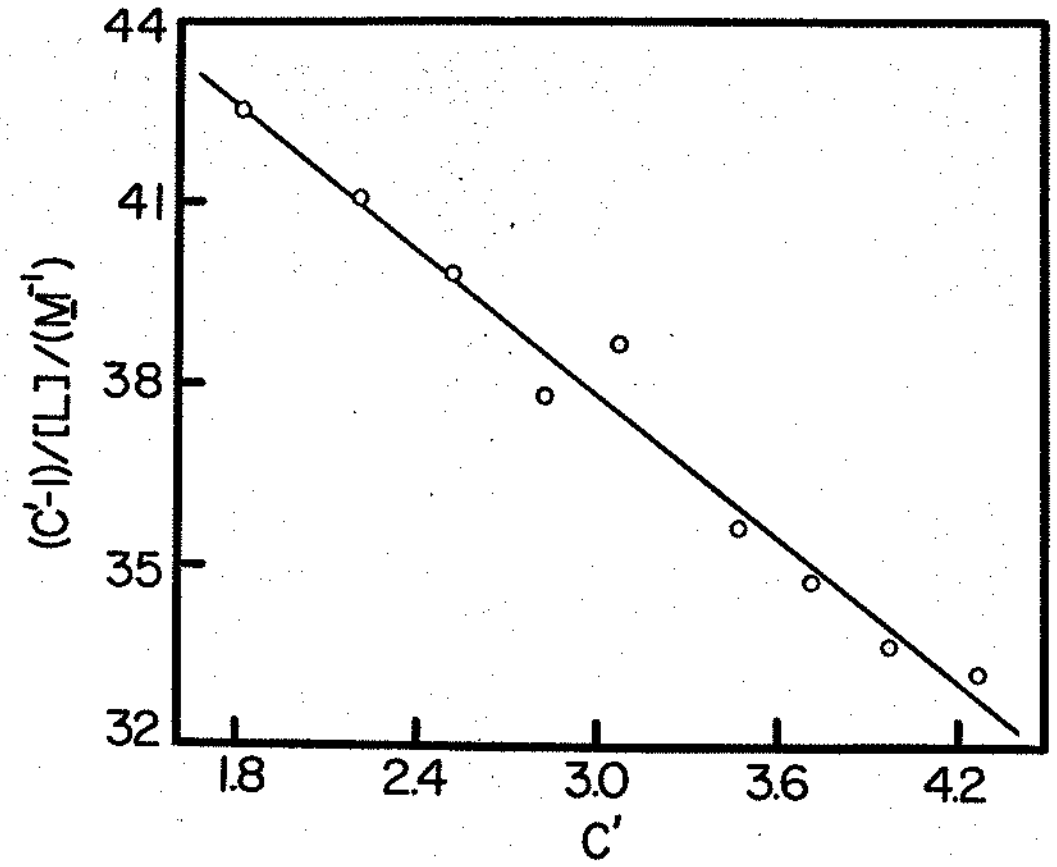
44
41
38
35
32
(C'-1)/[L]/(M⁻¹)
1.8
2.4
3.0
3.6
4.2
C'

to Eq. (37). Compounds 28-30 and 33 were Case II systems. Fig. 33 is a plot of C' vs. L_t for compound 29 (imidazole). The linear plot of C' vs. [L] is shown in Fig. 34. The potentiometric data of compounds 27, 32, and 34 were interpreted as Case III systems. Fig. 35 is the diagnostic plot of C' vs. L_t for compound 34 (isoquinoline), a Case III system. The linear plot to obtain stability constants is shown in Fig. 36.

Table LI lists the stability constants for these amine substrates. $K_{12a} = 0$ for all the systems. The assignments to Case I and II systems were tested as described in the preceding sections. It is obvious that the K_{12b} values for compounds 28, 29, 31 and 33 are not significant. For compounds 27, 32 and 34, the K_{12b}'s are finite, which is reasonable by definition of Case III systems. Compound 30 seems to have a significant K_{12b} at the 95% confidence level. However, the correlation coefficients (R^2) are 100% when it was treated as a Case II system and 0.3% as a Case III system. Therefore, the Case II system provides a better description of this system.

The significance of the intercepts in Eq. (38) for Case II systems was analyzed as shown in Table LII. Though the intercepts of compounds 28 and 30 were statistically different from unity, the same conclusion was drawn as described previously on the basis of the correlation coefficients.

Figure 33. Plot of C' vs. L_t for imidazole:α-cyclodextrin system.

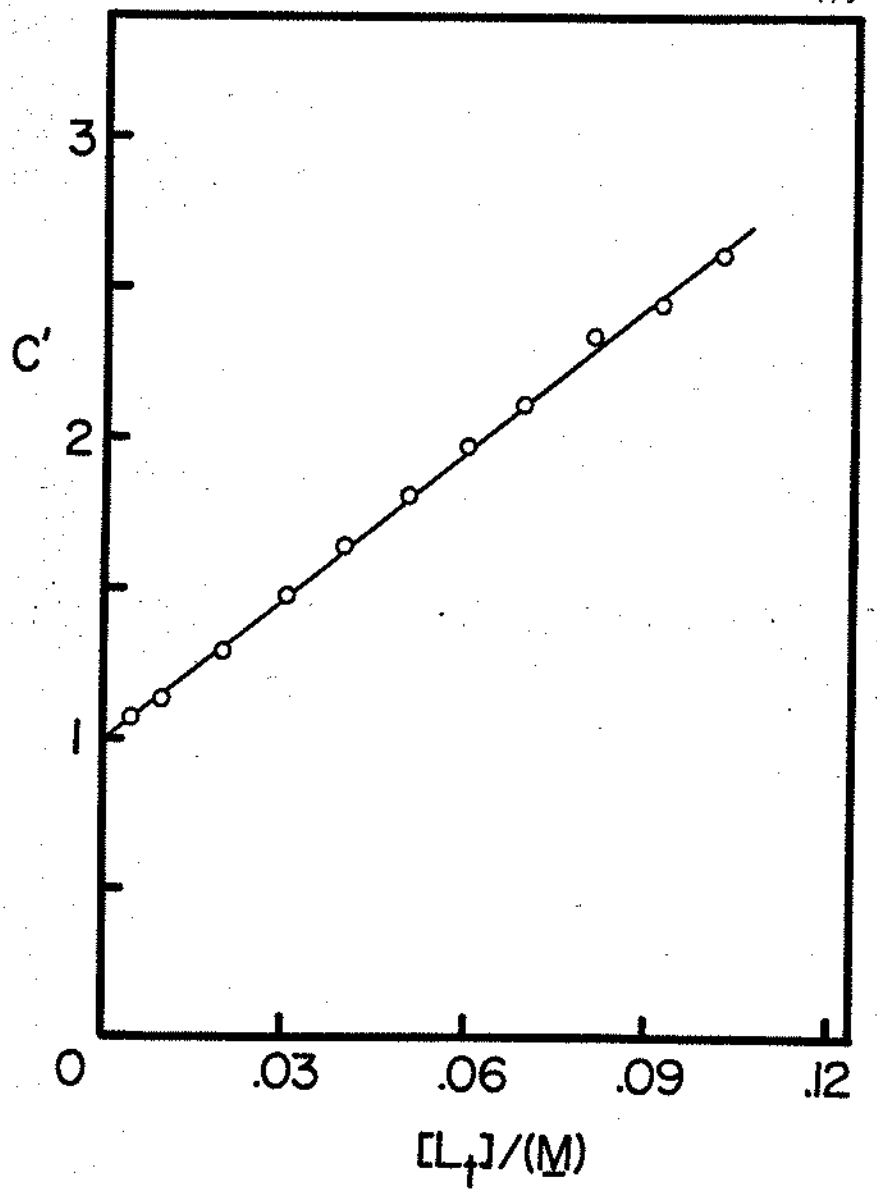
C'
3
2
1
0
.03
.06
.09
.12
[L_t]/(M)

Figure 34. Plot of Eq. (38), with subscripts a and b interchanged, for imidazole:α-cyclodextrin system.

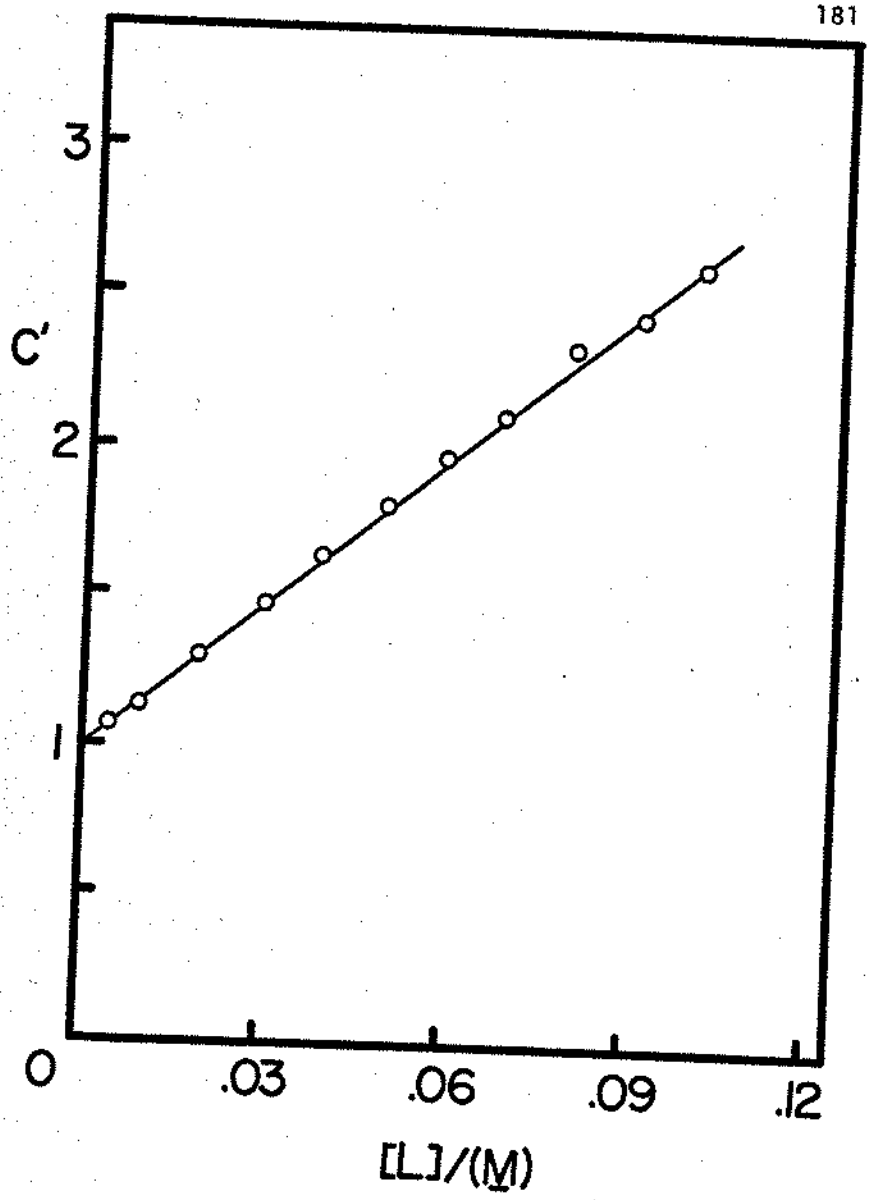
3
2
1
0
C'
.03
.06
.09
.12
[L]/(M)

Figure 35. Plot of C' vs. L_t for isoquinoline:α-cyclodextrin system.

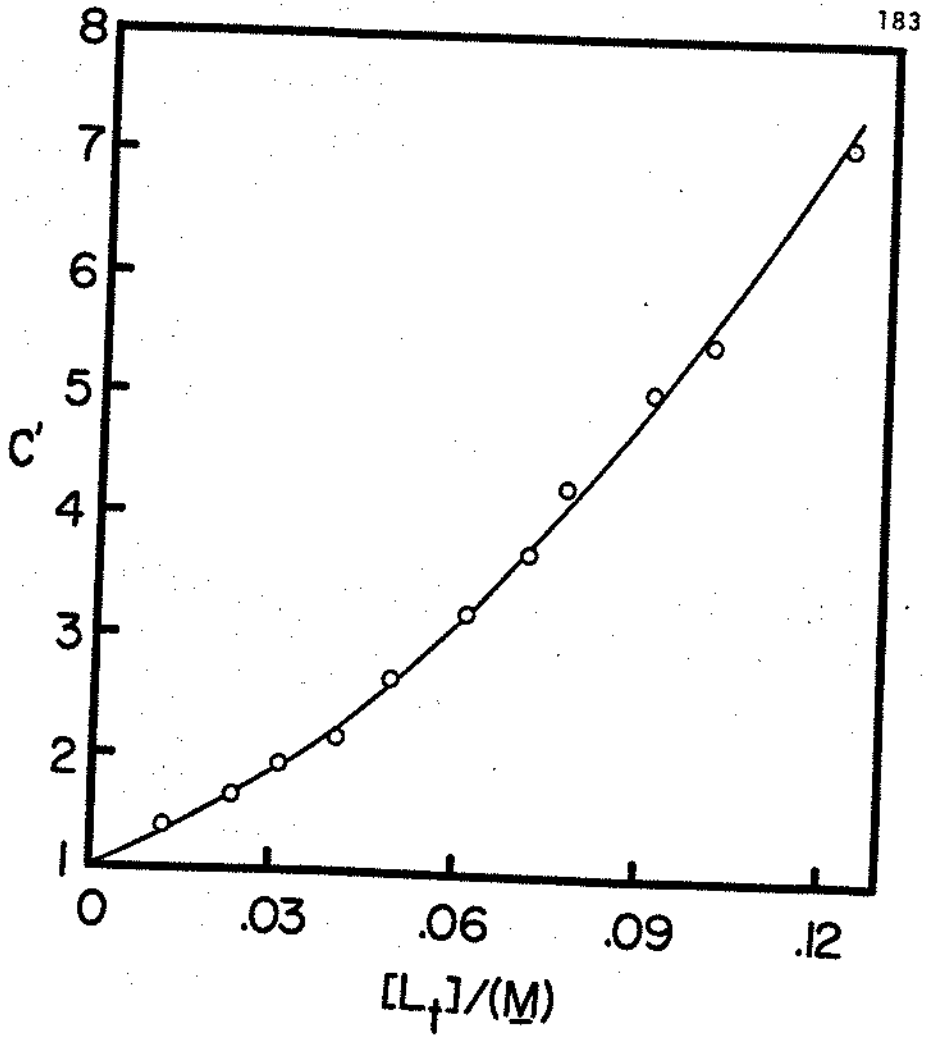
8
7
6
5
4
3
2
1
C'
0
.03
.06
.09
.12
[L_t]/(M)

Figure 36. Plot of Eq. (42), with subscripts a and b interchanged, for isoquinoline:α-cyclodextrin system.

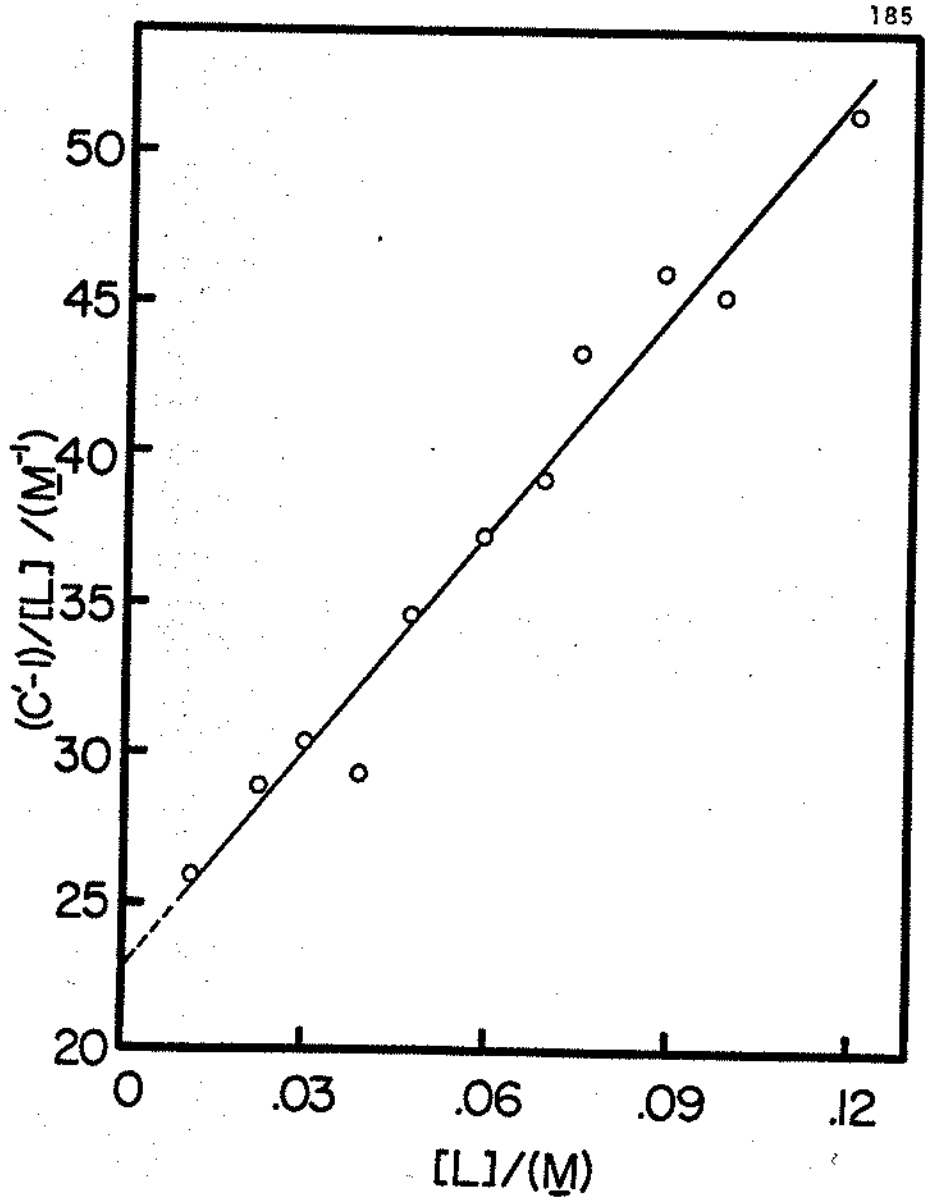
50
45
40
35
30
25
20
0
.03
.06
.09
.12
(C'-1)/[L] /(M⁻¹)
[L]/(M)

Table LI. Stability constants for α-cyclodextrin complexes of some amines at 25.0 ± 0.1°C.

No.	Amine	K^a_{11b}/M^{-1}	K^a_{12b}/M^{-1}	K^a_{11a}/M^{-1}
27	Benzylamine	17.4 (0.35)	4.01 (0.26)	0
28	Phenethylamine	26.4 (0.17)	-0.44 (0.16)	0
29	Imidazole	16.3 (0.23)	0.05 (0.37)	0
30	N-Methylimidazole	13.4 (0.09)	0.81 (0.23)	0
31	4-Nitroimidazole	49.8 (0.81)	-0.00064 (0.16)	3.98 (0.25)
32	4-t-Butylpyridine	84.7 (5.98)	20.13 (1.75)	0
33	Quinoline	28.6 (0.73)	0.63 (0.48)	0
34	Isoquinoline	22.7 (0.95)	10.76 (0.76)	0

[a]Standard deviation in parentheses.

Table LII. Student's t-test for the significance of intercept = 1 in Case II amines.

No.	Amine	Intercept[a]	t^b	$t^c_{(n-2,\ 0.025)}$
28	Phenethylamine	1.06 (0.012)	5.417	2.201
29	Imidazole	0.99 (0.013)	0.80	2.262
30	N-Methylimidazole	0.98 (0.005)	3.278	2.262
33	Quinoline	0.97 (0.048)	0.532	2.228

[a]Standard deviation in parentheses.

[b]$t = \frac{\text{intercept} - 1}{\text{standard deviation of intercept}}$

[c]Student's t-values at n-2 degrees of freedom, 95% confidence level.

VI. DISCUSSION

A. Evaluation of the Potentiometric Method

For complexing systems in which the full 4-parameter Eq. (32) is not required, this potentiometric method with graphical treatment of data is simple, rapid and effective. Because of the linear graphing forms, the usual least-squares statistical treatment is appropriate: the error in the abscissa is much smaller than that in the ordinate, as is required by the conventional treatment. The great sensitivity of the quantity $(C - 1)/[L]$ at low [L] values made it necessary to reject some data points at very low [L] in the plots according to Eqs. (37), (42) and (49). The data reported in this thesis were obtained at α-cyclodextrin concentrations varying from 0.01 M to 0.13 M, except for some Case I systems whose K_{11a} and K_{11b} were relatively large so that, according to Eq. (35), the pH changes were not sensitive to high ligand concentration. These systems were 4-cyanophenol and 4-nitrophenol, for which systems the linear form, Eq. (37), applied up to a concentration of 0.07 M.

The assumption that activity coefficients are constant as L_t changes is fundamental to the interpretation of potentiometric data in terms of 1:1 and 1:2 complex formation. It is conceivable that the observation of finite 1:2

stability constants represents a measurement of changing activity coefficients rather than actual 1:2 complexation. Gelb et al. (79) described evidence that ionic activity coefficients are not changed as a consequence of changes in cyclodextrin concentration. That K_{12a} values for several acids, and K_{12b} for some phenols and amines, were found to be negligible suggests further that activity coefficient changes are not responsible for the observed 1:2 stability constants. Nevertheless the role of cyclodextrin in modifying the properties of the solvent cannot be overlooked as a possible complicating factor in such studies.

A preliminary study showed that there was no counter-ion effect. Either sodium or potassium ion present in the solutions gave identical pH changes under the experimental condition. However, the role of ionic strength remains to be studied.

Several prior studies of the benzoic acid:α-cyclodextrin and 4-nitrophenol:α-cyclodextrin systems have been described in the literature. Tables LIII and LIV list these chronologically. The earliest benzoic acid potentiometric result (78) obtained by curve-fitting is now rejected. It is evident that the method developed in this thesis is capable of generating stability constants that are consistent with those obtained by other techniques and in other laboratories. Wong (115) reported that the

Table LIII. Comparison of stability constants for the benzoic acid:α-cyclodextrin system.[a]

Method	K_{11a}/M^{-1}	K_{11b}/M^{-1}	Ref.
Competitive spectrophotometry	1050	--	76
Kinetics	--	12.3	7
Thermometry	1000	--	116
Potentiometry	1400	38	78
Proton NMR	233; 800	9.8	143
Potentiometry	751	10.5	79
Solubility	500	--	19
UV spectrophotometry	660	--	19
Competitive spectrophotometry	--	13	77
Competitive spectrophotometry	810	--	This work
Potentiometry	722	11.2	This work

[a]At 25°C; ionic strengths differ.

Table LIV. Comparison of stability constants for the 4-nitrophenol:α-cyclodextrin system.[a]

Method	K_{11b}/M^{-1}	K_{11a}/M^{-1}	Ref.
Competitive spectrophotometry	2230	290	64
Thermometry	--	126	116
Potentiometry	2200	200	78
UV spectrophotometry	2512	190	95
Polarography	2439	--	90
Potentiometry	2143	211	79
UV spectrophotometry	2720	250	19
Potentiometry	2382	270	115
Potentiometry	2408	245	This work
UV spectrophotometry	--	249	This work
Competitive spectrophotometry	--	249	This work

[a]At 25°C; ionic strengths differ.

curve-fitting method was successful only when applied to phenols, when a convergence to a unique set of results occurred. His results are compared with those obtained in this work, as shown in Table LV; good agreement between the two methods is observed except for 4-iodophenol.

An advantage of this potentiometric method is that it yields information about the complexing of both the conjugate acid and base forms of the substrate simultaneously. A limitation is that it can serve as an independent method only when the system includes two (or fewer) complex equilibria, that is, when the equation has two (or fewer) parameters. For the 3-parameter Case IV system, it was judged necessary to make use of a separate experimental determination of one of the parameters. This combination of several techniques is essential if the equation has 4 parameters, as in the cinnamic acid system (111).

A relatively high concentration of substrate was required to achieve adequate buffer capacity in the potentiometric measurement. This condition excluded a number of relatively insoluble compounds which might complex extensively with cyclodextrins.

The potentiometric method developed in this work is a powerful tool in studying complexation of ionizable substrates. The method can further be extended to study non-ionizable substrates. A competitive potentiometric method,

Table LV. Comparison of stability constants for the *para*-substituted phenols:α-cyclodextrin system.[a]

X[b]	K_{11a}	K_{12a}	K_{11b}	K_{12b}
I	2316 (1157)	0 (0)	3955 (1987)	2 (2)
Cl	272 (277)	0 (0)	488 (501)	3 (4)
Br	704 (752)	0 (0)	1221 (1301)	5 (5)
CN	158 (158)	0 (0)	662 (651)	0 (0)
NO_2	245 (270)	0 (0)	2408 (2382)	0 (2)

[a] The numbers in the parentheses are from Ref. (115). The data were obtained by a curve-fitting method, while the numbers not in the parentheses are from Table XXXII.

[b] X in X-C_6H_4-OH.

theoretically based on the competition of the non-ionizable substrate and an ionizable substrate of known stability constants for the binding site on cyclodextrin molecule, is described in Appendix C. The method seems worthy of further investigation.

B. Evaluation of Methyl Orange Competitive Spectrophotometric Method

The K_{11a} determined by methyl orange (MO) competitive spectrophotometry for the 4-nitrophenol:α-cyclodextrin system, as shown in Table LIV, is in excellent agreement with values obtained by other techniques. Therefore, the method is applicable and is useful when the complexation is accompanied by no significant substrate spectral change. However, there are several points to be noticed in applying this method:

1) It determines K_{11a} only. The method was developed on the basis that MO and the substrate form 1:1 complexes with α-cyclodextrin, and this is the case for MO in acid medium (118). In alkaline pH, however, Cramer et al. (64) found that higher stoichiometric ratios were present.

2) It was suggested in the Theory section that low R_c values, in Eq. (82), be used such that the effect due to substrate-indicator complexation (SI) is minimized and R_c is a good approximation of R in Eq. (59). The experimental

R_c values ranging from 1.0 to 3.0 gave linear relationships following Eq. (69), with an intercept of unity being obtained. Curvature was observed at higher R_c values, possibly because of SI complex formation. It was not pursued further, since adjustment can be made to overcome this effect. The spectrum of MO was not altered by the presence of the substrate.

3) The graphical MO technique was applied also to the benzoic acid system. The K_{11a} value found from Eq. (69) was 810.3 $\underline{M}^{-1}$, somewhat larger than the value of 722 found by potentiometry (Table XVII), but considerably lower than the value 1050 reported by Casu and Ravà with their version of the MO method (76). Taking into account possible SI formation, with an estimate of K_{SI} = 25 $\underline{M}^{-1}$ based on area overlap (120) led, with Eq. (101), to K_{11a} = 815.8 $\underline{M}^{-1}$. The discrepancy between the potentiometric and MO results is not understood. Though outside the estimated confidence limits of the potentiometric result, it should be pointed out that the MO result is not in obvious error, as revealed by the comparisons in Table LIII.

4) In the equilibrium Eq. (54), competition occurs only if the amount of L is limited. That is, if $L_t >> S_t$ and $L_t >> I_t$, there would be adequate free L present, and addition of S would not displace any significant amount of L from IL. Thus L_t and S_t must be of comparable magnitudes

though L_t can be very much greater than I_t. This argument is correct if $K_{11I} \simeq K_{11S}$, so that S and I have comparable affinities for L. In case $K_{11S} >> K_{11I}$, then a smaller concentration of S would be adequate to displace I from IL. In case $K_{11S} < K_{11I}$, S_t should be larger in order to compete effectively.

Generally, in graphical methods, the greatest sensitivity is achieved when the slope is near 1. Following Eq. (69), K_{11S} (K_{11a}) is determined from the slope, therefore the method is most sensitive when $K_{11S} \simeq K_{11I}$. It would be desirable to have a range of indicators whose K_{11I} values vary with K_{11S}. The linear graphing form is appropriate for the conventional least-squares fitting, since the error in abscissa (R), which is calculated directly from experimental data, is smaller than that in the ordinate (S_t/P), which includes both R and an estimated K_{11I}.

C. A Stoichiometric Model of Cyclodextrin Complexes

The model of cyclodextrin complex formation developed earlier (97,115) can be applied to interpret the stability constants obtained in this work.

Let g-G represent the substrate (guest) molecule, the lower and upper case letters signifying two binding sites; let h-H represent the cyclodextrin (host), the lower and

upper case letters standing for the two rims of the cavity, which are different chemically. Then all possible 1:1 inclusion complexes may be represented as follows, where it is assumed that, within each orientation, the energy distribution of positional isomers is so narrow that only a single complex need be considered:

1:1 Complexes	Symbol
g-G h-H	gH
g-G H-h	gh
G-g h-H	GH
G-g H-h	Gh

It is also possible, in principle, to form 2:1 and 1:2 inclusion complexes:

2:1 Complexes	Symbol	1:2 Complexes	Symbol
g-G G-g H-h	GH-hG	g-G h-H H-h	Hg-GH
g-G g-G H-h	GH-hg	g-G h-H h-H	Hg-Gh
G-g g-G H-h	gH-hg	g-G H-h h-H	hg-Gh
G-g G-g H-h	gH-hG	g-G H-h H-h	hg-GH

There appear to be no reports of 2:1 complexes of organic substrates with α-cyclodextrin, therefore it is not necessary to invoke the 2:1 stoichiometry to describe the systems quantitatively. The model then leads to the inference that the guest molecule can enter only one end of the host (say H). It follows that there are only two 1:1 complexes (gH and GH) and one 1:2 complex (Hg-GH). The model thus leads to a great simplification of the stoichiometric possibilities.

The observed K_{11} value is the sum of the stability constants for all isomeric 1:1 complexes (117), hence for the case being considered:

$$K_{11} = K_{gH} + K_{GH} \tag{115}$$

The 1:2 complex can be formed via the gH or the GH route:

$$gH + h\text{-}H \rightleftharpoons Hg\text{-}GH \qquad K' \tag{116}$$

$$GH + h\text{-}H \rightleftharpoons Hg\text{-}GH \qquad K'' \tag{117}$$

The observed stability constant (K_{12}) is given by:

$$K_{12} = \frac{[Hg\text{-}GH]}{([gH] + [GH])[h\text{-}H]} \tag{118}$$

and becomes

$$K_{12} = \frac{K'K''}{K' + K''} \tag{119}$$

It is also seen that

$$\frac{K'}{K''} = \frac{K_{GH}}{K_{gH}} \qquad (120)$$

Writing $K' = aK_{GH}$, with Eq. (120) it follows that $K'' = aK_{gH}$. Combination with Eq. (119) gives

$$K_{12} = \frac{aK_{gH}K_{GH}}{K_{gH} + K_{GH}} \qquad (121)$$

The factor a is a measure of the extent of interaction between the two sites in a 1:2 complex. Several types of behavior can be classified:

1) Independent binding sites (a = 1). Then Eq. (121) becomes $K_{12} = K_{gH}K_{GH}/K_{11}$, or

$$\frac{1}{K_{12}} = \frac{1}{K_{gH}} + \frac{1}{K_{GH}} \qquad (122)$$

i.e., the 1:2 dissociation constant is equal to the sum of the 1:1 dissociation constants. With Eqs. (115) and (122), the isomeric stability constants K_{gH} and K_{GH} can be evaluated. This has been used to describe small molecule-protein interactions with two independent binding sites (144). Some α-cyclodextrin systems with cinnamic acid derivatives have been interpreted in this way (97).

2) Identical binding sites. Then g = G, therefore

$$K_{gH} = K_{GH} = K_{11}/2 \qquad (123)$$

$$K_{12} = aK_{11}/4 \qquad (124)$$

3) Competitive binding sites ($a < 1$).

4) Cooperative binding sites ($a > 1$).

To solve for the isomeric constants in cases 3) and 4) some assumptions are necessary, since there are three unknowns in Eqs. (115) and (121). Suppose we choose two substrates, g-G and d-D, having very similar structures; e.g., one end of each substrate (say G and D) is essentially identical, then there are four equations with six unknowns to describe the stability constants:

$$K_{11g} = K_{GH} + K_{gH} \qquad K_{11d} = K_{dH} + K_{DH} \qquad (125)$$

$$K_{12g} = \frac{aK_{gH}K_{GH}}{K_{gH} + K_{GH}} \qquad K_{12d} = \frac{a'K_{dH}K_{DH}}{K_{dH} + K_{DH}} \qquad (126)$$

The assumptions are made that

$$K_{GH} = K_{DH} \qquad (127)$$

$$a = a' \qquad (128)$$

Then all the parameters can be solved combining Eqs. (125) to (128). Reasonable substrates are 1,4-disubstituted benzenes. However, the assumptions made in Eqs. (127) and (128) are limited to substrates in which extensive resonance delocalization between the two ends of the molecule cannot take place; if such delocalization occurs, identical

binding sites on the two substrates cannot be assumed.

The model as expressed in Eqs. (115) and (121) is useful in directing attention to the nature of K_{11} and K_{12}, since it reveals that K_{12} is actually a constant for the formation of a 1:1 complex from an already formed 1:1 complex. Though some chemically reasonable assumptions are required in using the two equations with three unknowns, the model leads to the interpretations of experimentally determined stability constants in terms of specific site binding constants.

Before further analysis of the stability constants determined in this work, the model described above will be used to discuss the possibility that special cases may occur other than the four assigned in the potentiometric method.

For an ionizable substrate in 1:1 + 1:2 complex systems, there are four possible stability constants, namely K_{11a}, K_{12a}, K_{11b} and K_{12b} in Eq. (32). There are therefore 16 possible combinations of these constants. As shown in Table LVI, these are: one case of no K values (parameters), four cases of 1-parameter, six cases of 2-parameter, four cases of 3-parameter and one case of 4-parameter systems.

A question arises: To what extent must all of them be considered? According to the stoichiometric model, if

Table LVI. Possible special cases of an ionizable substrate in 1:1 and 1:2 complex systems.

Case Code	K's Present	Case Designation*
1	--	
2	K_{11a}	II
3	K_{12a}	
4	K_{11b}	II'
5	K_{12b}	
6	K_{11a}, K_{12a}	III
7	K_{11a}, K_{11b}	I
8	K_{11a}, K_{12b}	
9	K_{12a}, K_{11b}	
10	K_{12a}, K_{12b}	
11	K_{11b}, K_{12b}	III'
12	K_{11a}, K_{12a}, K_{11b}	IV
13	K_{11a}, K_{12a}, K_{12b}	
14	K_{11a}, K_{11b}, K_{12b}	IV'
15	K_{12a}, K_{11b}, K_{12b}	
16	K_{11a}, K_{12a}, K_{11b}, K_{12b}	

*Case designations are consistent with those described for potentiometric method in the Theory section.

K_{11} = 0 then K_{12} must be zero, because it is assumed that the 1:2 complex is formed via the 1:1 complex. Therefore if a finite K_{12} exists, the corresponding K_{11} must also exist. Consequently, Case No. 3, 5, 8-10, 13 and 15 in Table LVI need not be considered. Case 1 contains no stability constants, and Case 16 is the general case, which described the cinnamic acid systems (97). The remaining seven possible cases are thus assigned appropriately to the four special cases as described in the Theory section, since if C < 1 [Eq. (32)]. C' = 1/C was defined and K_{11a} becomes K_{11b}, thus Case II' is equivalent to Case II and in the same manner, Case III' = Case III and Case IV' = Case IV. Therefore the four special cases assigned in the potentiometric method include all the possible cases and are sufficient to describe the complex system in which the full 4-parameter Eq. (32) is not required. Nevertheless, we should be aware that some of the seven cases not being considered here may be physically present especially when $K_{12} >>> K_{11}$, which may occur when a >>> 1.

D. Interpretation of Stability Constants

1. Benzoic Acids

Fig. 37 is a Hammett plot of the K_{11a} and K_{11b} data in Table XVII. The obvious result is that these quantities vary with substituent constant in opposite ways.

Fig. 37. Hammett plots of K_{11a} (open circles) and K_{11b} (filled circles) for 4-substituted benzoic acids; data from Table XVII.

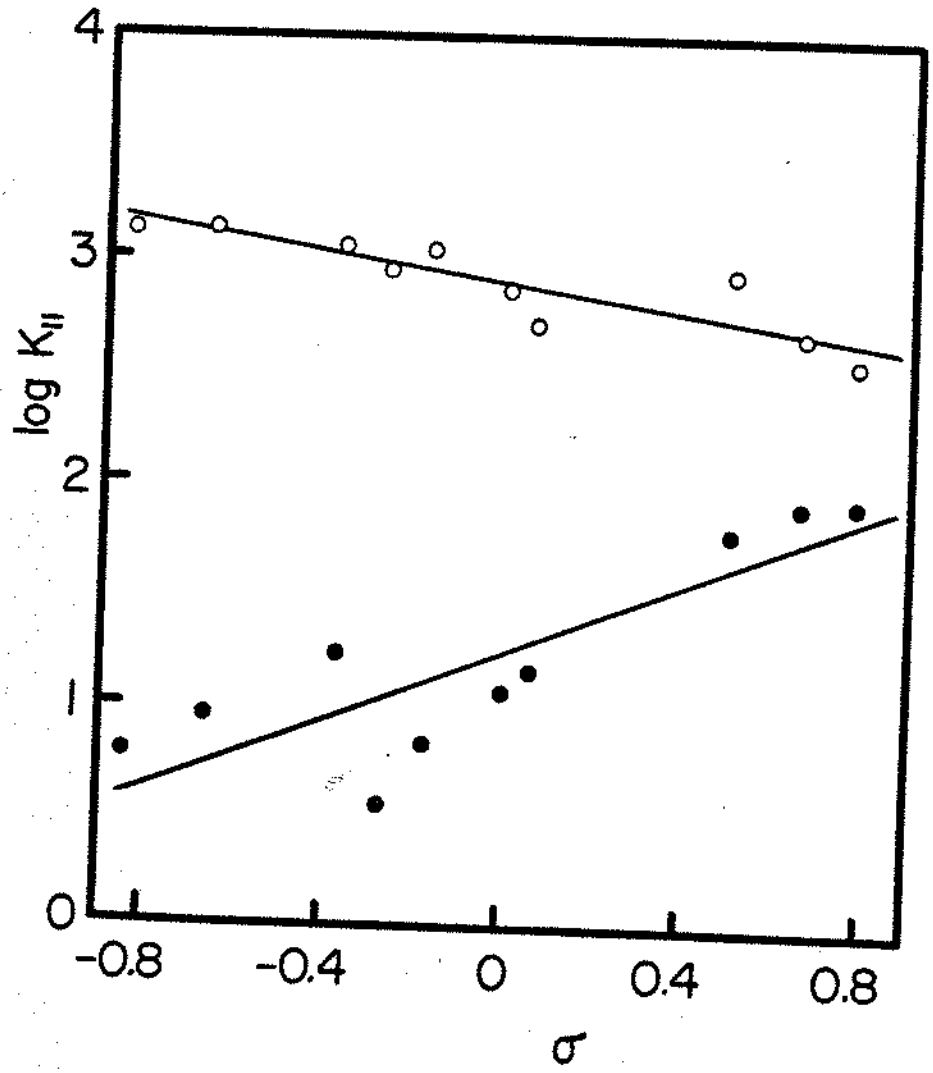
4
3
2
1
0
log K_{II}
-0.8
-0.4
0
0.4
0.8
σ

The complexation constants for this series can be described by the following equations:

$$\log K_{11a} = 2.89 - 0.31\sigma \quad (129)$$
$$(0.11) \quad (0.04) \quad (0.07)$$

$$\log K_{11b} = 1.23 + 0.77\sigma \quad (130)$$
$$(0.27) \quad (0.08) \quad (0.17)$$

where σ is the Hammett substituent constant and the numbers in parentheses are standard deviations of the quantities immediately above them, in the units to which they appear in the equation. The correlations show the trends rather than precise relationships.

Casu and Ravà (76) studied K_{11a} for some of these acids; their constants are different from those in Table XVII, however, the general behavior is the same, namely that the slope (rho value) is negative. Electron withdrawing X groups decrease complex stability in the conjugate acid series.

This behavior is explicable if K_{11a} represents primarily binding at the COOH end of the substrate molecule. The binding interaction is increased by an increase in electron density at the binding site, hence is associated with a negative rho value. This hypothesis is supported by proton NMR data (143) and ^{13}C NMR results (79) on benzoic

acid, which indicate the carboxyl group enters the cavity.

K_{11b} is always smaller than K_{11a} for the same substrate. This is consistent with the view that K_{11a} represents mainly COOH-site binding. Upon ionization of this group, its affinity for the cavity is greatly decreased because of the high polarity of COO^- and the nonpolarity (relative to the solvent) of the cavity. Therefore K_{11b} represents binding at the remaining site, namely X. The more electron-withdrawing the X group, the higher the electron density at the binding site, thus the larger is K_{11b}. Since K_{11b} describes X-site binding, the correlation with σ for X is not expected to be as precise as when the substituent is distant from the reaction site.

If K_{11a} describes mainly COOH-site binding, then K_{12a} must represent mainly binding at the X-site. The model predicts that K_{12a} should respond to X-substituent effects in the same way that K_{11b} does, since they describe roughly the same process. Table XVII shows that this is indeed the case, in a general way; both K_{11b} and K_{12a} tend to increase together, and to trend in the opposite sense to K_{11a} along the sigma scale. The binding at the X-site, K_X, becomes larger as σ gets larger; finally K_X becomes comparable with K_{COOH} when $\sigma_X \simeq \sigma_{COOH}$. Then a finite K_{12} is observed. Compounds with <u>para</u>-substituents having sigma values close to that of COOH will be interesting to study.

Note that the Hammett plot suggests if a substituent with sufficiently large σ were available, K_{11b} would become larger than K_{11a}. This might not result in $\Delta pK_a'$ becoming negative, however, because K_{12a} will also increase.

The Hammett correlations indicated that the electron density at the binding site is a primary determinant for the stability of the complex. Other factors than electronic density affecting binding site affinity must be considered also. For example, K_{11b} for substrates 1-3 in Table XVII seems anomalously high. These are the only X groups capable of functioning as hydrogen-bond donors, and this capability may increase complex stability. The trend in K_{12a} for compounds 8-10 appears to oppose that for K_{11b}, and this may be the result of some additional factors, which could include size, shape, polarity, and polarizability. In fact, K_{12a} for these substrates seems to be a resultant of the electronic density effect measured by σ, and the X-site polarity as measured by group dipole moments. These dipole moments are, for X = $COCH_3$, 3.00D; CN, 4.39; NO_2, 4.21 (145). An increase in site polarity will tend to decrease the site binding constant (97), and both K_{11b} and K_{12a} may reflect this effect superimposed on the electron density effect.

This model of complexing suggests that K_{12} values are useful sources of information. Writing Eqs. (115) and

(121) as

$$K_{11} = K_X + K_Y \tag{131}$$

$$K_{12} = \frac{aK_XK_Y}{K_{11}} \tag{132}$$

where X and Y signify the two binding sites on the substrate $X\text{-}C_6H_4\text{-}Y$, shows that K_{12} can be zero only if $a = 0$ or if one of the site binding constants (K_X or K_Y) is zero, according to Eq. (132). Now since K_{11b} describes mainly X-site binding, K_{12b} represents binding at the COO^- site; and it was found that $K_{12b} = 0$ for all substrates. Moreover the existence of finite K_{12a} values (substrates 8-10) means that a is finite for these acid substrates, which suggests that it will also be finite in the corresponding base substrates. It follows that K_{12b} is zero as a consequence of the site binding constant for COO^- being zero. Letting K_{Yb} represent this quantity, and K_{Xb} be the X-site binding constant in the conjugate base series, it follows that $K_{11b} = K_{Xb} + K_{Yb} = K_{Xb}$; that is, K_{11b} can be identified solely with the binding at site X.

Extension to the acid series requires the assumption that K_{Xb} for binding to X in the base series is identical with K_{Xa} for binding to X in the acid series. The assumption seems to be reasonable since the negative charge on COO^- is localized. The X-binding sites on either acid or

base forms of the aromatic acid can be assumed to be identical. Then $K_{11a} = K_{Xa} + K_{Ya} = K_{Xb} + K_{Ya} = K_{11b} + K_{Ya}$, and the site binding constant K_{Ya} for the COOH site is given approximately by $K_{11a} - K_{11b}$.

With these estimates of K_{Xa} ($= K_{11a} - K_{11b}$) and K_{Ya} ($= K_{11b}$), Eq. (132) becomes

$$K_{12a} = \frac{aK_{11b}(K_{11a} - K_{11b})}{K_{11a}} \qquad (133)$$

which leads to estimates of these substrates. For compounds 1-7, a = 0; for no. 8, a = 0.51; no. 9, a = 0.38; no. 10, a = 0.33. Because of the several approximations, these estimates may not be accurate, but they seem reasonable in magnitude.

A different set of assumptions leads to another way to estimate a. Combining Eqs. (131) and (132) gives Eq. (134):

$$K_{11} = \frac{K_{11}K_{12}}{aK_Y} + K_Y \qquad (134)$$

If a and K_Y are non-zero and essentially constant, a plot of K_{11} vs. $K_{11}K_{12}$ will be linear. Fig. 38 is the plot of Eq. (134) for the 4-CH_3CO, CN and NO_2 benzoic acids. A reasonably straight line is obtained indicating the assumptions are valid. a is found to be 0.25 which is similar in magnitude to the earlier estimates. K_Y is 136 M^{-1}. The assignment of this value (to the X or COOH site) requires additional information or assumptions.

Fig. 38. A plot of Eq. (134) for 4-CH_3CO, CN, NO_2 benzoic acids.

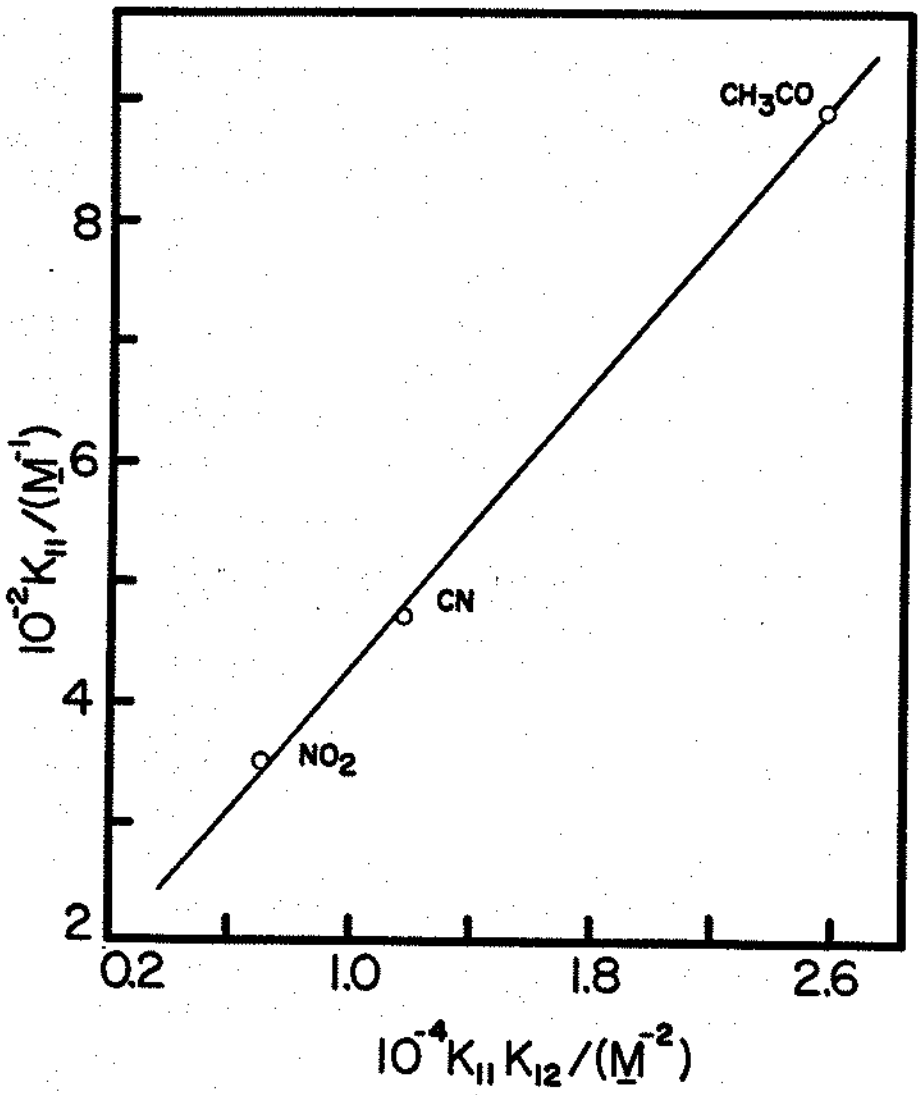
CH3CO
CN
NO2
8
6
4
2
0.2
1.0
1.8
2.6
10^-2 K11 / (M^-1)
10^-4 K11 K12 / (M^-2)

2. Phenols

The general result that K_{11b} is greater than K_{11a} for all the phenols is observed in Table XXXII. This indicates that the anion appears to "partition" into the cyclodextrin cavity more favorably than does the neutral form. K_{11a} and K_{11b} trend in the same way along the sigma scale, as shown in Fig. 39. The greater the electron-withdrawing ability in the X site, the stronger the complex stability, except for halogen substituents. These data suggest that, in both the conjugate acid and base series, the para-substituted end is the primary binding site in the 1:1 complexes.

Scattering is observed in the Hammett plots, the K_{11a} and K_{11b} values of halogen substituted phenols being anomalously high. Obviously, other factors must be taken into account. It is proposed that complex stability is determined by binding site electron density (which usually is expressed in the substituent constant sigma), polarizability (which is measured in terms of molar refraction, R_D) and polarity (which is indicated in dipole moment, μ) besides the size and shape. The first two factors favor stability, while the polarity opposes it. The Hammett substituent constants (σ), molar refractions (R_D) of monosubstituted benzenes X-C_6H_5 and the dipole moment (μ) of phenols are listed in Table LVII. The data in Table XXXII

Fig. 39. Hammett plots of K_{11a} (open circles) and K_{11b} (filled circles) for phenols; data from Table XXXII.

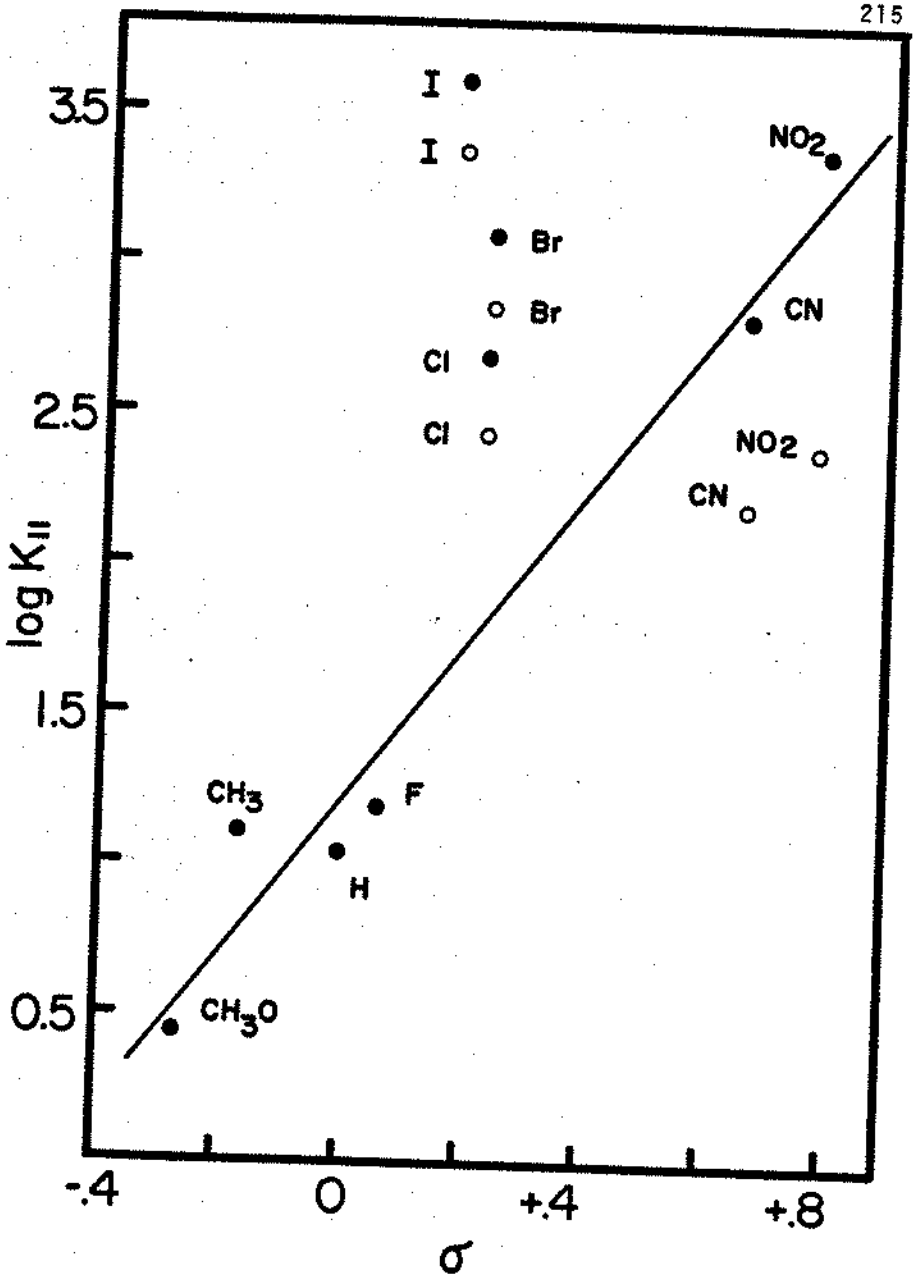
3.5
2.5
1.5
0.5
log K_{II}
I
I
Br
Br
Cl
Cl
NO_2
CN
NO_2
CN
CH_3
F
H
CH_3O
-.4
0
+.4
+.8
σ

Table LVII. Hammett substituent constants (σ), molar refraction (R_D) of monosubstituted benzenes and dipole moments (μ) of phenols.

X[a]	σ	R_D[b]	μ[c]
OCH_3	-0.268	32.91	1.92
CH_3	-0.17	31.12	1.37
H	0	26.19	1.52
F	0.062	26.07	2.17
I	0.18	39.03	2.13
Cl	0.227	31.15	2.19
Br	0.232	33.97	2.19
CN	0.66	31.48	4.93
NO_2	0.778	32.69	5.05

[a] X in $X\text{-}C_6H_4\text{-}OH$.

[b] Calculated according to $R_D = (\frac{n^2 - 1}{n^2 + 2})\frac{M}{d}$ for $X\text{-}C_6H_5$ where n = refractive index, M = molecular weight, and d = density.

[c] From Ref. (146).

are described by the following equations:

$$\log K_{11b} = -1.41 + 5.33\sigma + 0.15R_D - 0.81\mu \quad R^2 = 99\% \quad (135)$$
$$(0.13) \quad (0.42) \quad (0.34) \quad (0.01) \quad (0.08)$$

$$\log K_{12b} = 0.78 - 1.22\sigma \quad R^2 = 81\% \quad (136)$$
$$(0.18) \quad (0.10) \quad (0.42)$$

$$\log K_{11a} = -0.96 + 0.12R_D - 0.10\mu \quad R^2 = 99\% \quad (137)$$
$$(0.06) \quad (0.37) \quad (0.01) \quad (0.02)$$

$$K_{12a} = 0 \quad (138)$$

The numbers in the parentheses are the standard deviations. Again, these correlations have no quantitative theoretical significance because of the nature of the measures of polarizability and polarity, but they indicate the roles of these factors.

It was stated previously as a hypothesis that the electron density at the binding site is the primary determinant in the binding stability. Eq. (137) indicates that the polarizability of the substituent plays a more important part in this series. The easier the electron density can be distorted, the greater the strength of binding. Fig. 40 shows how K_{11a} varies as a function of R_D.

Fig. 40. K_{11a} of phenols plotted against molar refraction (R_D) of the corresponding monosubstituted benzene; K_{11a} data from Table XXXII.

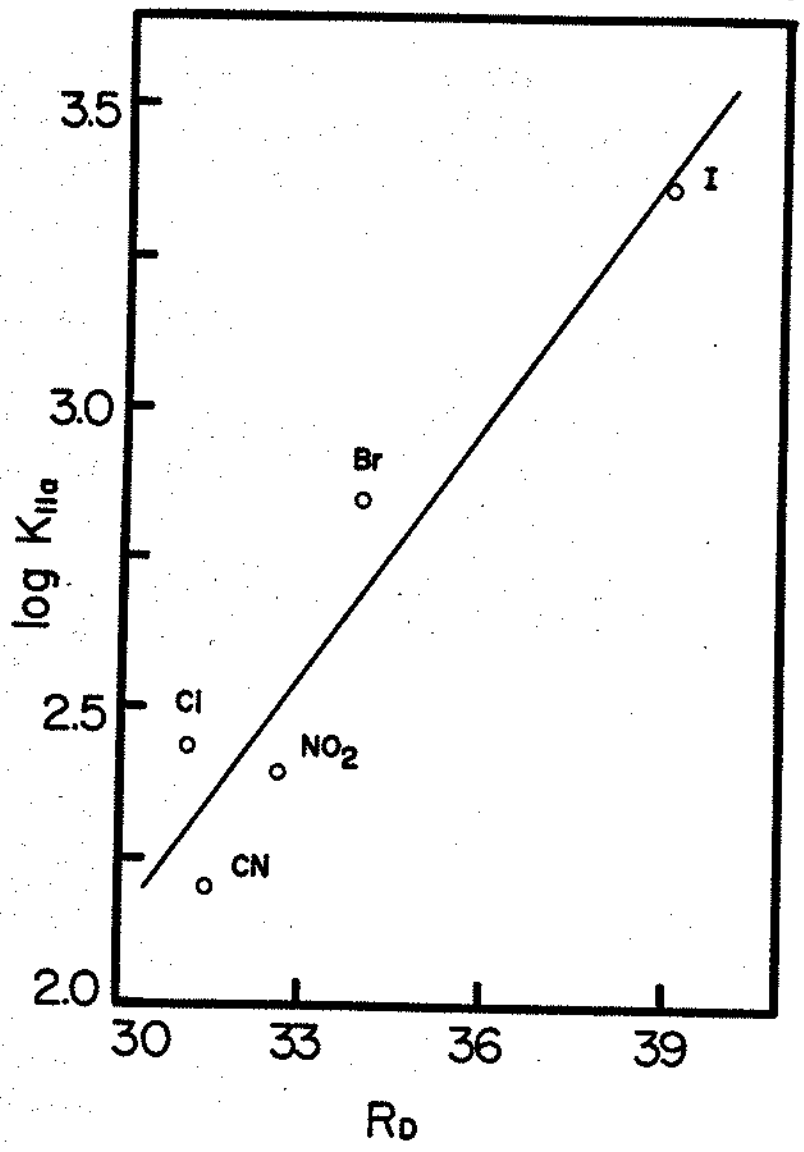
3.5
3.0
2.5
2.0
log K_{IIa}
I
Br
Cl
NO_2
CN
30
33
36
39
R_D

When X = Cl, Br, I, there is relatively high electron density at X binding site by the electron-withdrawing inductive effect, and they are extremely polarizable. Thus the binding constants K_{11a} and K_{11b} are anomalously high as shown in the Hammett plots, Fig. 39.

Estimation of a values using the argument from the benzoic acid discussion probably is not warranted. The systems are more complicated because of the possibility for the extensive electron delocalization between the phenol or phenolate group and the para-substituted group, as illustrated:

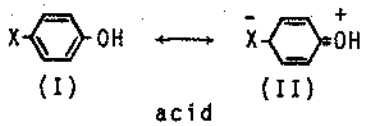

(I) acid (II)

and

(III) base (IV)

It therefore cannot be expected that the group X has identical properties in the conjugate acid and base forms of the substrate.

That $K_{11b} > K_{11a}$ for phenols may seem surprising because of the presumed greater polarity of the anion. The resonance forms in structures (I)-(II) and (III)-(IV) are

extreme cases. The actual species has just a single average electron distribution. Neutral phenols, especially those having electron-withdrawing X groups, are highly dipolar species, as revealed by their dipole moments. Upon ionization extensive delocalization of the unit excess charge over the entire molecule occurs, thus the electron density at site X for the anion is increased. This favors complexing with the anion. In addition, the anion may actually be less "polar" than the neutral form because of the delocalization of the charge, whereas charge separation occurs in the neutral form, which again favors complexing with the anion. Therefore, it may be concluded that highly localized negative charges (as in the benzoate series) will result in destabilization, but delocalized charge (as in the phenolate series) may be stabilizing.

K_{11a} for the phenol $^{-}OOC\text{-}C_6H_4\text{-}OH$ is evidently the same quantity as K_{11b} for the benzoic acid anion $HO\text{-}C_6H_4\text{-}COO^{-}$. Discussing this as a benzoate it was concluded that the COO^{-} site binding was negligible, leaving binding at OH to account for the observed binding. On the other hand, it was concluded here that binding at the OH site in phenols is probably negligible. This inconsistency suggests that it may not be permissible to make a common assignment of binding mode to all the members of a series. In this case the negative charge on the carboxylate may oppose the usual

electron release by the hydroxy group, leaving it more susceptible to binding.

If it is correct that X is the main binding site for K_{11b}, then K_{12b} must represent binding at the phenolate site. The general trend should be that K_{12b} increases in the opposite direction to K_{11b}. Thus the negative rho value observed in Eq. (136) is reasonable. However, not all compounds show a finite K_{12b}. The compounds having K_{12b} values all can donate electron charge by the resonance effect (X = Cl, Br, I) or possess large negative sigma (X = OCH_3); that is, they have substituents that can tolerate a positive charge as follows:

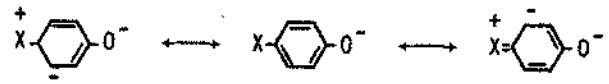

(V) (III) (VI)

Structure (IV) will not be important. This resonance effect (V-VI) may sufficiently counter the electron release of the phenolate site to allow significant binding at that site and result in finite K_{12b} values.

However, in phenolates having electron withdrawing X groups, the electronic structures are:

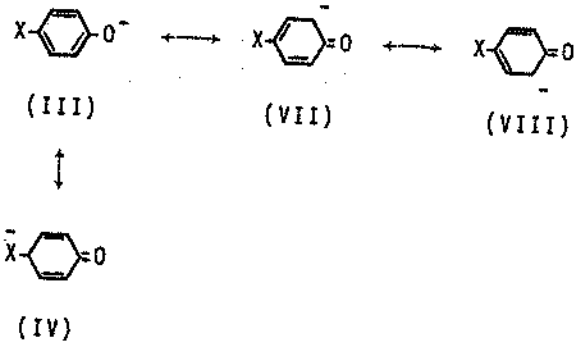

(III) (VII) (VIII)

(IV)

When X has a high tolerance for negative charge, which is reflected in a large positive σ value, then structure (IV) will be highly favored, and the electron charge (i.e., the excess density on the oxygen) will be distributed very largely between structures (III) and (IV). Therefore the binding at phenolate end does not occur because of low electron density, i.e., $K_{12b} = 0$ for these compounds.

In unionized phenols, the resonance forms in structure (II) result in low electron density at the OH binding site, therefore that $K_{12a} = 0$ for all the substrates is explicable.

3. Anilines and Amines

The data in Table XLI for the aniline derivatives show a rough trend of K_{11b} with electron-withdrawal by the 4-substituent, indicating that the X site is the primary binding site. 4-Methylaniline appears to bind anomalously strongly. The binding of 4-aminobenzoic acid may be

enhanced by hydrogen-bonding. The binding constants are described by Eq. (139)

$$\log K_{11b} = \underset{(0.39)}{1.70}\sigma + \underset{(0.31)}{0.05}R_D \quad (0.005) \qquad (139)$$

4-Aminoaniline is symmetrical. From Eqs. (123) and (124), the site binding constant $K_{NH_2} = 1.1$ and $a = 0$. However, this estimate of $\underline{a}$ must be considered in light of the experimental uncertainty in K_{12}. For example, suppose $\underline{a}$ were equal to 0.35, which is a typical $\underline{a}$ value determined in benzoic acid series. Then with Eq. (124) we calculate $K_{12b} = 0.20$. This value is experimentally indistinguishable from zero; hence the estimate $a = 0$ based on $K_{12b} = 0$ is not definitive.

Since in 4-aminoaniline the X group is NH_2, with $\sigma = -0.66$, it is expected that any X group having a more positive σ will reduce binding at NH_2 site. Thus the isometric binding constant for the NH_2 group should be in the range of 0 to 1.1, which is very small. Therefore K_{11b} for the anilines can be interpreted as essentially the isomeric binding constant for the X site.

If this is so, it can be predicted that K_{11a} for phenols and K_{11b} for anilines are comparable, since the two substrate series are electronically very similar; compare the resonance forms in structures (IX)-(X) for anilines and

(I)-(II) for phenols.

(IX) (X)

Fig. 41 is the plot of K_{11b} of anilines vs. K_{11a} of phenols. The trend is generally in agreement with the prediction, also it shows that K_{11b} of the anilines is greater than K_{11a} of the phenols in most of the cases. These stability constants are comparable since they are primarily for binding to the same X site: the binding to the other site is very small, as proved by the very small K_{12b} values.

K_{11a} is zero in most of the anilines. The finite K_{11a} corresponds to binding at the X-site because the anilinum site is positively charged, and the charge is localized at that amino site. Thus not only is the cation polar, it also has less electron density at the X-site than the amine base, therefore K_{11a} is smaller than K_{11b} in this series. $K_{12a} \approx 0$ for all the anilines, which is obviously reasonable.

The stability constants for benzylamine, phenethylamine and heterocyclic amines in Table LI show that these amines form weak complexes with α-cyclodextrin. The K_{11b} increase with the increase in the carbon chain of aniline, benzylamine and phenethylamine probably is a result of the

Fig. 41. A plot of K_{11b} of anilines against K_{11a} of phenols. Data from Tables XXXII and XLI.

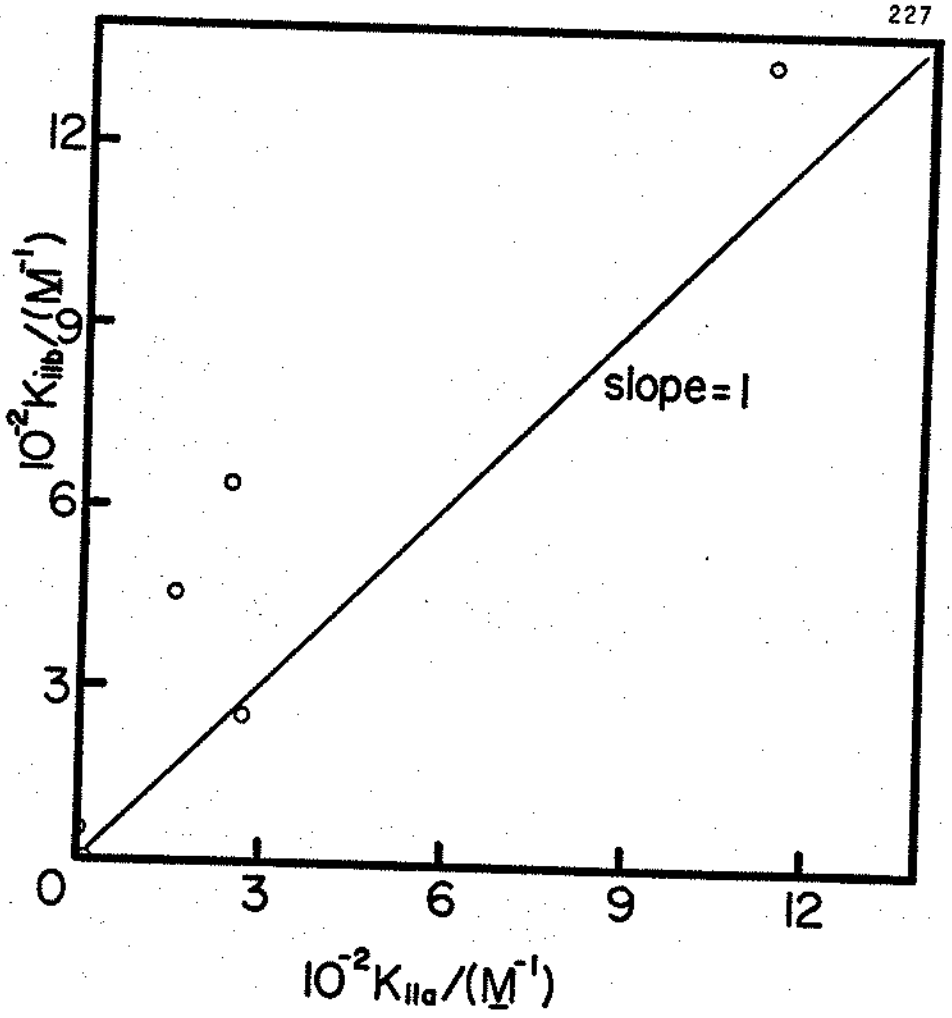
12
9
6
3
0
3
6
9
12
slope = 1
$10^{-2}K_{IIb}/(M^{-1})$
$10^{-2}K_{IIa}/(M^{-1})$

change in hydrophobicity of the molecule, which aids the "partitioning" of the substrate from polar solvent medium to the relatively apolar cyclodextrin cavity.

A three times stronger binding for 4-nitroimidazole than imidazole suggests that the 4-nitro substituted end is the primary binding site. The high dipole moment of imidazole, μ = 6.2 (147), indicates the involvement of a charge separation in the resonance forms as,

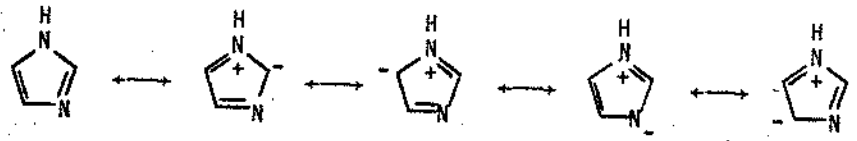

A large decrease in dipole moment of N-methylimidazole, μ = 3.6 (148), supports that the 1-N end is electron deficient.

The relatively high stability constants of K_{11b} and K_{12b} for 4-t-butylpyridine indicate binding occurs at both ends of the molecule. The spacial conformation of the substituent may not be very important; as long as the size allows it to fit into the cavity, complexation occurs (other factors being considered the same).

Quinoline and isoquinoline have very similar 1:1 binding constants in base forms probably because of their similarity in electronic properties. However, an explanation for the effect of the structure of isoquinoline on the finite K_{12} formation requires further investigation.

E. Conclusion

Macroscopically, it is concluded that for benzoic acids, K_{11a} describes mainly binding at COOH site, K_{11b} at X-site and K_{12a} at X-site; for phenols, both K_{11a} and K_{11b} describe X-site binding; and for anilines, K_{11b} and K_{11a} describe primarily X-site binding. Assume binding to the other site of the molecule is very small and negligible, the X-site binding constants for constant Y in molecule $X\text{-}C_6H_4\text{-}Y$ are obtained from the K_{11} data and listed in Table LVIII. The Table enables making Hammett plots across the rows. Two Hammett plots for X = CN and NO_2, shown in Fig. 42, are very satisfactory. The data points of $Y = O^-$ are not included in the plots because σ_{O^-} is not available, but the four points are sufficient to see the correlation. This leads to the result, for molecule $X\text{-}C_6H_4\text{-}Y$, that correlation can be made with X at constant Y, and with Y at constant X. The more electron donating Y is, the stronger the binding at X and vice versa. But for very small binding constants, i.e., when X is electron donating, K_X is not very sensitive to the nature of Y, e.g., compare K_H for $Y = O^-$, NH_2, OH^-, COO^-, and COOH. K_H is almost a constant.

Further analysis of the model, solving Eqs. (131) and (132) for K_X and K_Y, where the assignment of groups X and Y is arbitrary, gives:

Table LVIII. X-site binding constants for X-C_6H_4-Y.

	1:1 K_X binding site constant for Y =					
X	O^-	NH_2	OH	COO^-	COOH	NH_3^+
$NHCH_3$				6.1	0	
NH_2		1.1		9.0	0	
OH				16.6	0	
OCH_3	2.73	6.6	0	3.5	0	
CH_3	13.9	57.6	0	6.6	0	37.05
H	10.9	8.8	0	11.2	0	
COO^-		0	0			
F	15.6		0	14.2	0	
I	3955		2316			
Cl	488	250.5	272			68.6
Br	1221		704			
COOH		1341	1130			
CH_3CO				60.3	28.8	
CN	662	451	158	79.2	25.0	
NO_2	2408	635	245	81.0	20.2	

Fig. 42. Hammett plot of K_X in Table LVIII against σ of Y site; X = CN (open circles), X = NO_2 (filled circles).

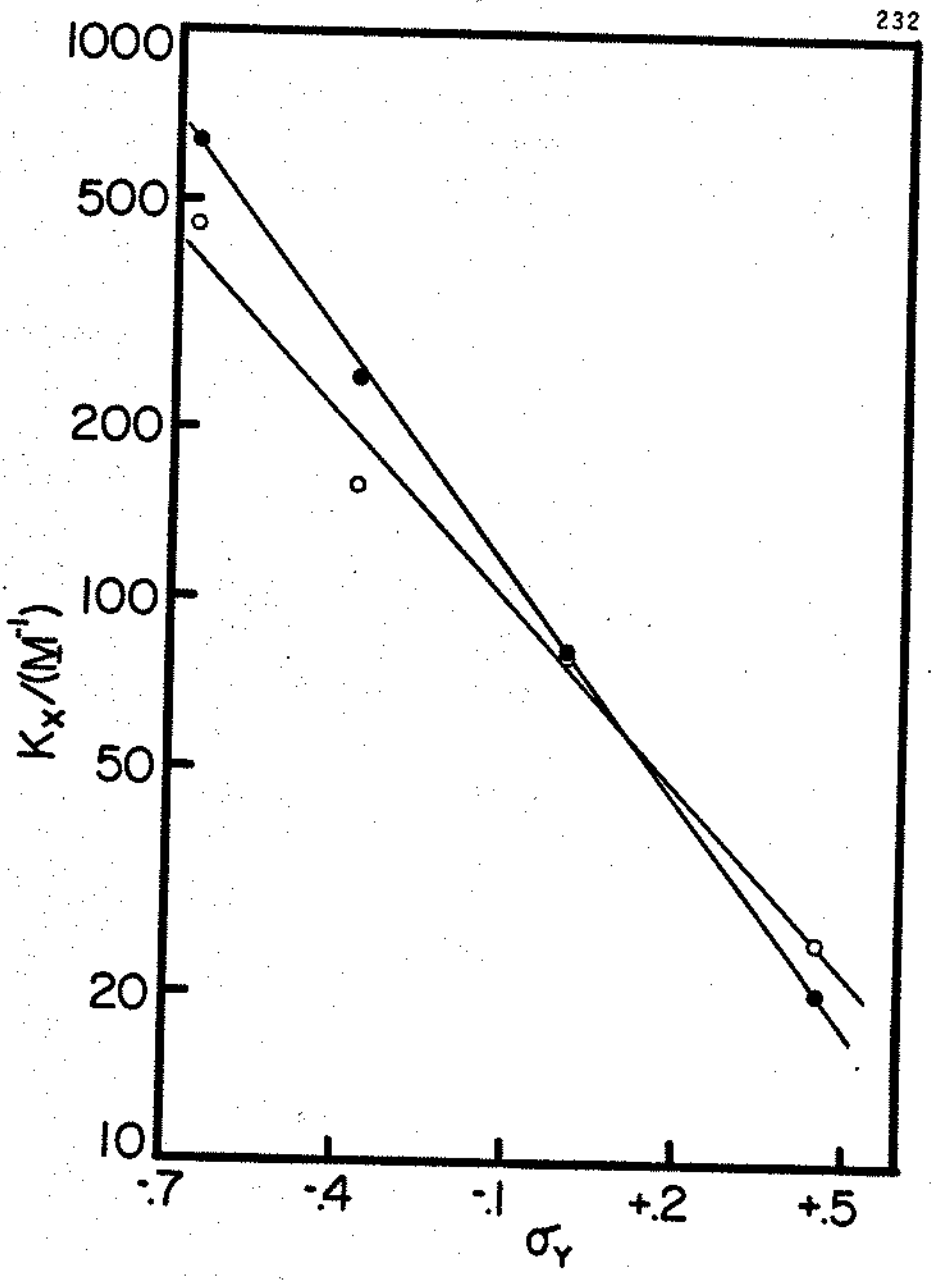
1000
500
200
100
50
20
10
$K_x/(M^{-1})$
-.7
-.4
-.1
+.2
+.5
σ_Y

$$K_Y = \frac{aK_{11} \pm \sqrt{aK_{11}(aK_{11} - 4K_{12})}}{2a} \qquad (140)$$

Eq. (145) puts a limit on the value of a. First, the equation cannot be valid if a = 0, though it is a meaningful result according to Eq. (132). Second, Eq. (140) can only be physically valid if the quantity in the square root is positive or zero, hence

$$aK_{11} \geq 4K_{12} \qquad (141)$$

or

$$a_{min.} = \frac{4K_{12}}{K_{11}} \qquad (142)$$

The $a_{min.}$ values (minimum of a) for some of the complex systems studied are calculated and shown in Table LIX. Systems with $K_{12} = 0$ indicate that either one of the site binding constants is zero or that a = 0. 4-Methoxyphenolate must be a cooperative system since a > 1. Other systems having finite K_{12} values are assumed to be non-cooperative systems. If $a = a_{min}$, then $aK_{11} = 4K_{12}$ and Eq. (140) and (131) gives

$$K_X = K_Y = K_{11}/2 \qquad (143)$$

Any larger value of a will increase K_Y and decrease K_X (or vice versa, since the designation is arbitrary). Therefore, $K_{11}/2$ is a minimum value for one of the binding sites and

Table LIX. Minimum a values for α-cyclodextrin: 1,4-disubstituted benzene systems ($X\text{-}C_6H_4\text{-}Y$).

	$a_{min.}$ for Y =		
X	OH	O^-	NH_2
NH_2	-	--	0
OCH_3	-	19.4	0
CH_3	-	0	0.272
H	-	0	0
COO^-	0	--	0
F	-	0	-
I	0	0.0024	-
Cl	0	0.025	0
Br	0	0.015	-
COOH	0	--	0
CN	0	0	0
NO_2	0	0	0

K_{11} is a maximum value. The sum of the two site binding constants is K_{11}. The general limits of the two site binding constants are therefore:

$$K_{11}/2 \leq K_X \leq K_{11}$$

$$K_{11}/2 \geq K_Y \geq 0$$

If $\underline{a}$ is not greater than one, the limits can be approximately written as

$$K_{11}/2 \leq K_X \leq (K_{11} - K_{12})$$

$$K_{11}/2 \geq K_Y \geq K_{12}$$

For closer estimation of K_X and K_Y, several chemically reasonable assumptions have been made. These are, for various systems:

(1) $a = 1$; which was used in cinnamic acid systems (97).
(2) $K_Y = 0$ or $a = 0$, when $K_{12} = 0$.
(3) $\underline{a}$ and K_Y are constant in a series; which was applied in benzoic acid series as described in Discussion section.
(4) $\underline{a}$ is identical for substrates of similar size.

When the substrate is symmetrical, i.e., X = Y, Eq. (123) allows the site binding constants to be calculated.

The *a* values calculated according to assumptions (2) and (3) for 4-CH_3CO, CN and NO_2 benzoic acids are summarized in the following:

Assumptions	a for X = CH_3CO	CN	NO_2
a and K_Y constant	0.25	0.25	0.25
$K_{COO^-} = 0$, $K_X^{COOH} = K_X^{COO^-}$	0.51	0.38	0.33

The results show reasonable agreement. It would not be far off to take a typical number of a = 0.35 for the acid compounds and, by use of assumption (4) above, for all the 1,4-disubstituted benzenes.

The site binding constants can, therefore, be calculated based on the assumptions described above and Eq. (140) with a = 0.35 for all the 1,4-disubstituted benzenes studied. The results are collected in Table LX. The binding site assignments are: when $K_{12} = 0$, K_{11} corresponds to the binding constant for the primary binding site and the other site has zero binding constant; when K_{12} is finite, according to Eq. (140), the larger number calculated corresponds to the binding of the primary site and the other binding constant corresponds to the other binding site. The sum of the two equals K_{11}.

It would be useful to know how large K_{12} might

Table LX. Site binding constant estimates for the X-site in X-C_6H_4-Y.

Y \ X	K_X[a] O^-	MeNH	NH_2	OH	MeO	Me	H	COO^-	F	I	Cl	Br	COOH	MeCO	CN	NO_2	NH_3^+
O^-					-[b]	14	11		16	3948	479	1209			662	2408	
MeNH								0					1301				
NH_2			1.1		6.7	43	8.8	0			251		1341		451	635	0
OH					0	0	0	0	0	2316	272	704	1130		158	245	
MeO	-[b]		0	0				0					884				0
Me	0		15	0				0					1091				0
H	0		0	0				0					722				0
COO^-		6.1	9.0	17	3.5	6.6	11		14					60	79	81	
F	0			0				0					504				
I	6.8			0													
Cl	8.9		0	0													0
Br	13			0													
COOH		0	0	0	0	0	0		0					92	88	73	
MeCO								0					797				

CN	0			0			0			384
NO_2	0			0			0			278
NH_3^+			0		37	0			69	

[a] K_X is calculated according to Eq. (140), a = 0.35.

[b] A cooperative system a cannot be 0.35.

actually be when it has been experimentally determined to be zero. One approach to solve this problem is to take into account the experimental uncertainties in K_{12} determinations. Only the uncertainties of K_{12} for Case I and II systems are needed, since for Case III and IV systems the K_{12} values are finite, by definition. Using Case IV equations to analyze a Case I system, and Case III equations for a Case II system, K_{12} values and their standard deviations are obtained. (This approach is the same as described in Results section in testing the appropriateness of case assignments.) The upper limit of an actual K_{12} that is still not significantly different from zero at 95% confidence level is then calculated and shown in Table LXI. In other words, these are the minimum values for K_{12} that would have to be ovserved for us to conclude that K_{12} is finite.

Using Eq. (140) with the upper limits of K_{12} and a = 0.35, the corresponding maximum site binding constants (say K_Z) are calculated in Table LXI. Z-site is the one other than the primary binding site on the substrate, following the general conclusion for binding site assignments. It is observed in Table LXI that the uncertainties in K_{12} and K_Z are roughly inversely related to K_{11}, which means assumption (2) is more accurately applied if K_{11} is high.

Table LXI. Upper limit of K_{12} and specific site binding constant K_Z to account for zero.

Substrate[a]			Std. dev.	Upper limit of[b]	Z-site	
X	Y	K_{11}	of K_{12}	K_{12}	designation	K_Z[c]
NH_2	NH_2	2.26	(0.10)[d]	--	NH_2	(0.23)[e]
CH_3O	NH_2	6.71	0.31	0.21	NH_2	0.67
H	NH_2	8.81	0.39	0.51	NH_2	1.8
H	O^-	10.9	0.21	0.91	O^-	4.3
CH_3	O^-	13.9	0.36	0.74	O^-	2.6
F	O^-	15.6	0.95	1.12	O^-	4.5
Cl	NH_2	250	0.16	0.47	NH_2	1.4
F	COOH	504	0.08	0.20	F	0.6
CN	O^-	661	0.08	0.28	O^-	0.8
H	COOH	722	0.13	0.27	H	0.8
CH_3O	COOH	884	0.07	0.16	CH_3O	0.5
CH_3	COOH	1091	0.07	0.16	CH_3	0.5
OH	COOH	1130	0.06	0.09	OH	0.3
CH_3NH	COOH	1301	0.14	0.31	CH_3NH	0.9
NH_2	COOH	1341	0.10	0.20	NH_2	0.6
NO_2	O^-	2408	0.16	0.25	O^-	0.7

[a] X, Y in X-C_6H_4-Y.

[b] At 95% confidence level.

[c] Calculated according to Eq. (140) with upper limit of K_{12} and a = 0.35.

[d] Std. dev. of K_{11}. According to Eq. (123) identical site binding constant depends on K_{11}.

[e] $t_{(n-2,\ 0.025)}$ x std. dev. of K_{11}.

Table LX is arranged in order of sigma values for the substituents such that the binding constants show the trend with site electron density, modified by polarizability and polarity. Comparing the site binding constants in Table LX with the corresponding significant values in Table LXI, apparently all the finite site binding constants are significant. The estimates in Table LX imply the presence of appreciable fractions of two isomeric 1:1 complexes from substrates lying close to the diagonal, and this phenomenon should be most readily detected for substrates lying in the lower right corner of the table. Substrates whose entries lie farthest from the diagonal are most likely to generate simple 1:1 complex systems, i.e., $K_X = K_{11}$ and $K_Y = 0$ (or vice versa). The largest bindings are in the upper right quadrant. The diagonal of the table represents symmetrical substrates, whose study will go far to establish the validity of the model and of the binding site assignments.

Table LX is valuable because it enables the estimation of K_{11} for any substrate by summing the two appropriate entries from the table, allowing X to be each substituent in turn.

REFERENCES

1. A. Villiers, Compt. Rend. Acad. Sci. Paris, 112, 536 (1891).
2. F. Schardinger, Wien. Klin. Wochenschr., 17, 207(1904).
3. F. Schardinger, Zentr. Bakteriol. Parasitenk. II, 29, 188(1911).
4. A. O. Pulley and D. French, Biochem. Biophys. Res. Commun., 5, 11(1961).
5. P. R. Sundarajan and V. S. R. Rao, Carbohydr. Res., 13, 351(1970).
6. J. A. Thoma and L. Stewart, "Starch: Chemistry and Technology," Vol. I. R. L. Whistler and E. F. Pashall (eds.), Academic Press, New York, pp. 209-249 (1965).
7. R. L. Van Etten, J. F. Sebastian, C. A. Clowes and M. L. Bender, J. Am. Chem. Soc., 89, 3242(1967); ibid., 89, 3253(1967).
8. D. W. Griffiths and M. L. Bender, Adv. Cat., 23, 209 (1973).
9. V. R. S. Rao and J. F. Foster, J. Phys. Chem., 67, 951(1963).
10. B. Casu, M. Reggiani, G. G. Gallo and A. Vigivani, Tetrahedron, 24, 803(1968); ibid., 22, 3061(1966).

11. M. L. Bender and M. Komiyama, "Cyclodextrin Chemistry," Springer-Verlag, New York, 1978.

12. L. H. Tung, Hua Hsueh Tung Pao, 2, 68(1981).

13. R. I. Gelb, L. M. Schwartz, J. J. Bradshaw and D. A. Laufer, Bioorg. Chem., 9, 299(1980).

14. F. Cramer, G. Mackensen and K. Sensse, Chem. Ber., 102, 494(1969).

15. F. Cramer, Rec. Trav. Chim., 25, 891(1956).

16. F. Cramer and W. Dietsche, Chem. Ber., 92, 1739(1959).

17. W. Saenger, Angew. Chem. Int. Ed. Engl., 19, 344 (1980).

18. D. French, M. L. Levine, J. H. Pazur and E. Norberg, J. Am. Chem. Soc., 71, 353(1949).

19. T. W. Rosanske, Ph.D. Thesis, University of Wisconsin, Madison, WI 53706.

20. M. A. Swanson and C. F. Cori, J. Biol. Chem., 172, 797(1948).

21. D. French, M. L. Levine, and J. H. Pazur, J. Am. Chem. Soc., 71, 356(1949).

22. S. Veibel and S. Hjorth, Acta Chem. Scand., 6, 1355 (1952).

23. J. Szejtli and Zs. Budai, Acta Chim. Acad. Sci. Hung., 91, 73(1976).

24. F. R. Senti and S. R. Erlander, "Non-Stoichiometric Compounds." L. Mandelcorn, Academic Press, New York, pp. 588-601 (1964).

25. M. Komiyama and H. Hirai, Chem. Lett., 1251(1980).

26. F. Cramer, "Einschlussverbindungen." Springer, Heidelberg (1954).

27. F. Cramer, Angew. Chem., 73, 49(1961).

28. J. I. Lach and T.-F. Chin, J. Pharm. Sci., 53, 924 (1964).

29. N. Hennrich and F. Cramer, J. Am. Chem. Soc., 87, 1121(1965).

30. M. L. Bender, Trans. N. Y. Acad. Sci., 29, 301(1967).

31. C. Van Hooidonk and J. C. A. E. Breebaart-Hansen, Recl. Trav. Chim. Pays-Bas, 89, 289(1970).

32. K. Flohr, R. M. Paton and E. T. Kaiser, Chem. Commun., 1621(1971).

33. D. E. Tutt, and M. A. Schwartz, Chem. Commun., 113 (1970); J. Am. Chem. Soc., 93, 767(1971).

34. M. Komiyama and M. L. Bender, J. Am. Chem. Soc., 99, 8021(1977).

35. F. Cramer, U. Bergmann, P. C. Manor, M. Noltemeyer and W. Saenger, Justus Liebigs Ann. Chem., 1169(1976).

36. F. Cramer and G. Mackensen, Angew. Chem., 78, 641 (1966).

37. Y. Iwakura, Uno, F. Toda, S. Onozuka, K. Hattori and M. L. Bender, J. Am. Chem. Soc., 86, 3680(1964).

38. M. Komiyama, E. J. Breaux and M. L. Bender, Bioorg. Chem., 5, 393(1976).

39. Y. Kitaura and M. L. Bender, Bioorg. Chem., 4, 237 (1975).

40. W. B. Gruhn and M. L. Bender, Bioorg. Chem., 3, 324 (1974).

41. J. Emert and R. Breslow, J. Am. Chem. Soc., 97, 670 (1975).

42. I. Tabushi, K. Shimokawa, N. Shimizu, H. Shirakata and K. Fujita, J. Am. Chem. Soc., 98, 7855(1976).

43. I. Tabushi, K. Fujita and L. C. Yuan, Tetrahedron Lett., 2503(1977).

44. R. Breslow and L. E. Overman, J. Am. Chem. Soc., 92, 1075(1970).

45. I. Tabushi, N. Shimizu, T. Sugimoto, M. Shiozuka and K. Yamamura, J. Am. Chem. Soc., 99, 7100(1977).

46. Y. Matsui, T. Yokoi and K. Mochida, Chem. Lett., 1037 (1976).

47. R. Breslow and P. Campbell, J. Am. Chem. Soc., 91, 3085(1969).

48. I. Tabushi, K. Yamamura, K. Fujita and H. Kawabuko, J. Am. Chem. Soc., 101, 1019(1979).

49. K. Uekama, F. Hirayama and M. Daiguji, Chem. Lett., 327(1978).

50. F. Hirayama and K. Uekama, Chem. Pharm. Bull., 27, 435(1979).

51. D. French, Adv. Carbohydr. Chem., 12, 189(1957).

52. F. Cramer and H. Hettler, Naturwissenschaften, 54, 625(1967).

53. W. Saenger, "Environment Effects on Molecular Structure and Properties," B. Pullman (ed.), pp. 265-305, D. Reidel Publ. Co., Dordrecht, Holland.

54. S. G. Frank, J. Pharm. Sci., 64, 1585(1975).

55. M. L. Bender and M. Komiyama, "Bioorganic Chemistry," Vol. 1, Chap. 2, E. E. VanTamelen (ed.), Academic Press, New York (1977).

56. R. J. Bergeron, J. Chem. Educ., 54, 204(1977).

57. J. F. Wojcik and R. P. Rohrbach, J. Phys. Chem., 79, 2251(1975).

58. F. Cramer and F. M. Henglein, Angew. Chem., 68, 649 (1956).

59. H. Schlenk, D. M. Sand and J. A. Tillotson, J. Am. Chem. Soc., 77, 3587(1955).

60. J. L. Lach and J. Cohen, J. Pharm. Sci., 52, 137 (1963).

61. P. V. DeMarco and A. L. Thakkar, Chem. Commun., 2 (1970).

62. A. L. Thakkar and P. V. DeMarco, J. Pharm. Sci., 60, 652(1971).

63. M. Eigen and L. C. De Maeyer, "Technique of Organic Chemistry," Vol. III, Part 2, S. L. Friess, E. S. Lewis, and A. Weissberger (eds.). Interscience Publisher Inc., New York, 1963.

64. F. Cramer, W. Saenger, H.-Ch. Spatz, J. Am. Chem. Soc., 89, 14(1967).

65. R. P. Rohrback, Z. J. Rodriguez, E. M. Eyring and J. F. Wojcik, J. Phys. Chem., 81, 944(1977).

66. N. Yoshida and M. Fujimoto, Chem. Lett., 1377(1980).

67. M. Eigen, Ber. Bunsenges. Physik. Chem., 64, 115 (1960).

68. W. Broster and W. Lautsch, Z. Naturforsch., 8B, 711 (1953).

69. P. A. Kramer and K. A. Connors, Amer. J. Pharm. Educ., 33, 193(1969).

70. K. Uekama, M. Otagiri, Y. Kanie, S. Tanaka and K. Ikeda, Chem. Pharm. Bull., 23, 1421(1975).

71. M. Otagiri, T. Miyaji, K. Uekama and K. Ikeda, Chem. Pharm. Bull., 24, 1146(1976).

72. T. Miyaji, Y. Kurono, K. Uekama and K. Ikeda, Chem. Pharm. Bull., 24, 1155(1976).

73. H. A. Benesi and J. H. Hildebrand, J. Am. Chem. Soc., 71, 2703(1949).

74. R. J. Bergeron and W. P. Roberts, Anal. Biochem., 90, 844(1978).

75. Von W. Lautsch, W. Bandel and W. Broser, Z. Naturforsch., 11B, 282(1956).

76. B. Casu and L. Ravà, Ric. Sci., 36, 733(1966).

77. R. I. Gelb, L. M. Schwartz, B. Cardelino and D. A. Laufer, Anal. Biochem., 103, 362(1980).

78. K. A. Connors and J. M. Lipari, J. Pharm. Sci., 65, 379(1976).

79. R. I. Gelb, L. M. Schwartz, R. F. Johnson and D. A. Laufer, J. Am. Chem. Soc., 101, 1869(1979).

80. R. I. Gelb, L. M. Schwartz, C. T. Murray and D. A. Laufer, J. Am. Chem. Soc., 100, 3553(1978).

81. J. L. Cohen and K. A. Connors, Amer. J. Pharm. Educ., 34, 197(1970).

82. H. Schlenk and D. M. Sand, J. Am. Chem. Soc., 83, 2312(1961).

83. J. L. Cohen and K. A. Connors, Amer. J. Pharm. Educ., 31, 476(1967).

84. J. P. Behr and J. M. Lehn, J. Am. Chem. Soc., 98, 1743(1976).

85. D. J. Wood, F. E. Hruska and W. Saenger, J. Am. Chem. Soc., 99, 1735(1977).

86. K. Uekama, F. Hirayama, N. Matsuo, and H. Koinuma, Chem. Lett., 703(1978).

87. H. Kondo, H. Nakatani and K. Hiromi, Carbohydr. Res., 52, 1(1976).

88. R. J. Bergeron and P. McPhie, Bioorg. Chem., 6, 465 (1977).

89. S. Yamaguchi and T. Tsukamoto, Nippon Kagaku Kaishi, 1856(1976).

90. T. Osa, T. Matsue and M. Fujihara, Heterocycles, 6, 1833(1977).

91. K. Harata, Bull. Chem. Soc. (Japan), 51, 2737(1978).

92. H. Kondo, H. Nakatani and K. Hiromi, J. Biochem., 79, 393(1976).

93. G. E. Hardee, M. Otagiri and J. H. Perrin, Acta Pharm. Succ., 15, 188(1978).

94. W. Saenger, M. Noltemeyer, P. C. Manor, B. Hingerty and B. Klar, Bioorg. Chem., 5, 187(1976).

95. R. J. Bergeron, M. A. Channing, G. J. Gibeily and D. M. Pillor, J. Am. Chem. Soc., 99, 5146(1977).

96. F. Cramer, Angew. Chem., 68, 115(1956).

97. T. W. Rosanske and K. A. Connors, J. Pharm. Sci., 69, 564(1980).

98. K. A. Connors, S. F. Lin and A. B. Wong, J. Pharm. Sci., in press.

99. K. Harata, Bull. Chem. Soc. (Japan), 50, 1416(1977).

100. G. Nemethy and H. A. Scheraga, J. Chem. Phys., 36, 3401(1962).

101. M. Komiyama and M. L. Bender, J. Chem. Phys., 100, 2259(1978).

102. K. Lindner and W. Saenger, Angew. Chem., 90, 738 (1978); Angew. Chem. Int. Ed. Engl., 17, 694(1978).

103. P. C. Manor and W. Saenger, Nature, 237, 392(1972); J. Am. Chem. Soc., 96, 3630(1974).

104. W. Saenger and M. Noltemeyer, Angew. Chem. Int. Ed. Engl., 13, 552(1974).

105. B. Hingerty and W. Saenger, J. Am. Chem. Soc., 98, 3357(1976).

106. J. M. MacLennan and J. J. Stezowski, Biochem. Biophys. Res. Commun., 92, 926(1980).

107. R. J. Bergeron and M. P. Meeley, Bioorg. Chem., 5, 197(1976).

108. E. S. Hall and H. J. Ache, J. Phys. Chem., 83, 1805 (1979).

109. I. Tabushi, Y. I. Hiyosuke, T. Sugimoto and K. Yamamura, J. Am. Chem. Soc., 100, 916(1978).

110. R. I. Gelb, L. M. Schwartz, and D. A. Laufer, J. Am. Chem. Soc., 100, 5875(1978).

111. K. A. Connors and T. W. Rosanske, J. Pharm. Sci., 69, 173(1980).

112. W. A. Pauli and J. L. Lach, J. Pharm. Sci., 54, 1745 (1965).

113. A. Wishnia and S. L. Lappi, J. Mol. Biol., 82, 77 (1974).

114. R. Bergeron, Y. Machida and K. Block, J. Biol. Chem., 250, 1223(1975).

115. A. B. Wong, Ph.D. Thesis, University of Wisconsin, Madison, WI 53706.

116. E. A. Lewis and L. D. Hansen, J. Chem. Soc. Perkin Trans. II, 2081(1973).

117. K. A. Connors and J. A. Mollica, J. Pharm. Sci., 55, 772(1966).

118. W. Broser, Z. Naturforsch., 8B, 722(1953).

119. J. A. Mollica, Jr. and K. A. Connors, J. Am. Chem. Soc., 89, 308(1967).

120. J. L. Cohen and K. A. Connors, J. Pharm. Sci., 59, 1271(1970).

121. P. A. Kramer and K. A. Connors, Amer. J. Pharm. Ed., 33, 193(1969).

122. P. A. Kramer and K. A. Connors, J. Am. Chem. Soc., 91, 2600(1969).

123. K. A. Connors, M. H. Infeld, and B. J. Kline, J. Am. Chem. Soc., 91, 3597(1969).

124. H. Stelmach and K. A. Connors, J. Am. Chem. Soc., 92, 863(1970).

125. M. DeVylder and D. DeKeukeleire, Bull. Soc. Chim. Belg., 87, 9(1978); ibid., 87, 497(1978).

126. P. Pfeiffer, O. Angern, and L. Wang, Hoppé-Seyler's Z. Physiol. Chem., 164, 197(1927).

127. C. Zerbe and F. Jage, Brennstoffch., 16, 88(1935).

128. P. Pfeiffer, K. Kollbach and E. Haack, Justus Liebigs Ann. Chem., 460, 147(1928).

129. D. D. Perrin, W. L. F. Armarego and D. R. Perrin, "Purification of Laboratory Chemicals," Pergamon Press, Long Island City, New York, 1966.

130. J. F. T. Berliner and O. E. May, J. Am. Chem. Soc., 49, 1007(1927).

131. A. V. Few and J. W. Smith, J. Chem. Soc., 1, 753 (1949).

132. H. R. Snyder, C. T. Elston and D. B. Kellom, J. Am. Chem. Soc., 75, 2014(1953).

133. W. E. Deming, "Statistical Adjustment of Data," Dover Publ., New York, p. 18 (1943).

134. A. G. Worthing and J. Geffner, "Treatment of Experimental Data," John Wiley and Sons, Inc., London, p. 242 (1943).

135. P. A. Kramer, Ph.D. Thesis, University of Wisconsin, Madison, WI 53706.

136. C. L. Perrin, "Mathematics for Chemists," Wiley-Interscience, New York, p. 159 (1970).

137. J. Johnston, Proc. Roy. Soc. (London), A78, 82(1906).

138. P. O. Lumme, Suom. Kemistil., 30B, 168(1957).

139. R. N. Mattoo, Trans. Faraday Soc., 52, 1462(1956).

140. A. V. Willi, Z. Physik. Chem. N. F., 27, 233(1961).

141. A. I. Biggs and R. A. Robinson, J. Chem. Soc., 388 (1961).

142. M. M. Fickling, A. Fischer, B. R. Mann, J. Packer and J. Vaughan, J. Am. Chem. Soc., 81, 4226(1959).

143. R. J. Bergeron, M. A. Channing, and K. A. McGovern, J. Am. Chem. Soc., 100, 2878(1978).

144. I. M. Klotz, Acc. Chem. Res., 7, 162(1974).

145. E. S. Gould, "Mechanism and Structure in Organic Chemistry," Holt, Rinehart and Winston, New York, 1959, p. 62.

146. A. L. McClellan, "Tables of Experimental Dipole Moments," Vol. 2, Rahara Enterprises, El Cerrito, Cal., 1974.

147. W. Hückel and W. Jahnentz, Chem. Ber., B74, 652(1941).

148. W. Hückel, J. Datow, and E. Simmersbach, Z. Physik. Chem., A186, 129(1940).

APPENDICES

A. Equations to Calculate [L] in Potentiometric Method

Free ligand concentration [L] is estimated by combining Eq. (34) with the appropriate special case of Eq. (32).

$$L_t = [L] + S_t\left[\frac{M}{2A} + \frac{N}{2B}\right] \tag{34}$$

where

$$A = 1 + K_{11a}[L] + K_{11a}K_{12a}[L]^2$$

$$B = 1 + K_{11b}[L] + K_{11b}K_{12b}[L]^2$$

$$M = K_{11a}[L] + 2K_{11a}K_{12a}[L]^2$$

$$N = K_{11b}[L] + 2K_{11b}K_{12b}[L]^2$$

$$C = \frac{1 + K_{11a}[L] + K_{11a}K_{12a}[L]^2}{1 + K_{11b}[L] + K_{11b}K_{12b}[L]^2} \tag{32}$$

Case I: $K_{12a} = 0$, $K_{12b} = 0$. Then

$$A = 1 + K_{11a}[L]$$

$$B = 1 + K_{11b}[L]$$

$$M = K_{11a}[L]$$

$$N = K_{11b}[L]$$

and Eq. (32) becomes

$$C = \frac{1 + K_{11a}[L]}{1 + K_{11b}[L]} \tag{35}$$

Let $R = K_{11a}/K_{11b}$, then $K_{11a} = R \cdot K_{11b}$. Substituting into Eq. (35) gives

$$K_{11b} = \frac{(C - 1)}{(R - C)[L]} \tag{A-1}$$

Substituting A, B, M, N and Eq. (A-1) into Eq. (34), after rearranging gives

$$[L] = L_t - \frac{(C - 1)(R + C) \cdot S_t}{2C(R - 1)} \tag{A-2}$$

Which is equivalent to Eq. (A-3).

$$[L] = L_t - \frac{S_t}{X + 1} \tag{A-3}$$

where

$$X = \frac{(C + 1)(R - C)}{(C - 1)(R + C)}$$

Case II: $K_{11b} = 0$, $K_{12b} = 0$, $K_{12a} = 0$. Then

$$A = 1 + K_{11a}[L]$$

$$B = 1$$

$$M = K_{11a}[L]$$

$$N = 0$$

and

$$C = 1 + K_{11a}[L] = A \tag{38}$$

Substituting these equations into Eq. (34) gives

$$L_t = [L] + \frac{S_t K_{11a}[L]}{2C} \qquad (A\text{-}4)$$

Substituting $K_{11a}[L]$ from Eq. (38) into Eq. (A-4) gives

$$[L] = L_t - \frac{(C - 1)S_t}{2C} \qquad (A\text{-}5)$$

[L] can be calculated directly from experimental C values.

Case III: $K_{11b} = 0$, $K_{12b} = 0$. Then

$$A = 1 + K_{11a}[L] + K_{11a}K_{12a}[L]^2$$

$$B = 1$$

$$M = K_{11a}[L] + 2K_{11a}K_{12a}[L]^2$$

$$N = 0$$

and

$$C = 1 + K_{11a}[L] + K_{11a}K_{12a}[L]^2 = A \qquad (40)$$

Substituting A, B, M, N, and C into Eq. (34) gives

$$L_t = [L] + \frac{S_t(K_{11a}[L] + 2K_{11a}K_{12a}[L]^2)}{2C} \qquad (A\text{-}6)$$

From. Eq. (40),

$$K_{11a}K_{12a}[L]^2 = (C - 1) - K_{11a}[L] \qquad (A\text{-}7)$$

Substituting Eq. (A-7) into Eq. (A-6) becomes

$$L_t = [L](1 - \frac{S_t K_{11a}}{2C}) + \frac{S_t(C - 1)}{C} \qquad (A\text{-}8)$$

Rearranging Eq. (A-8) becomes

$$[L] = \frac{2C(L_t - S_t) + 2S_t}{2C - S_t K_{11a}} \tag{41}$$

Case IV: $K_{12b} = 0$. Then

$$A = 1 + K_{11a}[L] + K_{11a}K_{12a}[L]^2$$

$$B = 1 + K_{11b}[L]$$

$$M = K_{11a}[L] + 2K_{11a}K_{12a}[L]^2$$

$$N = K_{11b}[L]$$

and

$$C = \frac{1 + K_{11a}[L] + K_{11a}K_{12a}[L]^2}{1 + K_{11b}[L]} \tag{43}$$

$$= A/B$$

Substituting C = A/B into Eq. (34) gives

$$L_t = [L] + \frac{S_t(\frac{M}{C} + N)}{2B} \tag{A-9}$$

Substituting B, M, N and C into Eq. (A-9) gives

$$L_t = [L] + \frac{S_t(K_{11a}[L] + 2K_{11a}K_{12a}[L]^2 + CK_{11b}[L])}{2C(1 + K_{11b}[L])} \tag{A-10}$$

From Eq. (43),

$$K_{11a}K_{12a}[L]^2 = (C - 1) + CK_{11b}[L] - K_{11a}[L] \tag{A-11}$$

Combining Eqs. (A-11) and (A-10) gives

$$L_t = [L] + \frac{S_t(2C - 2 - K_{11a}[L] + 3CK_{11b}[L])}{2C(1 + K_{11b}[L])} \qquad \text{(A-12)}$$

Rearranging Eq. (A-12) as a function of [L], a quadratic equation is obtained:

$$K_{11b}[L]^2 + [1 + S_t K_{11b}(\tfrac{3}{2} - \tfrac{R}{2C}) - L_t K_{11b}][L] - [L_t - \frac{S_t(C - 1)}{C}] = 0 \qquad (45)$$

where $R = K_{11a}/K_{11b}$

B. Equation for [L] and the Determination of K_{11} in Spectrophotometric Method

The conventional Benesi-Hildebrand spectrophotometric method to determine stability constant of 1:1 complex is well known (73).

The interaction of substrate and ligand to produce a complex is expressed as

$$S + L \rightleftharpoons SL$$

and the corresponding stability constant is defined as:

$$K_{11} = [SL]/[S][L] \qquad (B\text{-}1)$$

Assume Beer's Law is followed by all species. The absorbance of substrate (A_o) in the absence of ligand is given by Eq. (B-2).

$$A_o = \epsilon_S b S_t \qquad (B\text{-}2)$$

where ϵ_S is the molar absorptivity of the substrate, and b is the cell pathlength in cm. In the presence of ligand at a total molar concentration L_t, the absorbance of the solution is

$$A_L = \epsilon_S b[S] + \epsilon_L b[L] + \epsilon_{11} b[SL] \qquad (B\text{-}3)$$

where brackets represent the molar concentration, and ϵ_L and ϵ_{11} are the molar absorptivities of the ligand and the

(SL), respectively. Combining Eq. (B-3) with the mass balances on S and L, gives

$$A_L = \varepsilon_S b S_t + \varepsilon_L b L_t + \Delta\varepsilon b[SL] \qquad (B\text{-}4)$$

where $\Delta\varepsilon = \varepsilon_{11} - \varepsilon_S - \varepsilon_L$. The L_t term in Eq. (B-4) can be deleted if the absorbance of the solution is measured relative to a reference containing identical ligand concentration. Eq. (B-4) becomes

$$A_L' = \varepsilon_S b S_t + \Delta\varepsilon b[SL] \qquad (B\text{-}5)$$

Combining Eqs. (B-1), (B-2) and (B-5) gives

$$\Delta A/b = K_{11}\Delta\varepsilon[S][L] \qquad (B\text{-}6)$$

where $\Delta A = A_L' - A_o$. Eq. (B-1) combines with mass balance on S gives

$$[S] = S_t/(1 + K_{11}[L]) \qquad (B\text{-}7)$$

and substituting Eq. (B-7) into Eq. (B-6) gives

$$\Delta A/b = K_{11}S_t\Delta\varepsilon[L]/(1 + K_{11}[L]) \qquad (B\text{-}8)$$

A linear form of Eq. (B-8) is to take the reciprocal of this equation:

$$b/\Delta A = 1/K_{11}S_t\Delta\varepsilon[L] + 1/S_t\Delta\varepsilon \qquad (B\text{-}9)$$

The stability constant K_{11} is taken as the ratio of

intercept/slope from the linear plot of $1/\Delta A$ vs. $1/[L]$. In a system if the consumption of ligand by the substrate is small enough to be neglected, then [L] can be approximated by L_t, and K_{11} is obtained by a plot of $1/\Delta A$ vs. $1/L_t$.

However, the approximation may not be adequate. Eq. (B-10) relates [L] to L_t by combining Eq. (B-1) with the mass balance on L.

$$[L] = L_t/(1 + K_{11}[S]) \qquad \text{(B-10)}$$

The approximation that $[L] = L_t$ sustains only when $K_{11}[S] << 1$, i.e., either or both K_{11} and [S] is small. A more general form to determine K_{11} by Eq. (B-9) using [L] which is solved by the following equations. Substituting into Eq. (B-10) from Eq. (B-7) gives

$$[L] = L_t(1 + K_{11}[L])/(1 + K_{11}[L] + K_{11}S_t) \qquad \text{(B-11)}$$

Rearranging Eq. (B-11) and expressing in terms of [L], gives

$$[L]^2 - (L_t - S_t - \frac{1}{K_{11}})[L] - L_t/K_{11} = 0 \qquad \text{(B-12)}$$

[L], therefore, can be calculated from the quadratic equation in Eq. (B-12) where K_{11} is first estimated from the plot of $1/\Delta A$ vs. $1/L_t$. Iteration is carried out until K_{11} essentially does not change.

C. A Competitive Potentiometric Method

Analogous to the methyl orange competitive spectrophotometric method, a competitive potentiometric method is proposed to study the stability constants of non-ionizing substances.

Suppose a substrate HA (weak acid) forms complex with cyclodextrin to give a $\Delta pK_a'$ change, as in the usual potentiometric method. The stability constants of the system can be determined as described in this work. However, to study the complexation of cyclodextrin with a second substrate (S) that does not undergo ionization within the pH covered in measuring pK_a' of HA, we set up a system of HA and [L], measure its pH and see how the addition of S perturbs the pH, which allows the determination of complex stability constant for S.

Assume 1:1 stoichiometry in both S and HA complexes with cyclodextrin:

$$HA \rightleftharpoons H^+ + A^-$$

$$S + L \rightleftharpoons SL$$

$$HA + L \rightleftharpoons HAL$$

$$A^- + L \rightleftharpoons AL^-$$

The corresponding stability constants are

$$K_a = \frac{[H^+][A^-]}{[HA]} \qquad (C\text{-}1)$$

$$K_{11s} = \frac{[SL]}{[S][L]} \qquad (C\text{-}2)$$

$$K_{11a} = \frac{[HAL]}{[HA][L]} \qquad (C\text{-}3)$$

$$K_{11b} = \frac{[AL^-]}{[A^-][L]} \qquad (C\text{-}4)$$

As in Case I system, in the absence of S, ΔpK_a° is related to [L] in Eq. (C-5).

$$\Delta pK_a^\circ = \log \frac{1 + K_{11a}[L]}{1 + K_{11b}[L]} = \log C \qquad (C\text{-}5)$$

The mass balances on the acid substrate (A_t), the second non-ionizable substrate (S_t), and ligand concentration (L_t) are:

$$A_t = [HA] + [A^-] + [HAL] + [AL^-] \qquad (C\text{-}6)$$

$$S_t = [S] + [SL] \qquad (C\text{-}7)$$

$$L_t = [L] + [HAL] + [AL^-] + [SL] \qquad (C\text{-}8)$$

Substituting Eqs. (C-1), (C-3) and (C-4) into Eq. (C-6) gives

$$A_t = [HA]\left[\frac{A[H^+] + BK_a}{[H^+]}\right] \qquad (C\text{-}9)$$

where $A = 1 + K_{11a}[L]$ and $B = 1 + K_{11b}[L]$.

Substituting Eq. (C-2) into Eq. (C-7) gives

$$[S] = S_t/(1 + K_{11s}[L]) \qquad (C\text{-}10)$$

Combining Eqs. (C-1) to (C-4) with Eq. (C-8) to related L_t and [L] gives

$$L_t = [L](1 + K_{11s}[S]) + [HA]\left(\frac{M[H^+] + NK_a}{[H^+]}\right) \qquad (C\text{-}11)$$

where $M = K_{11a}[L]$ and $N = K_{11b}[L]$.

Put Eq. (C-10) into Eq. (C-11)

$$L_t = [L]\left(1 + \frac{S_t K_{11s}}{1 + K_{11s}[L]}\right) + [HA]\left(\frac{M[H^+] + NK_a}{[H^+]}\right) \qquad (C\text{-}12)$$

Eliminating [HA] in Eq. (C-12) by substitution from Eq. (C-9) gives a general relationship between [L] and L_t:

$$L_t = [L]\left(1 + \frac{S_t K_{11s}}{1 + K_{11s}[L]}\right) + A_t\left(\frac{M[H^+] + NK_a}{A[H^+] + BK_a}\right) \qquad (C\text{-}13)$$

The electroneutrality equation for this system is,

$$[Na^+] + [H^+] = [OH^-] + [A^-] + [AL^-] \qquad (C\text{-}14)$$

[S] is not included since it is assumed not ionizable, and $[Na^+]$ in Eq. (C-14) is the counter-ion to the conjugate base of the substrate, A^-. Combining Eq. (C-14) with preceding expressions gives

$$[Na^+] + [H^+] - [OH^-] = \frac{A_t BK_a}{A[H^+] + BK_a} \qquad (C\text{-}15)$$

Eq. (C-15) is comparable with Eq. (22). The presence of S

exerts its effect only through Eq. (C-13) by lowering [L]. In order to find K_{11s}, let

$$C_o = C \quad \text{when } S_t = 0$$
$$C_s = c \quad \text{when } S_t = S_t$$
$$[L]_o = [L] \quad \text{when } S_t = 0$$
$$[L]_s = [L] \quad \text{when } S_t = S_t$$

From Eq. (C-5),

$$C_o = \frac{1 + K_{11a}[L]_o}{1 + K_{11b}[L]_o} \tag{C-16}$$

and

$$C_s = \frac{1 + K_{11a}[L]_s}{1 + K_{11b}[L]_s} \tag{C-17}$$

where C_o and C_s are experimentally measured quantities as a function of L_t at $(L_t)_o$ and $(L_t)_s$, respectively. A hypothetical system of benzoic acid in presence of non-ionizable substrate S is set up. Fig. (C-1) is a plot of C_o vs. L_t for benzoic acid which is plotted according to the data in Table IX and a hypothetical plot of C_s vs. L_t is also generated in the Figure. The way to obtain C_s values here will be described later.

In Fig. C-1, along the horizontal line ab, C is constant, so $[H^+]$ is constant according to Eq. (C-5), and therefore [L] must be constant. From the analysis of C_o system, $[L]_o$ can be calculated at point d (in Fig. C-1) by

Fig. C-1. Plots of C vs. L_t. C_o curve is generated according to the data in Table IX for benzoic acid:α-cyclodextrin system. The hypothetical C_s curve is calculated according to Eq. (C-20) where S_t = 0.01 $\underline{M}$, K_{11s} = 250 $\underline{M}^{-1}$ and [L] is calculated from Eq. (36).

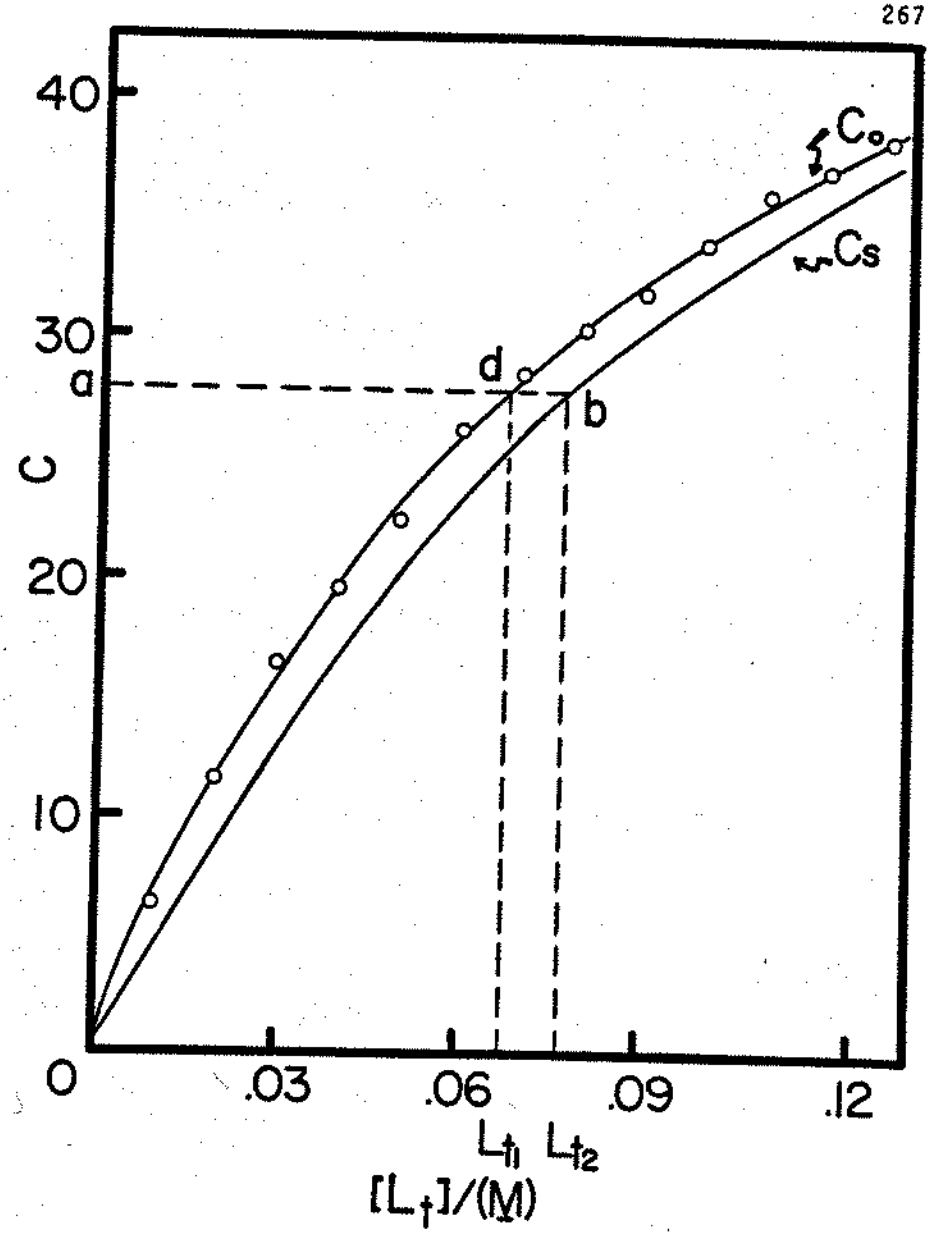
40
30
20
10
0
C
a
d
b
C_o
C_s
.03
.06
.09
.12
L_{t1}
L_{t2}
$[L_t]/(M)$

Eq. (36), then $[L]_s$ at point b is known, since they are identical.

Consider Eq. (C-13), let L_{t1} and L_{t2} be the total ligand concentration at points d and b, then

$$L_{t1} = [L]_o + A_t\left(\frac{M_o[H^+]_o + N_oK_a}{A_o[H^+]_o + B_oK_a}\right) \qquad (C\text{-}18)$$

$$L_{t2} = [L]_s\left(1 + \frac{S_tK_{11s}}{1 + K_{11s}[L]_s}\right) + A_t\left(\frac{M_s[H^+]_s + N_sK_a}{A_s[H^+]_s + B_sK_a}\right) \qquad (C\text{-}19)$$

Since $[H^+]_o = [H^+]_s$ and $[L]_o = [L]_s$ along the ab line, $A_o = A_s$, $B_o = B_s$, $M_o = M_s$ and $N_o = N_s$. Thus by subtraction:

$$L_{t2} - L_{t1} = \frac{S_tK_{11s}[L]}{1 + K_{11s}[L]} \qquad (C\text{-}20)$$

Let $\Delta L_t = L_{t2} - L_{t1}$, rearranging Eq. (C-20) gives

$$\Delta L_t = K_{11s}(S_t - \Delta L_t)[L] \qquad (C\text{-}21)$$

In Eq. (C-21), S_t is known, ΔL_t is measured according to the construction in Fig. C-1, and [L] at any point d on the C_o curve can be calculated according to Eq. (36) for Case I system. Therefore K_{11s} is the slope of a plot of ΔL_t vs. $(S_t - \Delta L_t)[L]$. The hypothetical system C_s in Fig. C-1 is calculated by assuming $S_t = 0.01$ M, $K_{11s} = 250$ M^{-1} in using Eq. (C-20) to find ΔL_t, and [L] is calculated from

the results of benzoic acid system. The maximum ΔL_t in this case is 0.01 M, when L_t ranging from 0.01 M to 0.13 M, which is equivalent to a 0.33 pH unit change by the presence of the second substrate. The method is worth further pursuing.